**Faculty of Science and Engineering**
**WA School of Mines: Minerals, Energy and Chemical Engineering**

**Develop an efficient and sustainable process for biodiesel production via transesterfication**

**Mariam Fares Abdulnabi Alsharifi**

**This thesis is presented for the degree of**
**Doctor of Philosophy**
**of**
**Curtin University**

**May 2020**

*Declaration*

To the best of my knowledge, I declare that, this thesis contains no material previously published any other person expect where due acknowledgment has been made. This thesis contains no material which has been accepted for the award of any other degree or diploma in any university.

## Acknowledgements

I would like to thank all those who supported me in bringing this study into reality. I would also like to thank HCED Iraq for giving me the opportunity of undertaking my PhD.

First, I thank my research supervisor, Dr Hussein Znad, for persuading me to take on this research, and his constructive recommendations and encouragement. I am extremely grateful to my associate supervisor, Prof Ming, for giving me valuable advice, assistance and support.

I would also like to thank Jason Wright for his endless and valuable suggestions and assistance in the setting up of the laboratory equipment and facilities used in this study. Special thanks to Dr Hussein Abid for his advices. My sincere thanks to Dr Roshanak

Doroushi for always being ready to help and her kind encouragement and friendship during the years I have been doing this research study.

I would like to thank the Department of Chemical Engineering and Chemical Engineering Laboratories of Curtin University for all their kind administrative assistance and the carrying out my laboratory work. I am extremely grateful to Karen Haynes, Andrew Chan, Araya Abera, Xiao Hua, Ann Carroll, for their support.

I would like to acknowledge my gratitude to all my family and friends for helping me survive all the stress and not letting me give up. This thesis would not have been possible without the support and love of my family: my spouse, Araz; my children, Zara, Shayan and Umit; and my parents, Fares and Zahra.

## *Dedication*

*To my beloved spouse, Araz*


*Thanks for your support and encouragement*


*To my parents, Fares and Zahraa*

*Thanks for your praying*

*To my siblings, Yhia, Fatima and Mohammed*

*To my precise kids, Zara, Shayan and Umit*

## Abstract

Biodiesel is mono-alkyl fatty acid esters and it is an attarctive alternative to the fossil fuel. It is produced from the transesterfication reaction of vegetable oil or animal fats by homogeneous or heterogeneous catalyst. This research focused on biodiesel production from heterogeneous catalyst to avoid the disadvantages of homogeneous catalysts minimize the

environmental issues by including waste cooking oil as a feedstock and waste biomass as a source of catalyst.

The development of heterogeneous catalyst for transesterification process by implanting lithium onto $TiO_2$ by wet impregnation process was investigated. A series of $Li/TiO_2$ was prepared with different amounts of Li (20, 30, 40 wt %) and at different calcination temperatures (450, 600, 750 °C). The $Li/TiO_2$ catalysts were characterized by several spectroscopic and analytical techniques like X-ray diffraction (XRD), Fourier-transform infrared spectroscopy (FT-IR), Brunauere Emmette Teller surface area (BET), Thermo gravimetric/ differential scanning calorimetry analysis (TGA/DSC) and Field Emission Scanning Electron Microscope (FESEM). The XRD study revealed that the insertion of Li improved the catalyst efficiency without any alteration in structure of $TiO_2$. $Li/TiO_2$ catalysts with 30 wt. % Li and calcined at 600 °C was found to be the most efficient with 98% transesterification yield. The best performance of catalyst was achieved with methanol to oil ratio of 24:1, 5 wt % of catalyst loading, at 55 °C reaction temperatures for 3 h of reaction time. The kinetic studies revealed the transesterification process was compatible with the zero order model. However the reusability decreases after every successive use.

A lithium based chicken bone (Li-Cb) composite has been synthesized by wet impregnation method followed by calcination at various temperatures (750, 800, 850, and 900 °C). The Li-Cb catalysts were characterized by FE-SEM, BET, XRD, TG-DSC and FT-IR. The catalytic activities of Li impregnated catalyst were described in term of basicity. 2 g of $LiNO_3$ impregnated in 7 g of Cb and calcinated at 850 °C (2Li-Cb850) were found as the best combination to synthesize the efficient catalyst for the transesterification of canola oil with 96.6% conversion to FAME in 3 h of reaction time along with 18:1 of methanol:oil molar ratio, catalyst loading of 4wt %, and reaction temperature of 60 °C. The pseudo-first order

model with 0.58 h$^{-1}$ rate constant (at 60 °C) and 16.9 kJ/mol activation energy was the best fitted to represent the transesterification kinetic. Moreover, the prepared catalyst (2Li-Cb850) showed sustained activity after being recycled and reused for 5 times with FAME content > 82%.

In this work, lithium/zinc based chicken bone catalyst (Li/Zn-Cb) was synthesised by wet impregnation method using different metal ratios (Li:Zn= 1:2, 2:2, and 2:1). The synthesised Li/Zn-Cb catalyst was characterized by FE-SEM, BET, XRD, TG-DSC and FT-IR. The feasibility and activity of Li/Zn-Cb catalyst for transesterification of waste canola oil (WCO) were investigated under different operation conditions. The results showed that integrating the chicken bone powder with Li:Zn=2:2 could enhance the FAME content significantly (60 times) to 98% at 60 ºC reaction temperature, 3.5 h reaction time, catalyst dosage of 4% and 18:1 molar ratio of MeOH/WCO. The kinetic studies revealed that transesterification reaction follows the pseudo first order model with 23.20 kJ mol$^{-1}$ activation energy ($E$a). The reusability studies show only 2% reduction in the FAME content after the 7$^{th}$ cycle of use. Moreover, the influence of ultrasonic was investigated and the results showed that the lower reaction time and catalyst dosage achieved the conversion to FAMEs close to that obtained without ultrasonic.

Finally, biodiesel production by Li/Zn-Cb catalyst from waste canola oiol was optimised by the response surface methodology (RSM) based on the Box–Benkhen design (BBD). Reaction temperature, methanol to oil molar ratio and catalyst dosage were the most significant parameters that influence positively on the conversion. Furthermore, the interaction between the reaction temperature and the molar ratio of methanol:oil influenced the conversion as showed by the statistical analysis and variance analysis (ANOVA). The experimental data fitted the quadratic model as shown from the determination coefficient ($R^2$

=0.98). The highest conversion to FAMEs of 97% was achieved at 17:1 of methanol:oil molar ratio, 4% of catalyst dosage and 56.3 °C of reaction temperature.

**List of publications**

*Journal Papers*

Alsharifi, M., Znad, H., Hena, S., & Ang, M. (2017). Biodiesel production from canola oil using novel Li/TiO2 as a heterogeneous catalyst prepared via impregnation method. ***Renewable Energy***, 114, 1077-1089.

Alsharifi, M., & Znad, H. (2019). Development of a lithium based chicken bone (Li-Cb) composite as an efficient catalyst for biodiesel production. *Renewable Energy*, *136*, 856-864.

Alsharifi, M., & Znad, H. (2020). Transesterification of waste canola oil by lithium/zinc composite supported on waste chicken bone as an effective catalyst. *Renwable Energy, 151*, 740-749.

Alsharifi, M., & Znad, H. (2019). Optimization of biodiesel production from waste canola oil by response surface methodology (RSM) (*Biochemical Engineering Journal* under prepartion).

*Conference papers*

Mariam Alsharifi, H. Znad, M. Ang, Lithium Ion Supported on $TiO_2$ Mixed Metal Oxides as a Heterogeneous Catalyst for Biodiesel Production from Canola Oil. ICESE 2017 :19th Int. Conf. on Energy Sources and Environment. Aug 24-25, 2017 Kuala Lumpur Malaysia.

## Table of Contents

**Chapter 4 Biodiesel production from canola oil using novel Li/TiO$_2$ as a heterogeneous catalyst prepared via impregnation method**

**Chapter 5   Development of a lithium based chicken bone (Li-Cb) composite as an efficient catalyst for biodiesel production**

## Chapter 6 Transesterfication of waste canola oil by lithium/zinc composite supported on waste chicken bone as an effective catalyst

## List of Figures

## List of Tables

and catalyst dosage along with the experimental and predicted response of ester conversion…………………………………………………………………………...

## List of Nomenclature and Abbreviations

$R_1$, $R_2$ and $R_3$       alkyl chains

SV           Saponification value

ANOVA         Analysis of variance

BBD           Box Behnken Design

| | |
|---|---|
| RSM | response surface methodology |
| CCD | central composite design |
| Cb | Chicken bone |
| WCO | Waste cooking oil |
| FFA | Free fatty acid |
| DG | Diglycerides |
| FAME | Fatty acid methyl esters |
| FT-IR | Fourier Transform infrared |
| BET | Brunauer-Emmett-Teller |
| MG | Monoglycerides |
| TG | Triglycerides |
| GC | Gas chromatography |
| GL | glycerol |
| Me | methyl ester |
| Mw | molecular mass |
| rpm | revolutions per minute |
| XRD | X-ray diffraction |
| X | conversion |
| S.D. | Standard devation |
| df | degree of freedom |
| (C4 –C24) | Fatty acid methyl esters mixture standard |
| MS | Mass spectroscopy |
| MeOH | methanol |
| FE-SEM | Field emission scanning electron microscope |
| TGA/DSC | Thermo gravimetric/ differential scanning calorimetry |
| BJH | Barrett Joyner Halenda |
| MPa | Pressure |
| COOR | Carbonyl group |
| $RO^-$ | Alkoxide ion |
| FAAE | fatty acid alkyl esters |
| MMOs | Mixed metal oxides |
| Conv. | Conversion |
| PKO | palm kernel oil |

| | |
|---|---|
| HC | hydrodynamic cavitation |
| PTC | phase transfer catalyst |
| WFO | waste frying oil |
| R | Reactants |
| P | Products |
| ROH | Alcohol |
| A | Oil and triglyceride molecule |
| B | Alcohol |
| C | Glycerol |
| D | Fatty acid alkyl ester |
| AV | acid value of feedstock |
| atm | Atmosphere |
| $k1$ | Forward reaction rate constant |
| $k2$ | Reverse reaction rate constant |
| $t$ | Time (min, h) |
| $T$ | Reaction temperature (K) |
| $Ea$ | Activation energy (kJ/mol) |
| $R$ | Universal gas constant (8.314 $kJmol^{-1}K^{-1}$) |
| $A$ | Frequency factor |
| $k$ | Reaction rate constant ($h^{-1}$) |
| $X_{Me}$ and Y | Conversion to FAMEs |
| $Wt. \%$ | Weight percentage |
| $K_{Me}$ | reaction rate constants for the zero order |
| $V$ | Volume of KOH solution required for the titration |
| $C$ | Molarity of the KOH solution |
| $M$ | Molecular weight of KOH (56.1 g/gmol) |
| $m$ | Mass of sample (g). |
| $N$ | Normality of KOH, |
| $V$ | Volume of KOH consumed by 1g fat (ml) |
| $V_b$ | Volume of HCL used for the Blank titration |
| $V_t$ | Volume of HCL used for the test titration |
| $\Sigma A$ | Sum of the areas under all peaks from C4:0 to C24:1 |
| As | Area under the peak of methyl octanoate used as the internal standard |

| | |
|---|---|
| CS | Methyl octanoate solution concentration (mg/ mL) |
| VS | Internal standard solution volume (mL) |
| m | FAMEs sample weight (mg). |
| rpm | Rotations per minute |
| $\lambda$ | x-ray wavelength |
| Å | Unit of x-ray wavelength |
| kV | Kilo volt |
| mA | Milli amper |
| h | Hour |
| K | Kelvin |
| $\theta$ | Theta |
| $\mu$ | Micro |
| H_ | Hammett acidity or basicity (basic strength) |

# CHAPTER 1
# Introduction

## 1.1 Background and motivation

Increasing the demand for energy consumption as a vital feature of rapid growth of population and industrialization has created environment issues. The annual energy consumption is estimated at 12 billion tons of oil. About 80% of energy is from fossil sources and the highest portion (about 58%) used for transportation section [1]. Furthermore, there is an expectation that the energy consumption will rise to 53% by 2030 [2]. Rising demand for energy to meet the human needs means increasing the concerns towards the environment which is represented by air pollution from fossil fuel combustion, global warming and $CO_2$ emission. Moreover, some studies have stated that the natural sources of fuel such as fossil fuel reserves will be exhausted in future which are not renewable sources [3]. Thus, efforts have been intensely devoted for using renewable energy sources (such as hydrogen, wind, natural gas, solar and biodiesel) as an alternative to the conventional fuels.

Biodiesel has emerged as promising alternative solution for petroleum-based fuel. The main features of biodiesel fuel are biodegradability, renewability, non-toxic fuel, and environmentally-friendly. Flash point of biodiesel is quite high (150 ºC) that makes it safe for handling and storage. Thus, its exhaust emissions of hydrocarbons, NOx, CO, $CO_2$ is lower [4, 5]. Moreover, using biodiesel minimizes the emission of SOx gases as it has no sulfur. Therefore, utilization of biodiesel as a fuel could reduce the emissions of petroleum- based fuel by 40-60% [6]. In addition, the viscosity of biodiesel is high and its heating value is low because of its polar structure (high $O_2$ level). Biodiesel could be used as pure or blended to increase its stability such as B20 which means 20% of biodiesel is mixed with 80%diesel [2, 7].

Biodiesel is chemically known as mono alkyl esters of long chain fatty acids, according to the definition of American Society for Testing and Materials (ASTM). Transesterification process is a process for fracturing down the triglyceride molecules (fat animals or vegetable

oils) by short alcohol chain such as methanol or ethanol in the presence of a catalyst [8]. If the transesterification reaction is carried out with methanol then the reaction is called methanolysis and the product is fatty acid methyl ester (FAME). However, if the reaction is conducted with ethanol then the reaction is ethanolysis and fatty acid ethyl esters (FAEE) is the product [9,10]. Transesterification includes three steps of reaction for converting triglycerides to the final products (biodiesel and glycerol). Firstly, triglycerides (TAG) are converted to di-glycerides (DG), then di-glycerides to mono-glycerides (MG) and finally mono-glycerides to glycerol. A mono-alkyl ester of fatty acid is produced in each of the three steps as shown in scheme (1-1).
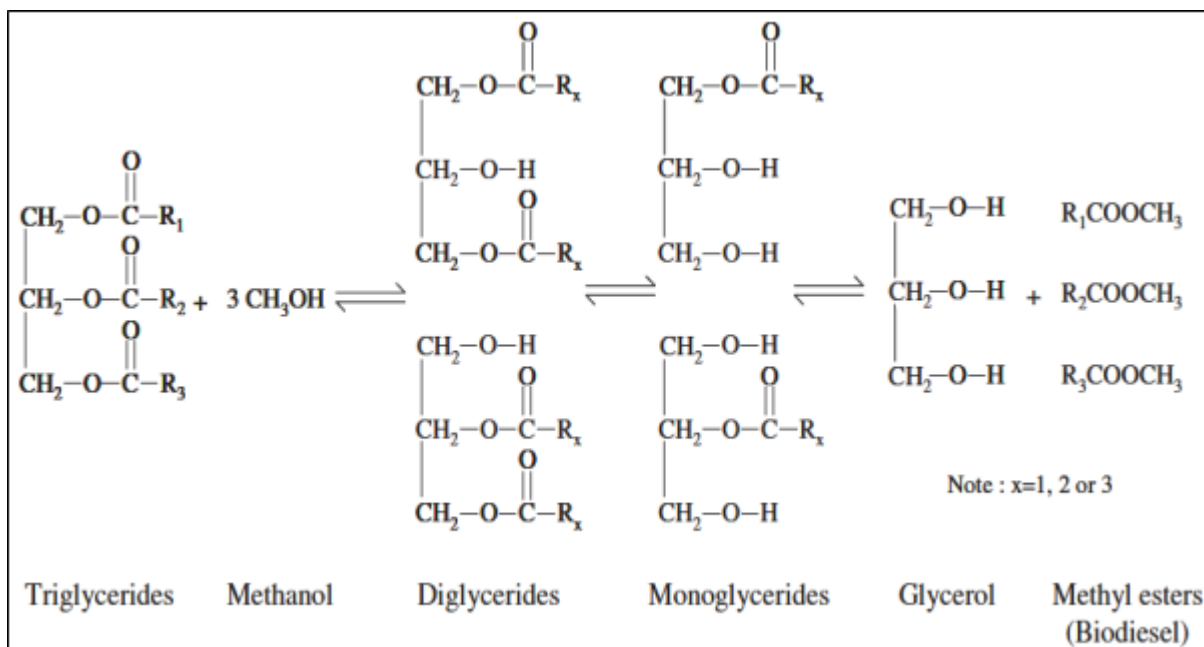


**Scheme 1.1.** Three steps of Methanolyation process of a triglyceride. $R_1$, $R_2$ and $R_3$ are alkyl chains [11].

The factors that significantly affect the transesterification yield and the quality of FAME, are the quality of oil feedstock such as free fatty acid (FFA) content, the nature and amount of catalyst, the type of acyl acceptor (alcohol), the reaction temperature and time, and the ratio of alcohol to oil. Many studies have been published to investigate the influence of these parameters on the quality of final product [4]. In addition, the quality of the final product

must be evaluated according to the requirement of EN 14214 and ASTM D6751. Thus, various feedstocks and catalysts could affect the quality and quantity of produced biodiesel. In spite of the characteristics of biodiesel, the process of its production is expensive. Therefore, some solutions have been proposed in order to solve this challenge such as using low grade feedstock, using mild operating conditions, and utilizing biowaste as a source of catalyst. Thus, the work in this thesis is designed to investigate the process efficiency under atmosphere pressure and mild temperature, using waste oil as a cheap source of feedstock and modified waste chicken bone as a biowaste-based catalyst.

## 1.2 Scope and objectives

The main objectives of this PhD thesis are devoted to develop and enhance an efficient process for biodiesel production via transesterification. To achieve this aim, different catalysts based on lithium oxide will be modified and investigated to produce biodiesel from waste and fresh canola oil. The following are the specific objectives:

1) Synthesising, characterization, and kinetic evaluation of $Li/TiO_2$ mixed-oxide catalyst for efficient transesterification of fresh canola oil and waste canola oil.

2) Prepartaion, characterization, and evaluating a chicken bone-based solid catalyst (Li-Cb) for biodiesel production from fresh and waste canola oil.

3) Prepartaion, characterization, and evaluating a mixed metal chicken bone-based solid catalyst (Li/Zn-Cb) for transesterification of waste canola oil

4) Optimization the transesterfication process of the waste canola oil (WCO) using (Li/Zn-Cb) catalyst by Box Behnken Design method.

5) Investigate the influence of ultrasonic irradiation on transesterification of waste canola oil.

## 1.3 The significance of the work

- The mild operation conditions reduce the cost of the process by avoiding the high pressure and temperature equipments. It was reported that alkali earth metals in the catalyst structure results in mild operating temperature, thus, lithium was seleted for this purpuse after impregnated on $TiO_2$.

- Waste animal bones have been used as a catalyst for the transesterfication process with relatively limited oil covnversion. To the best of our knowledge, no detailed studies have been established for the combination of waste chicken bones with alkali earth metals (lithim) and/or amphoteric metal (zinc). Thus, the role of lithium and/or zinc loaded chicken bone in the transesterfication performance is investigated.

- Using low quality feedstock results in economic biodiesel production process. However, this kind of feedstock has a high content of water and free fatty acid which affect the process efficiency by saponification reaction in the presence of basic catalyst. So, pretrearment step is necessary to esterfiy the FFA in easterification reaction by acidic catalyst which put more cost in the process. Therefore, preparing a catalyst that could handle the esterfication and transesterfication in a single step is of great interest. Zinc is an amphoteric metal that presents the acidic and basic properties is chosen to produce biodiesel from waste canola oil.

- Many studies have been conducted to investigate the influence of ultrasonic on the homogeneous-transesterfication process. In this study we first reported the ultrasonic influence on the heterogeneous transesterfication using chicken based catalyst.

## 1.4 The structure of thesis

This thesis comprises of **8** chapters which are linked systematically in order to achieve the targeted objectives. These chapters are briefly described in the following sections, and also demonstrated in scheme 1-2:

*Chapter 1 P*rovides a general overview of the present research work which includes a brief background of the thesis topic, the main problems facing the energy demand and the alternative renewable energy, and the thesis's main objectives and structure.

*Chapter 2 C*overs the literature review of the biodiesel production processes and its fundamentals.

*Chapter 3 D*escribes the experimental methods and set-up, materials, and analytical equipment used in this study.

*Chapter 4 I*nvestigates the biodiesel production from canola oil via Li/TiO$_2$ as a solid catalyst and elaborates the kinetic of the process.

*Chapter 5 I*nvestigates the kinetic results of the lithium based chicken bone (Li-Cb) catalyst as an efficient catalyst for biodiesel production.

*Chapter 6 I*nvestigates and evaluates the efficiency of Li-Zn supported chicken bone (Li/Zn-Cb) catalyst for methyl esters production using waste canola oil. Also compare the performance of the catalyst with and without ultrasonic conditions.

*Chapter 7 O*ptimising the transesterification of the waste canola oil using Li/Zn-Cb catalyst applying Box Behnken Design (BBD) method.

*Chapter 8 I*ntroduces the main conclusions drawn from this thesis and also suggests the potential recommendations for further expanding this work.

```
                    ┌─────────────────────┐
                    │     CHAPTER 1       │
                    │    Introduction     │
                    └─────────────────────┘
                              │
                              ▼
                    ┌─────────────────────┐
                    │     CHAPTER 2       │
                    │  Literature review  │
                    └─────────────────────┘
                              │
                              ▼
          ┌──────────────────────────────────────────┐
          │              CHAPTER 3                    │
          │    Experimental Methods and Design        │
          └──────────────────────────────────────────┘
```

**CHAPTER 1**
Introduction

**CHAPTER 2**
Literature review

**CHAPTER 3**
Experimental Methods and Design

Metal oxides

Chicken bone based catalysts

Fresh oil

Waste oil

Fresh oil

Waste oil

**CHAPTER 4**

Biodiesel production from canola oil using novel Li/TiO2 as a heterogeneous catalyst prepared via impregnation method

**CHAPTER 5**

Development of a lithium based chicken bone (Li-Cb) composite as an efficient catalyst for biodiesel production

**CHAPTER 6**

Transesterfication of waste canola oil by lithium/zinc composite supported on waste chicken bone as an effective catalyst

**CHAPTER 7**

Optimization of biodiesel production from waste canola oil by response surface methodology (RSM)

**CHAPTER 9**

Conclusion and Recommendations

**Scheme 1.2.** Thesis structure.

# CHAPTER 2
# Literature Review

## 2.1 Background of biodiesel

Biodiesel is a biofuel that consists of a mixture of mono-alkyl-fatty acid esters. In contrast to fossil fuels which cause environmental damage from the emission of greenhouse gasses, biodiesel is renewable, non-toxic, sulphur-free, and biodegradable. Moreover, the sources of current conventional fuels are not sustainable. Thus, biodiesel is a promising substitute to reduce environmental pollution and address shortages of fossil fuel reserves. [12, 13]

Over the past few decades, many studies have demonstrated biodiesel production from vegetable oils and animal fats by various methods which will be discussed further in the following sections. According to Vyas et al. [14], Rudolf Diesel (1858–1913), the inventor of the diesel engine, was the first person to use peanut oil in his engine as a fuel and since then, the concept of using vegetable oil as fuel was suggested. Different types of vegetable oils were used during the Second World War in emergencies as biofuel and illustrated that this could be a potential replacement for conventional fuel [15]. The historical background of the development of the biodiesel industry is demonstrated in Table 2-1.

Although biodiesel could be synthesised from animal fats and vegetable oils, utilization of these feedstocks is controversial as they are used for human nutrition. Additionally, competition for arable land results in additional costs on biodiesel fuel [16]. The latter is the main issue facing the production and trade of biodiesel. Therefore, researchers have focused on developing techniques to reduce the cost of biodiesel production, such as employing mild operating conditions, simplifying downstream processes, and using waste feedstock, as the feedstock consists of 70-95% of the total biodiesel production cost [17, 18].

**Table 2-1:** The historical background of biodiesel industry development.

| The historic period | Occasion | Ref. |
|---|---|---|
| 1900 | Rudolf Diesel fueled his diesel engine with peanut oil | [19] |
| 1937 | "Biodiesel" term was first proposed as a concept for fuel derivatives of vegetable oil by G. Chavanne's patent | [20] |
| 1938 | The idea of reducing vegetable viscosity was presented to make vegetable oil suitable for engines | [15] |
| 1930s-1940s | For emergency situations, vegetable oils were utilized as diesel fuels | [21] |
| 1970s | US and Brazil were motivated by OPEC to begin their programs to increase the productivity of biofuel due to rising risk surrounding power security | [1] |
| 1977 | Expedito Parente, a scientist from Brazil, patented the first industrial process for the successful production of biodiesel | [22] |
| 1979 | Transesterified sunflower oil was used and refined to diesel fuel standards in South Africa | [23] |
| 1980s | PROALCOOL was a program created by Brazil's Federal Government which implemented and regulated the use of hydrated ethanol as fuel | [24] |
| 1983 | Engine-tested biodiesel was completed and published | [25] |
| 1987 | The first pilot unit was constructed in Austria | [26] |
| 1989 | The first industrial scale unit was established | [26] |
| 2000-2009 | The annual production of biofuel increased from 15.8 to 80.1 million tons | [1] |
| January 2008 | The addition of 2% of biodiesel to conventional diesel (B2) was established by the National Program for the Production and Use of Biodiesel | [6] |
| 2011 | European Union and United States produced approximately $24.7 \times 10^9$ liter/year and $4.16 \times 10^9$ liter/year, respectively | [27] |

The catalysts also play a role in the cost of biodiesel production. Waste materials such as egg shells, animal bones, and rice husks are produced daily and contribute to environmental waste. If these biowastes are utilized as cost effective catalysts for biodiesel production, production costs are reduced while simultaneously reducing their environmental impact.

In this chapter, the latest literature review related to biodiesel production methods and biodiesel feedstock and factors affecting the transesterification reaction will be discussed. Additionally, transesterification kinetics and optimization will be reported.

## 2.2 Biodiesel production methods

Biodiesel can be produced from vegetable oils or fats by various approaches (blending, pyrolysis, micro-emulsion, and transesterification), Fig. 2.1. Directly using these oils in engines without modification causes engine malfunction. The viscosity of vegetable oil is higher than diesel fuel due to the presence of glycerine in its structure [15], which results in poor fuel atomization, incomplete combustion, and carbon deposition on the injector and valve seats. One of the most common approaches used for high quality biodiesel production is transesterification [3, 15, 28].
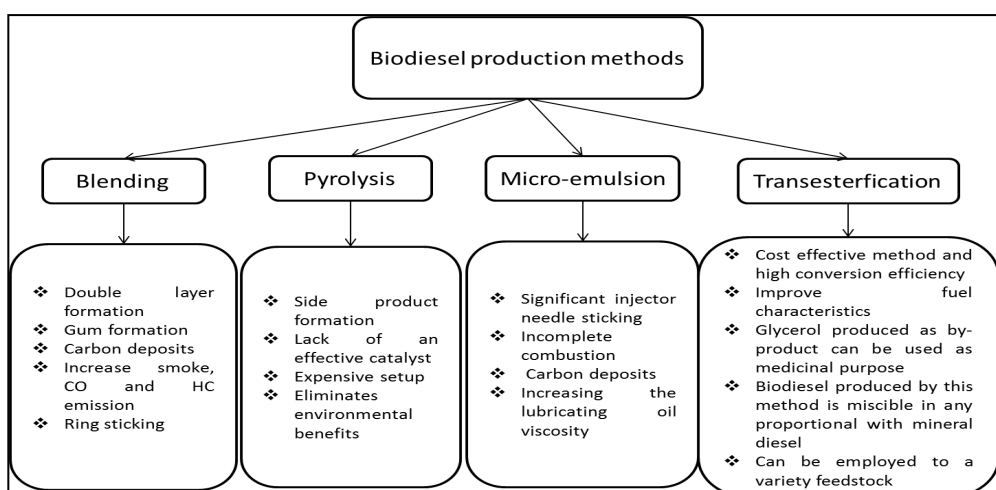


**Fig. 2.1.** Methods used for biodiesel production, adopted from Ramli et al. [18].

**2.2.1 Direct use and blending**

This method is defined as mixing or diluting the crude vegetable oil with diesel fuel to improve oil viscosity. Employing the vegetable oil directly as a fuel was discussed early in 1980. It was found that using pure food oil has some advantages owing to its heat content (80% of diesel fuel,) renewability, liquid nature-portability, and availability. However, long-term injection of diesel engines with vegetable oil causes some problems as a result of its high viscosity and lower volatility as well as its content of unsaturated hydrocarbon chains which are very reactive [29, 30].

**2.2.2 Microemulsion**

Another technique for biodiesel production is the micro-emulsion process, the aim of which is to solve the problem of the high viscosity of vegetable oil. A micro-emulsion is formed by mixing the vegetable oil with proper solvents. In this technique, solvents (methanol, ethanol, and 1-butanol) are used and investigated. Heavy carbon deposits and incomplete combustion are the main disadvantages of this technique [31].

**2.2.3 Pyrolysis**

Pyrolysis or thermal cracking process is another method for biodiesel production and it is carried out at high temperatures in the absence of $O_2$ to obtain pyrolysis products such as solid char residues, incondensable gases, and waxy liquid oil compounds. Researchers have reported contradictory observations regarding the reaction products since the paths of reaction are affected by the experimental conditions [32]. The advantages of this process are decreased processing cost, simplicity, low waste production, and no pollution [33]. The pyrolysis process is more suitable for processing waste cooking oil as stated by Ito et al [34].

## 2.2.4 Transesterification process

Transesterification is also known as alcoholysis, which is the reaction between animal fat or vegetable oil with alcohol (e.g. methanol or ethanol) to form esters and glycerol. The reaction rate is usually improved by a catalyst. Three types of catalyst could be used: alkali, acids, and enzymes [35]. It is the favored process in synthesising biodiesel since it can address and reduce vegetable oil viscosity. The main factors that affect the transesterification rate are the catalyst type, reaction temperature, alcohol: oil molar ratio, the water and free fatty acids (FFAs) content in the feedstock, and the reaction time [36]. There are numerous types of feedstock that can be used in this process.

## 2.3 Feedstock for transesterification reaction

One of the distinct advantages of biodiesel is that it can be synthesized from a wide range of feedstock sources, unlike petroleum-based fuels which are delimited to a specific geographical area. Fig. (2-2) shows the potential of biodiesel production from various sources of oil [37]. Biodiesel feedstock is divided into two major sources: conventional feedstocks which are edible oils and non-conventional feedstock which consist of non-edible oils, waste oil, and algae oil as shown in Fig. (2-3).
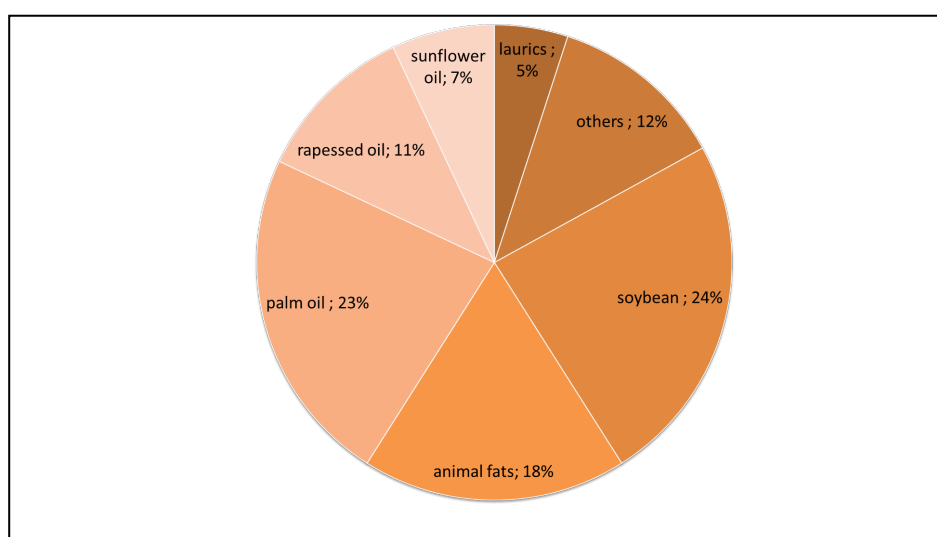


**Fig. 2.2.** Various feedstock for biodiesel production adopted from Gnanaprakasam et al.[37].
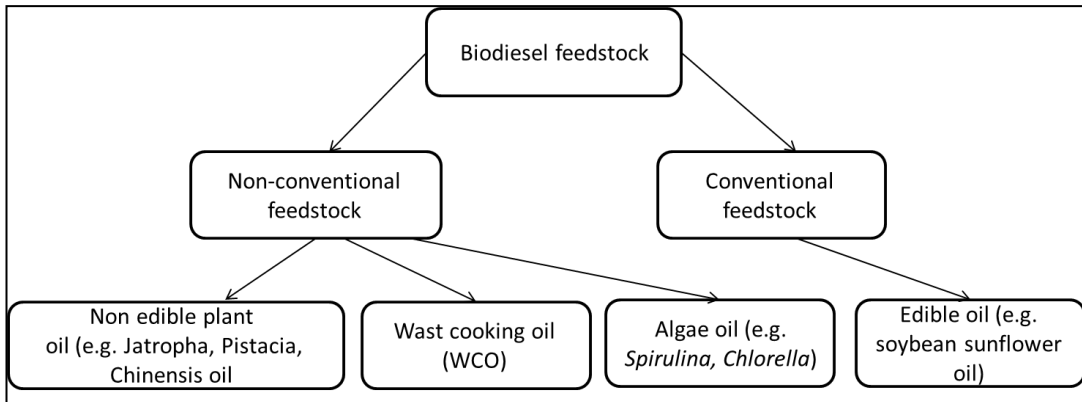
**Fig. 2.3.** The categories of biodiesel feedstock.

## 2.3.1 Edible / Conventional oils (first generation)

Conventional feedstock are edible oils which are also called "first generation feedstock," such as rapeseed, sunflower, soybean, and canola oil. This kind of feedstock is classified as first generation biofuel; it has been abundant since the commencement of agricultural trade and a simple transesterification process can be applied to this kind of feedstock [16]. About 95% of biodiesel production depends on agricultural food crops as a feedstock such as rapeseed oil (84%) and sunflower oil (13%) which represent the major contributors of edible feedstock, followed by 1% of palm oil and 2% of soybean, groundnut, coconut, peanut, corn and canola [38]. The quality of feedstock significantly affects the yield and properties of biodiesel. For instance, the composition of free fatty acid of the oil has great influence on the biodiesel properties; oils with high unsaturated acids produce unstable biodiesel as a result of oxidation. However, high content of saturated fatty acids in the feedstock produces poor cold flow properties in the resulting biodiesel which is not recommended for use in cold climates. [39]. Table 2-2 reports studies of various edible feedstock used for biodiesel production.

Using edible feedstocks for biodiesel production has sparked controversy associated with food vs. fuel and the world's food security. By raising the demand for vegetable oils, the cost

of vegetable oil-derived diesel and vegetable oil is increased, a critical factor that restricts the commercialization of biodiesel and will negatively affect the food economy [40,41]. Consequently, this issue encourages researchers to find more sustainable sources of feedstock.

**Table 2-2:** Edible feedstock for biodiesel production

| Edible Feedstock | Biodiesel production technique | Conv*; Yield ** (%) | Ref. |
| --- | --- | --- | --- |
| palm oil | Transesterification with methanol | 91.07** | [42] |
| palm oil | Transesterification with methanol | >98** | [43] |
| soybean oil | Transesterification with methanol | 99* | [44] |
| soybean oil | Transesterification with methanol | 90** | [45] |
| Safflower edible oil | Transesterification with methanol | ≈100** | [46] |
| canola oil | Transesterification with methanol | ≈100* | [47] |
| refined sunflower oil | Transesterification with ethanol | 100* | [48] |

### 2.3.2 Non-edible/ Non-conventional oils (second generation)

### 2.3.2.1 Non-edible plant oil

The plants of these feedstocks can grow in remote or waste regions, at the boundaries of arable lands, and can even be cultivated on irrigation channels so as not to compete with edible crops for human needs. Furthermore, these feedstocks are cheap, thus they could serve as the solution for reducing the cost of biodiesel. Based on the aforementioned features, these feedstocks have been considered as promising alternatives to the conventional sources [39]. Several attempts have been made to investigate biodiesel production from non-edible oils

(Table 2-3). As such, these feedstocks could reduce the need for using agricultural crops for biodiesel.

**Table 2-3:** Non-edible feedstock for biodiesel production

| Non-edible plant oil | Biodiesel production technique | Conv*/Yield **(%) | Ref. |
|---|---|---|---|
| Jatropha curcas oil | Transesterification with methanol | 75-90** | [49] |
| Jatropha oil | Transesterification with methanol | 83** | [50] |
| Jatropha curcas crude oil | Transesterification with methanol | 86.51** | [51] |

## 2.3.2.2 Domestic waste cooking oil (WCO)

Increasing global human populations and greater utilization of fast food restaurant chains have resulted in greater food consumption but also led to increasing amounts of food waste, particularly waste cooking oil, which is often incorrectly dumped into the environment due to poor strategies in managing this waste. This has resulted in damage to the environment, particularly to the aquatic environment as a consequence of pouring the waste cooking oil down the kitchen sink and then to sewage streams [52]. For instance, in China, waste cooking oil is disposed to water streams or soil. It is clear that employing WCO as an alternative feedstock for conventional biofuel feedstocks has both environmental and economic advantages, contributing to the effective management of waste cooking oil and improving biodiesel production which has a dual-impact: reducing the biodiesel production cost and reduction of greenhouse gas emissions from petroleum fuel [53]. Table 2-4 presents studies of waste oil based fuels. Thus, domestic waste cooking oil could be a potential source for biodiesel production at low cost.

**Table 2-4:** Waste cooking oil (WCO)-based biodiesel

| Waste oils | Biodiesel production technique | Yield (%) | Ref. |
|---|---|---|---|
| waste cooking oil | Transesterification with methanol | 97.71 | [54] |
| waste cooking oil | Transesterification with methanol | 90 | [55] |
| waste cooking oil | Transesterification with methanol | 93.1 | [56] |
| waste frying oil | Transesterification with methanol | 95.5 | [57] |
| used cooking oil | Transesterification with methanol | 93.6 | [58] |
| waste cooking oil | Transesterification with methanol | 91.4 | [59] |

### 2.3.3 Algae oil (third generation)

While second generation feedstock is a promising feedstock for biodiesel production, it is unlikely to be a sufficient source for all biodiesel production. Algae offer an interesting substitute as a renewable and sustainable fuel. Microalgae have been massively studied during the mid 70's as a non-edible based biodiesel feedstock. Microalgae have several benefits in comparison with crop feedstock which can be summarized as follows: (1) They are photosynthetic microorganisms which produce higher rates of biomass; (2) High rates of growth and high content of oil; (3) No demand for land as they can survive in non-arable lands and in saltwater, or even in wastewater [60]. Increasing lipid content of microalgae, culturing of algae, and characterization of algae biomass are currently of interest to researchers to demonstrate the potential of microalgae as an attractive substitutional feedstock for biodiesel production [61, 62]. Table 2-5 summarizes some studies regarding producing biodiesel from algae oil.

**Table 2-5:** Algae oil-based biodiesel

| Algae oil | Biodiesel production technique | Conv.*/Yield **(%) | Ref. |
|---|---|---|---|
| *Spirulina* | Extraction and transesterification by hexane as a solvent in a single stage | 79.50** | [63] |
| *Oedogonium* | Transesterification with methanol and sodium hydroxide | 98** | [65] |
| *Spirogyra sp* | As above | 95** | [65] |
| *Spirulina sp.* | In situ transesterification with toluene as a co-solvent | 76** | [66] |
| *Chlorella* | Acid-catalyzed in situ transesterification process | 92* | [68] |

## 2.4 Non-catalytic transesterification process (supercritical process)

In this process, the transesterification reaction is conducted without catalyst and under high temperature and pressure exceeding the critical points, for instance, the supercritical temperature for methanol is 240 ºC [69, 70]. Typically, the temperature of the supercritical reaction is more than 250 ºC, where under such severe conditions methanol in the liquid phase will be in the critical state where gas and liquid properties become indistinct [71]. This process has some advantages in comparison with the catalytic process, such as high production efficiency and simplified post process, since no catalyst separation step is needed [72]. Nevertheless, high temperature, pressure, and alcohol: oil molar ratios are required and the process should be carefully controlled. Rathore & Madras [73] demonstrated biodiesel production from edible and non-edible oils with the supercritical process. In their experiment, ethanol and methanol were studied to optimise the reaction conditions. They demonstrated that 50:1 molar ratio of alcohol: oil leads to the maximum oil conversion into methyl and ethyl esters at 300 ºC and 200 bar. The conversion under the aforementioned conditions was increased from 70% in 10 min to 85% in 40 min. However, higher conversion was observed

in the supercritical state of ethanol rather than methanol which was attributed to the solubility of ethanol which is closer to that of oil. Kiss et al. [74] investigated the effect of ethanol and methanol in the supercritical transesterification process for biodiesel production from rapeseed oil. At 42:1 alcohol to oil ratio and reaction temperature of 350 ºC, the highest conversions for methanol and ethanol were observed after 15 min of reaction time. In the case of methanol, the yield (93%) was 2% higher than the yield of ethanol (91%), however, the reaction pressure of ethanol (10MPa) was lower than the reaction pressure of methanol (12MPa). It was concluded that the effect of reaction conditions on the supercritical transesterification yield is as follows: temperature> time> pressure. The technology of non-catalytic transesterification is a promising alternative to make biodiesel production a robust and cost-effective process in the future.

## 2.5 Catalytic transesterification process

### 2.5.1 Alkaline (Base) catalysis

Numerous studies have been published on the transesterification reaction by basic homogeneous catalysts. Sodium hydroxide, potassium hydroxide, sodium methoxide, and potassium methoxide are intensively utilised as alkaline catalysts in the transesterification process. Generally, these catalysts are highly reacted under soft reaction conditions of temperature and pressure [4]. The mechanism of alkaline-catalysed transesterification reaction is shown in Scheme (2-1) [75]. The mechanism is summarized in the following four steps:

1. Producing the active species ($RO^-$) and protonated catalyst ($BH^+$) from the reversible reaction between the base catalyst and alcohol (ROH);

2. Nucleophilic attack of alkoxide ion (RO⁻) to the carbonyl group (COOR) in the triglyceride molecule (TG);

3. Formation of a tetrahedral intermediate which breaks down to form fatty acid alkyl esters (FAAE) and diglyceride ion;

4. Catalyst regeneration step involving the deprotonation of $BH^+$ by diglyceride ion to generate diglyceride (DG) and the catalyst (B).

The above steps will be repeated to the diglycerides (DG) and monoglycerides (MG), respectively, to conclude with formation of one molecule of glycerol (GL) and three molecules of alkyl esters.

Vicente et al. [76] demonstrated a comparison study of the activity of the most common basic homogeneous catalysts. These catalysts are sodium methoxide, potassium methoxide, sodium hydroxide, and potassium hydroxide which were employed to convert sunflower oil to biodiesel in a batch reactor. The FAME yield was nearly 100 % for $NaOCH_3$ and $KOCH_3$, however, it was lower for NaOH and KOH (85.9 and 91.67 wt. %, respectively). The losses in yield for the hydroxides were due to the saponification of triglyceride and dissolving of esters in glycerol [76]. Leung and Guo [77] applied methoxides and hydroxides of potassium and sodium (as base catalyst) for the transesterification reaction and they found that sodium hydroxide was the superior catalyst. However, base homogeneous catalyst results in soap formation due to the saponification reaction of free fatty acids (FFAs) that makes it unsuitable for feedstock with high FFAs and water content. Furthermore, the purification of biodiesel is difficult due to gel formation from soap that incurs biodiesel production additional cost and energy consumption [16, 78]. This problem can be addressed either by pretreatment of feedstock or by using acid homogeneous catalysts.
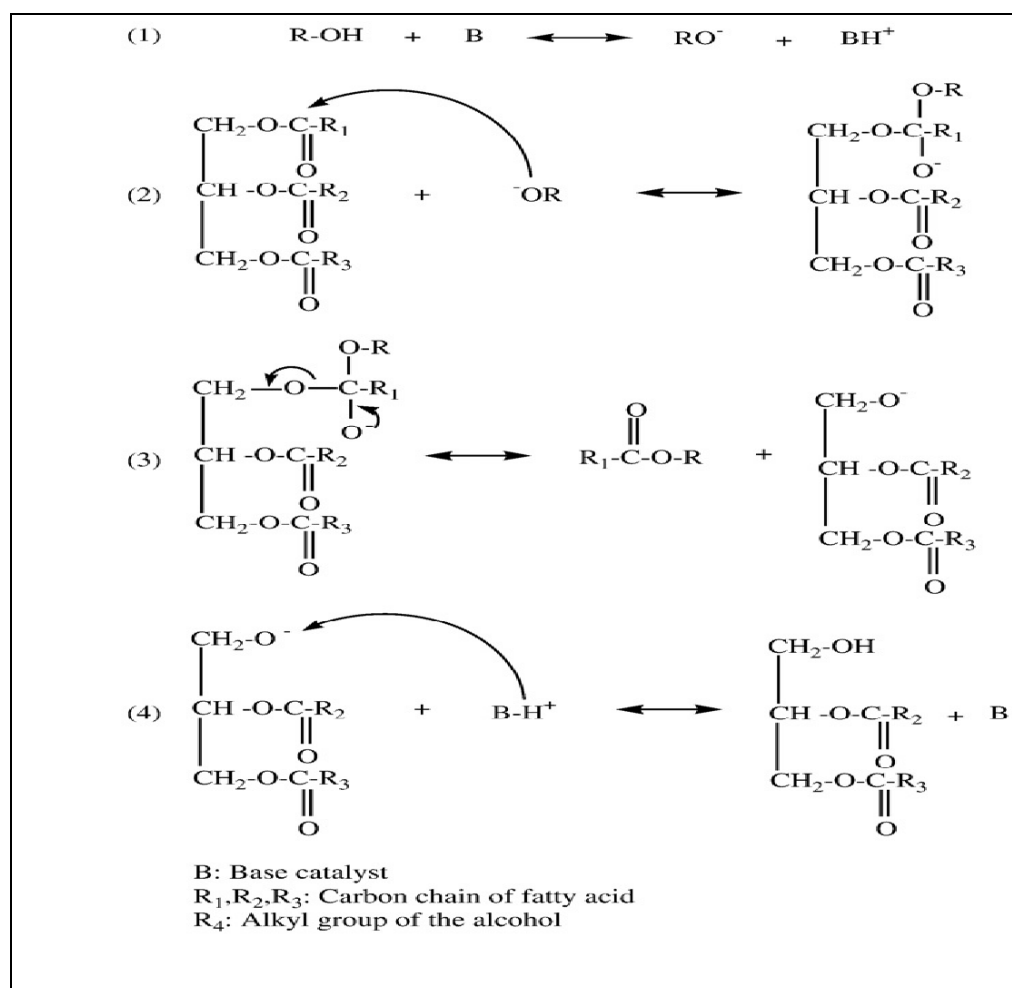
Scheme 2.1. Mechanism of homogeneous alkaline-catalysed triglyceride transesterification (adopted from Atadashiet al. [75].

## 2.5.2 Acidic catalysis

The most common acid catalysts include sulfuric acid, sulfonic acid, hydrochloric acid, organic sulfonic acid, ferric sulfate, etc. Unlike basic catalysts, they are suitable for feedstocks with high levels of water (i.e. $\geq 0.3$wt %) or FFAs (i.e. $\geq 0.5$wt %) [79, 80]. In addition, both esterification and transesterification reactions could be carried out simultaneously by acid catalysts [81]. The mechanism of soluble acid catalysis is illustrated in Scheme (2-2). The reaction pathway of transesterification in the presence of acid catalyst begins with the increased electrophilicity of the contiguous (adjoining) carbon atom as a

result of the carbonyl group protonation which exposes the carbonyl group of triglycerides to nucleophilic attack by alcohol to liberate intermediate molecules/moieties. The last step is dissociation of a tetrahedral intermediate and reactivation of the catalyst to generate diglyceride and ester. The sequence of the aforementioned steps is repeated to the diglyceride and monoglyceride to finally liberate glycerol (GL) accompanied by moieties of the fatty acid alkyl ester [82].
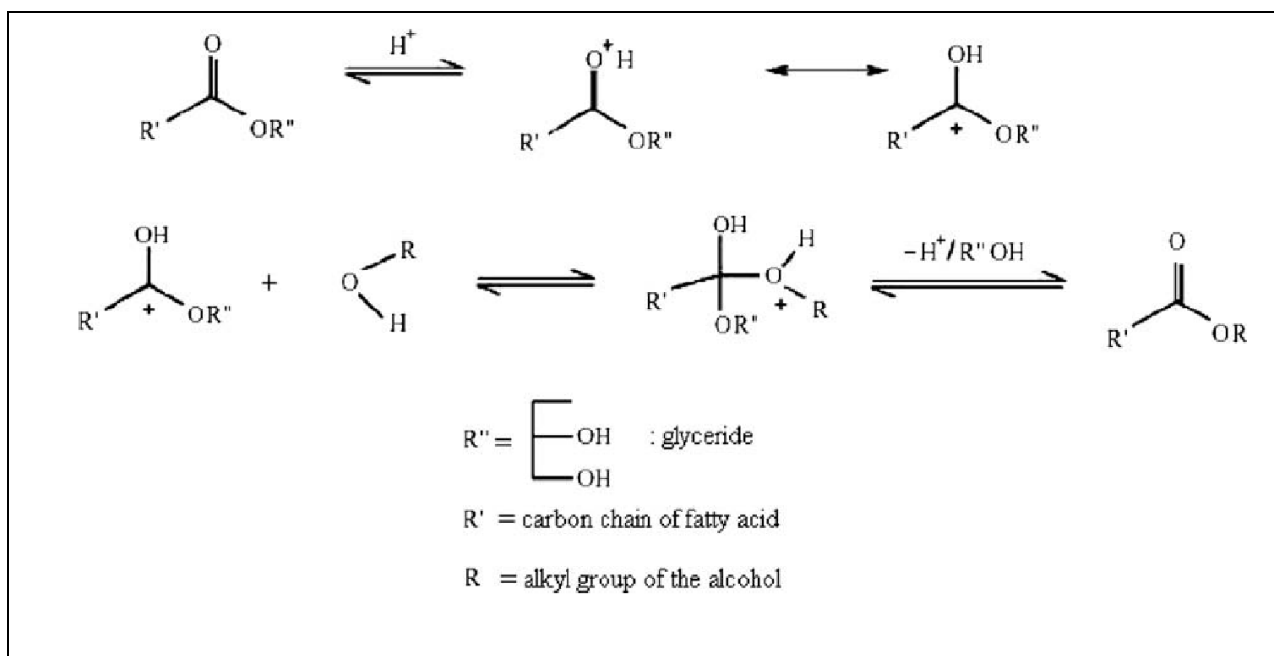


**Scheme 2.2.** Mechanism of homogeneous acid-catalysis for the triglyceride transesterification [83].

Among acid catalysts, sulfuric acid is popular in the acid-catalysed reaction from low grade oil or high free fatty acids oil due to its low cost [78]. It was reported that the main influencing factor in the acid-catalysed transesterification is alcohol to oil molar ratio and the reaction can be accelerated by adding excess amounts of alcohol [83, 84]. Thus, the acid-catalysed reaction requires harsh conditions such as long reaction time, high amounts of methanol, and high temperature, which in turn limits its application in the industrial scale in addition to causing reactor corrosion issues [75]. Table 2-6 presents previous studies on the homogeneous-catalysed biodiesel production. In summary, the solubility of homogeneous

catalyst increases the cost of biodiesel production as a result of the need for downstream processes to remove the soluble catalysts and purify the product. Solid (heterogeneous) catalysts may offer a substitute to overcome the issues related to the soluble (homogeneous) catalysts.

**Table 2-6:** Previous studies on the homogeneous-catalysed biodiesel production

| Base homogeneous catalyst | Conv.*/Yield** (%) | Ref. |
|---|---|---|
| potassium hydroxide (KOH) | 98.7 | [85] |
| sodium hydroxide (NaOH) | 85.3** | [77] |
| sodium methoxide (CH$_3$ONa) | 89** | [77] |
| **Acid homogeneous catalyst** | | **Ref.** |
| sulfuric acid (H$_2$SO$_4$) | 99** | [86] |
| methanesulfonic acid (CH$_3$SO$_3$H) | >90* | [87] |

## 2.6 Heterogeneous catalyst

Numerous studies have investigated various heterogeneous catalysts for enhancing biodiesel production under different operational conditions, such as reaction time, temperature, methanol amount, and catalyst loading.

### 2.6.1 Acid solid catalyst

The acid heterogeneous catalysts are suitable for feedstock with high acid value and water content which have the ability to stimulate the esterification and transesterification process to produce fatty acid alkyl ester. Table 2-7 shows some of the acid solid catalysts that have been

used in transesterification. These catalysts exhibit some drawbacks in the presence of a significant content of water as this prompts the hydrolysis reaction as a result of high interaction between water and the active sites [88].

## 2.6.2 Base solid catalyst

The use of base solid catalysts has an interesting advantage in biodiesel production by simplifying the production and purification processes. The cost of the production process could be reduced by applying the solid base catalyst which is recycled for future reactions and is easy to separate from the final product, with no need for washing the product to separate the catalyst. Batch or continuous process can be applied for this kind of catalyst [89]. Alkaline earth metal oxides (CaO, MgO, SrO, BaO, ZnO) are examples of the base solid catalysts that have been used for biodiesel production. Scheme (2-3) depicts the mechanism of CaO as an example of the heterogeneous base catalysed transesterification [75]. The mechanism of base solid catalyst is similar to the base soluble catalyst and was previously explained in section **2.5.1.** However, the affinity of this kind of catalyst towards moisture and water during storage is the catalyst's main drawback.
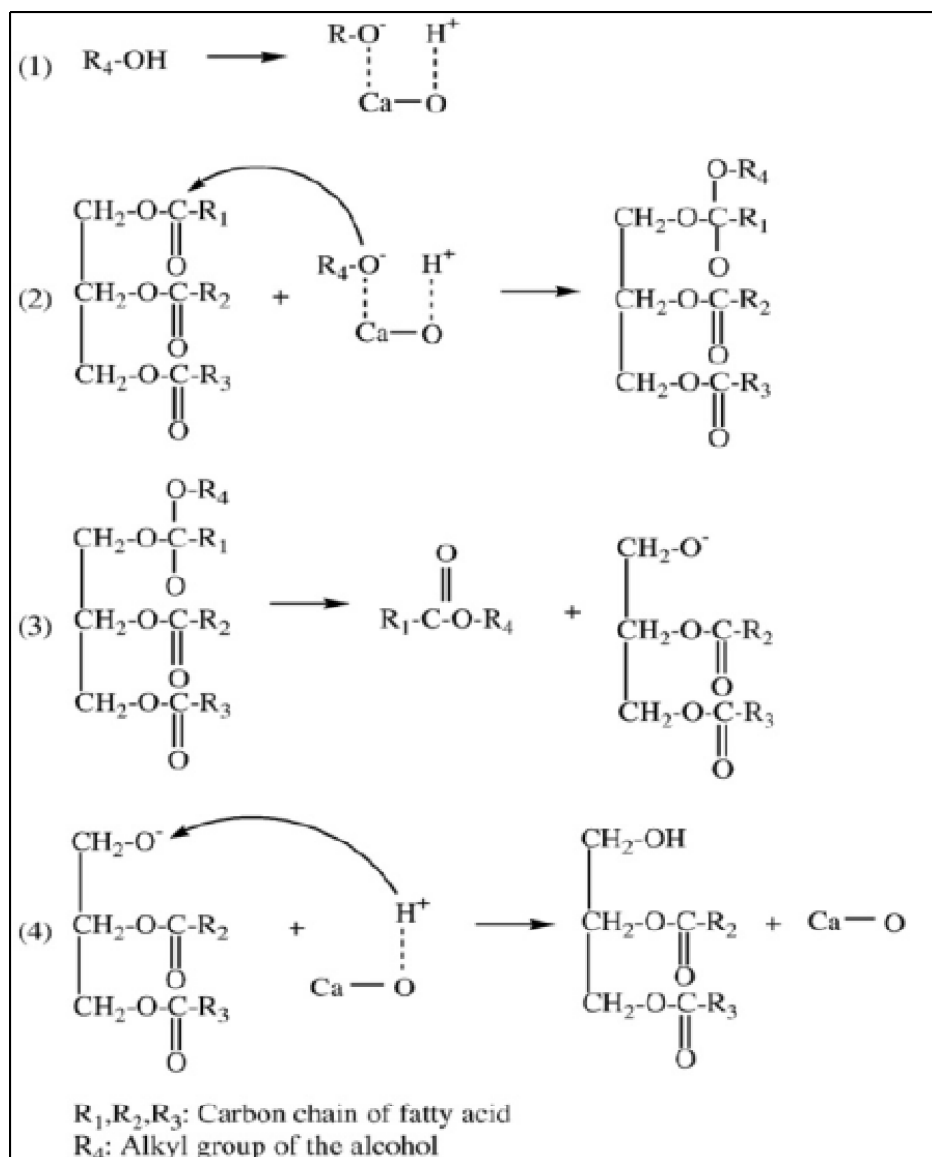
**Scheme 2.3.** The reaction mechanism of CaO in heterogeneous base catalyzed transesterification (reproduced from Atadashiet al. [78]).

Additionally, soap can be generated if the feedstock contains high FFAs thus reducing the process efficiency [80, 90]. Table 2-7 illustrates some investigations for the solid base catalyst.

**Table 2-7:** Solid base and acid catalysed transesterification

| Solid acid catalyst | Conv.*/ Yield ** | Ref. |
|---|---|---|
| $SO_4{}^{2-}/TiO_2$ (ST) | 97** | [91] |
| sulfonated graphene catalyst (GR-SO$_3$H) | 98** | [43] |
| chromium-tungsten (CrWO$_2$) | 86* | [92] |
| Sono-Sulfated zirconia nanocatalyst supported on MCM-41 (S-ZrO$_2$/MCM-41) | 96.9* | [93] |
| sulfonated ordered mesoporous carbon (OMC-SO$_3$H) | 73.59* | [94] |
| **Solid base catalyst** | **Conv.*/ Yield**** | **Ref.** |
| calcium oxide (CaO) | 95** | [95] |
| magnesium oxide (MgO) | 95* | [96] |
| strontium oxide (SrO) | 93* | [97] |
| MgO-KOH-20 | >98* | [98] |
| KOH/Al$_2$O$_3$ | 91.07** | [42] |

## 2.7 Mixed metal oxides

Several types of mixed metal oxides have been applied to biodiesel production such as Ca-La, Mg-Zn, CaMgO, Mg–Al and CaZnO. The literature reports that combination with other oxides such as rare earth, alkali, alkali earth or transition oxides leads to improvement of the catalyst physio-chemical properties and the catalyst structure as compared to the bulk metal oxide [55, 99, 100]. There are different methods for fabricating the mixed metal oxides (MMOs) such as co-precipitation and impregnation which are used in this work. The co-precipitation method has been adopted by several researchers for catalyst preparation [50, 51, 101, 102]. For instance, Mg-Zn mixed metal oxide catalysts with different Mg/Zn atomic ratios (0.5-10.0 at. %) were synthesised by the co-precipitation method.

Generally, the procedure is outlined as follows. First, the corresponding metal precursors ($Mg(NO_3)_2.4H_2O$ and $Zn(NO_3)_2.6H_2O$) are dissolved in deionized water under mixing to obtain a homogeneous solution. Then, the resulting solution is precipitated by the basic solution of $NaOH/Na_2CO_3$ (pH 10). The resulting solid precipitate is then filtered, washed, and allowed to dry at 100 ºC overnight. Thermal treatment is then required to obtain samples by calcination at different temperatures (in this case 800 ºC for 6 h) to obtain the mixed oxides [50].

Another fabrication method is impregnation [103, 104]. Kaur & Ali [105] have prepared the nanocrystalline lithium ion impregnated CaO catalyst (Li/CaO). In the preparation, calcium oxide (10 g) was suspended in deionized water (40 mL) and to this solution, an aqueous solution of $LiNO_3$ (10 mL) of desired concentration was added. The resulting slurry was then mixed for 2 h, evaporated to dryness, and heated at 120 ºC for 24 h. Different observations were reported regarding the effect of the preparation method on the catalyst structure and thus its impact on catalyst activity. For example, Lertpanyapornchai & Ngamcharussrivichai [99] have posited two synthesising methods for two mesoporous Sr–Ti mixed oxides (MST) which are the evaporation-induced self-assembly (EISA) method and sol–gel combustion (SGC) method. Both catalysts achieved high yield of FAME (>99.9 wt. %) when palm kernel oil was transesterified at different reaction temperature: (SGC) =170 ºC and (EISA) =150 ºC, respectively, and retaining other parameters (at molar ratio methanol:oil = 20:1, catalyst loading = 10 wt. % and reaction time = 3 h). However, MST–SGC activity reduced gradually during the reusability test as compared to MST–EISA which exhibited more tolerance to free fatty acids and water content in the feedstock. Conversely, leached metal species were observed from MST–EISA causing a significant homogeneous contribution and loss of basicity and catalytic efficiency after the first cycle. Table 2-8 summarises some mixed metal oxides used for fatty acid alkyl esters production. Additionally, the composition and the

operation conditions of the synthesized catalyst have an impact on its activity in converting triglyceride (TG) to biodiesel during the transesterification process. Wan et al. [106] have investigated the effect of the molar ratio of Mn/Zn on the performance of $MnCO_3/ZnO$ catalyst for FAMEs produced from soybean oil. It was found that triglyceride (TG) conversion and FAME yield were positively affected by Mn/Zn molar ratio. The triglyceride (TG) conversion and FAME yield were increased by insertion of Mn in comparison with only utilizing Zn complex, the conversion and yield were 25.6% and 18.22%, respectively. Mn/Zn molar ratio of 1:1 resulted in the highest efficiency, a slight reduction in the process efficiency was noticed with increasing Mn/Zn molar ratio. Moreover, the calcination temperature and time were optimised and found to be 573 K and 0.5 h, respectively.

**Table 2-8:** Mixed metal oxides (MMOs) for biodiesel production

| Mixed metal oxides (MMOs) | Preparation method | Conv.*/ Yield**(%) | feedstock | Ref. |
|---|---|---|---|---|
| Magnesium–lanthanum mixed oxide Mg/La (ML-3) | Co-precipitation | 100* | Sunflower oil and Jatropha oil | [107] |
| Mg-Zn | $CO_2$ precipitation (Mg3Zn1CO2ppt) | 90* | soybean oil | [101] |
| Potassium impregnated mixed oxides of lanthanum and magnesium (LaMg-3@10) | Co-precipitation | 96* | used cotton seed oil | [102] |
| Mg–Al mixed oxides | Thermal pre-treatment of hydrotalcite-like precursors at 450 ºC | 78** | rapeseed oil | [108] |
| Li/MgO and Li/Mg(Al)O | Impregnation | __ | Vegetable oil | [109] |
| Zn–Al | Co-precipitation | 76** | soybean oil | [110] |
| Ca/Zr mixed oxide (CaO/ZrO$_2$) | birch-templating route | 92.6** | rapeseed oil | [111] |

A novel β-potassium dizirconate (β-$K_2Zr_2O_5$) catalyst was prepared by the solid state reaction method. Among the various molar ratios of Zr/K (0.25:1, 0.50:1, 0.75:1, 1:1 and 1.25:1), 1:1 Zr/K molar ratio resulted in the highest conversion of 96.85 % in the transesterification reaction after reflux time of 2 h, reaction temperature of 65 ºC, and waste frying oil: methanol molar ratio of 1:10 at catalyst dosing of 4.0 wt. % [112]. Xie et al. [113] have synthesised $Fe_3O_4$/MCM-41/ECH/$Na_2SiO_3$ catalyst. It was found that $Fe_3O_4$/MCM-41 support was not active for TG conversion by the transesterification reaction as no FAME product was detected even after 10 h of reaction time. However, the magnetic $Fe_3O_4$/MCM-41 support was active when sodium silicate was loaded on it (97.4 % of oil conversion was achieved). The optimum conditions (3 wt. % of the catalyst, a methanol: soybean oil molar ratio of 25:1, and methanol reflux for 8 h of reaction time) resulted in high catalytic activity (conversion of 99.2 %).

## 2.8 Biocatalyst (Enzymatic biodiesel production)

There are notable issues surrounding chemical heterogeneous catalysts such as leaching issues during the reactions [16]. Therefore, enzyme catalysts have emerged as an alternative to chemical catalysts (base and acid). Lipases are the most common enzymatic catalysts. Catalysts can convert triglycerides and FFAs from varied feedstock to biodiesel by transesterification and esterification. The purity of the product from the enzymatic process is greater than for other catalytic processes. In addition, the enzymatic process is eco-friendly, producing less wastewater [16,4]. Biodiesel formation by applying enzyme catalysts has been investigated by many researchers using solvent and solvent-free system reactions. There have been several studies in the literature reporting enzyme transesterification in solvent-free systems, and also the effect of solvent on the stability and activity of the enzyme. Table 2-9

summarises some studies that deal with the enzyme catalyst in the solvent and solvent-free reactions. However, enzyme catalysts are expensive and can easily be deactivated so their use remains limited.

**Table 2-9:** Different investigated enzymes for biodiesel production.

| Enzyme | Solvent system | Conv.*/ Yield** (%) | Ref. |
|---|---|---|---|
| Novozyme 435 | solvent free | >99* | [114] |
| Lipozyme TL IM | solvent free | 81.73** | [115] |
| *Candida cylindracea* lipase | solvent free and tert-butanol solvent | 54.4** 71.6** | [116] |
| *Burkholderia* lipase | Hexane solvent | >90* | [117] |
| *Pseudomonas cepacia* | Solvent free | 98** | [118] |
| *Rhizopus orzyae* | Solvent free | 88–90** | [119] |
| combination of Lipase AY and Lipase AK | Solvent free | 89** | [120] |
| Novozyme 435 | Solvent free | 94.58** | [121] |
| *Rhizopus oryzae* | Solvent free | 80** | [122] |
| *Candida antarctica* lipase | *t*-butanol solvent | 97** | [123] |
| *Candida sp.* | Hexane solvent | 96* | [124] |

## 2.9 Natural and waste sources of catalyst

Different biowaste resources have been used as cost effective catalysts for biodiesel production via transesterification that make the cost of biodiesel production lower than that produced by other chemical catalysts. Recently, researchers have shown an increased interest in various natural materials as sources of calcium oxide. Viriya-Empikul et al. [125] investigated and compared the catalytic activities of industrial waste shells of egg, golden

apple snail, and meretrix venus for FAMEs production. The transesterification reaction of palm olein oils under the conditions of temperature = 60 ºC, methanol/oil molar ratio = 18:1, and catalyst dosage = 10 wt. % for 2h, resulted in conversion of 94.1 %, 93.2 %, 92.3 % for egg shell, golden apple snail shell, and meretrix venus shell, respectively. The descending activity was attributed to decreases of surface area and basicity of the strong base sites. Bet-Moushoul et al. [126] utilized five different sources of calcium oxide (CaO) (commercial CaO, egg shell, mussel shell, calcite, and dolomite) as a support for gold nanoparticles and proved their feasibility/ability as heterogeneous catalysts for sunflower oil transesterification for FAMEs production. The impregnation method was used to deposit the Nano gold particles on the CaO catalysts. The range of 90–97% conversion was obtained for all prepared samples after 3 h of reaction, 9:1 of $CH_3OH$: oil molar ratio, at 65 ºC of reaction temperature in the presence of 3% of catalyst. The authors also examined the significance of calcination temperature on catalyst activity in the conversion of waste mussel and egg shells to CaO after 4 hr of thermal treatment at various temperatures (600–900 ºC). Moreover, it was found that the quality of biodiesel produced from supported gold Nanoparticles (AuNPs) catalysts was higher than the biodiesel produced from commercial CaO catalysts.

Recent developments in the field of natural derived heterogeneous catalyst have led to a renewed interest in chicken bone based solid catalyst. Biodiesel production was studied by employing solid catalysts derived from waste chicken bones [127]. In this study, waste cooking oil was the feedstock in the transesterification reaction. The selected calcination temperature was 900°C, which exhibited a maximum FAME yield of 89.33% at the experimental conditions of 4 h of reaction time, methanol:oil molar ratio of 15:1, 65 ºC reaction temperature, catalyst dosage 5 wt. %, and mixing speed 500 rpm. This study showed that active basic site density on the catalyst surface as a result of optimal calcination temperature could be the reason for the high catalytic activity of prepared catalyst.

Suwannasom et al. [128] have synthesised and verified the effect of transesterification parameters for biodiesel production from waste cooking oil (WCO) with the use of waste chicken bone as a catalyst in the reaction. The calcium carbonate content in the waste chicken bone was converted to calcium oxide (CaO) at a calcination temperature of 800°C. Under the optimum conditions of catalyst concentration 3.0 wt. %, methanol to oil ratio of 3:1, and reaction temperature of 80 °C for 3 h, the maximum yield was achieved (96.31%).

The potential of wood ash as a heterogeneous catalyst for methyl esters synthesis was studied [129]. In this investigation, wood ash ($W_0$), calcined wood ash, and activated wood ash catalysts were prepared and their activity evaluated by ester conversion from Jatropha oil in the transesterification process. Wood ash itself is an alkaline substance in which the calcium phosphate silicate ($Ca_2SiO_4.0.05-Ca_3(PO_4)_2$) is the main component. It was found that alkalinity and the calcination treatment define catalyst activity. The activated wood ash with $K_2CO_3$ (99%) showed higher catalytic activity in comparison to calcined wood ash (98.7%) and $CaCO_3$ activated wood ash (91.7%) under the following conditions: 1:12 oil to methanol ratio, 5 mass fraction % catalyst dosage, and 3 h reflux time. Moreover, the produced methyl ester-based Jatropha oil was compatible with the ASTM D-6751 standards of biodiesel (FAMEs). Table 2-10 shows various sources of waste material used as catalyst for developing a cost effective biodiesel production process.

**Table 2-10:** Various sources of waste material as a catalyst in the transesterification

| Waste material | Derived catalyst | Feedstock | Conv.*/Yield** (%) | Ref. |
|---|---|---|---|---|
| chicken egg shell | CaO | Palm oil | 92* | [130] |
| quail egg shell | CaO | Palm oil | >98* | [131] |
| dolomite | $CaMg(CO_3)_2$ | Canola oil | 91.78** | [132] |
| calcite | $CaCO_3$ | palm kernel oil (PKO) | 46.8** | [133] |
| sheep bone | Hydroxyapatite | Palm oil | 96.78* | [134] |
| Rohu fish bone | $\beta$-$Ca_3(PO_4)_2$ | Soybean oil | 97.73** | [135] |
| mud crab *(Scylla serrata)* | CaO | Palm olein | 98.8* | [136] |
| shrimp | KF-CaO | Refined rapeseed oil | 89.1* | [137] |

## 2.10 Assisted techniques for the transesterification process

Many techniques are available to assist the transesterification process for biodiesel production, such as ultrasonic technique, hydrodynamic cavitation, ultra and high shear in-line and batch reactors, and microwave technique. In hydrodynamic cavitation (HC), cavitating conditions identical to acoustic cavitation are produced, which greatly aid in mixing immiscible liquids [138].  Furthermore, hydrodynamic cavitation has the potential for scaling-up in industrial-scale operations [139]. In ultra and high shear in-line or batch reactors, FAME could be produced in continuous, semi-continuous, and batch modes. Significant reduction in production time and increase in production volume can be achieved by this method [140].

In the microwave technique, the region of microwave radiation is located between infrared radiation and radio-waves. As reported by Marra et al. [141, the polar molecules are continuously oscillated by the absorbed microwave energy which cause heat generation as a consequence of the collisions and friction between the oscillated molecules, which leads to

raising the sample temperature and achieving high yield in a short time [142,143]. Ultrasound is defined as an oscillating sound with a high frequency (20 kHz and 100 MHz) exceeding human hearing limitation (16 and 18 kHz) [14,144]. The diffusion of sound waves through the liquid phase expands and compresses the medium space between the molecules. Thus, ultrasonic cavitation occurs, which is the formation, growth and collapse of micro-fine bubbles continuously in the liquid that is ultrasonically irradiated, thus, causing the formation and generation of shockwaves that enhance both energy and mass transfers in the liquid [145]. The ultrasound-assisted technology has been widely utilized in different areas of biological and chemical reactions because of its effect on improving the mass transfer between immiscible liquid–liquid interfaces in the solid reaction [138]. The ultrasound technique was applied in this work as an assisted technology for biodiesel production.

The influence of ultrasonication on transesterification for biodiesel production from various oil feedstocks has been investigated. Deshmane and Adewuyi [146] demonstrated the benefits of using ultrasound in comparison with magnetic stirring for the calcium methoxide-catalysed transesterification of soybean. Under ultrasound irradiation, more than 90% conversion was obtained at 65 °C reaction temperature using 1 wt. % catalyst loading and 9:1 methanol to oil molar ratio in 90 min. Ultrasonic cavitation enhanced the reaction rate and consequently reduced the reaction time from 150 min to 90 min.

Pukale et al. [147] have evaluated the effect of ultrasonic irradiation on the transesterification of waste cooking oil using different solid catalysts ($K_3PO_4$, $Na_3PO_4$, $Na_2HPO_4$, $NaH_2PO_4$, $KH_2PO_4$). Among the investigated catalysts, $K_3PO_4$ showed a high biodiesel yield (92%) under the optimum reaction conditions of oil to methanol molar ratio 1:6, catalyst loading of 3 wt. %, and reaction temperature of 50 ºC. The comparison study between sonication and conventional stirring illustrated that the high transesterification efficacy using ultrasound was

achieved from improving emulsification and mass transfer in the reaction mixture. Some reported studies regarding the effect of ultrasound are summarized in the Table 2-11.

**Table 2-11:** Previous reported ultrasonication studies for biodiesel production.

| Sonicat ion type | Freque ncy (kHz); power (W) | Feedsto ck | Catalyst type; loading (wt. %) | Temper ature (°C) | Alcohol type; alcohol to oil molar ratio | React ion time (min) | Conv.*; Yield ** (%) | Ref. |
|---|---|---|---|---|---|---|---|---|
| sonicati on bath | 40 kHz; 200W | Waste soybean oil | $H_2SO_4$; 3.5 | 60 | Methanol; 9:1 | 60 | 99.9* | [148] |
| sonicati on bath | 25 kHz; 210W | Palm fatty acid distillat e | $H_2SO_4$; 5 | 60 | Isopropano l; 5:1 | 275 | 75* | [149] |
| sonicati on by horn | 24 kHz; 200W | Cotton seed oil | NaOH; 2 | 60 | Methanol; 7:1 | 20 | 95* | [[150] |
| sonicati on by horn | 24 kHz; 200W | Sunflo wer oil | NaOH; 2 | 60 | Methanol; 7:1 | 20 | 95* | [151 |
| sonicati on bath | 20 kHz; 120W | Fatty acid odour | Zirconium-supported chlorosulfonic acid; 1 | 40 | Methanol;1 0:1 | 300 | 75* | [152] |
| sonicati on by horn | 20 kHz; 400W | Jatroph a oil | Activated carbon-supported tungstophosph oric acid; 4 | 65 | Methanol; 20:1 | 40 | 87.33* | [153] |
| sonicati on bath | 40 kHz; 160W | Palm oil | CaO; 3 | 65 | Methanol; 6:1 | 120 | 90* | [154] |
| sonicati on bath | 20 kHz; 130W | Palm, corn, Canola, sunflow er oils | SrO; 2.55 | 65 ± 2 | Methanol; 9:1 | 30.7 | 94* | [155] |

## 2.11 Factors affecting transesterification

### 2.11.1 Reaction temperature

The kinetics of the transesterification reaction are greatly affected by the reaction temperature. Higher temperature can lead to high biodiesel yield. The yield is expected to increase until reaching the optimum reaction temperature value [156]. When the reaction is carried out at a temperature lower than the boiling point of methanol (64.7 ºC) or ethanol (78 ºC), the reaction should be conducted with a reflux condenser to avoid alcohol evaporation [157]. Moreover, the conversion decreases if the reaction temperature becomes close to the alcohol boiling point due to the formation of alcohol bubbles which result in inhibition of the mass transfer over the interface of reactant phases [158]. Kumar and Ali [159] have investigated the effect of reaction temperature for transesterification of three types of oils (waste cotton seed oil (WCO), Jatropha oil (JO) and Karanja oil (KO) in the presence of 3.5-K-CaO catalyst (potassium ion impregnated calcium oxide) under atmospheric pressure. It was found that although there was conversion at 35 ºC, the reaction time was relatively longer, and increasing the reaction temperature from room temperature to 65 ºC resulted in reducing the reaction time and increasing the conversion. A high-pressure reactor is required when the reaction is carried out at high temperature exceeding the boiling point of alcohol. It was found that raising the reaction temperature from 60 ºC to 180 ºC increased the conversion of triglyceride (TG) from 18% to 99% as a result of changing methanol's physicochemical state [44].

### 2.11.2 Reaction time

Adequate contact time between reagents is required so the reactants can reach the active sites of the catalyst and for conversion to occur [160]. Hailegiorgis et al. [161] have investigated

biodiesel production in situ transesterification of methanol and Jatropha curcas L oil in the presence of phase transfer catalyst (PTC). Benzyltrimethylammonium hydroxide (BTMAOH) was used as a PTC in their study. It was found that the reaction time was highly affected by the phase transfer catalyst whereas, the reaction time was reduced to half (3.5 to 1.5 h) when BTMAOH as PTC was used with NaOH catalyst and the yield increased from 47.9% to 91.2%. Girish et al. [162] studied the effect of reaction time during the transesterification of waste frying oil (WFO) via employing natural white bivalve clam shells as a source of CaO catalyst after thermal treatment at 900 ºC for 4 h. The results revealed that the yield was improved when the reaction period was increased from 1.5 h to 3 h and the maximum yield was 95.84% at the reaction conditions of catalyst dosage of 8 wt. %, 18:1 methanol/oil molar ratio, and reaction temperature of 65 ºC. In addition, it was observed that the yield was decreased when reaction time was extended further, due to the formation of soap. The operating conditions were optimized by Dai et al. [163] for the transesterification reaction for methyl esters production via $LiALO_2$ catalyst. The results showed that the production was affected by the reaction time and the highest yield (97.5%) was after 2h of reaction at 65 ºC, catalyst amount was 6% (w/w), and methanol/oil molar ratio of 24:1.

## 2.11.3 Catalyst dosage

Catalyst dosage has a positive effect on the transesterification product. Increasing the catalyst dosage results in increasing the biodiesel production, however, the yield decreases or levels off beyond the optimum value of catalyst dosage due to soap formation, increasing the reaction mixture viscosity, or reaching the equilibrium state [164]. Table 2-12 shows the effect of catalyst dosage from previous investigations.

Liu et al. [111] have investigated the effect of catalyst dosage of $CaO/ZrO_2$ mixed oxide $C_{0.3}Z(T)$ in the range of 2-12 wt.%. Increasing the catalyst dosage from 2 to 8 wt. % led to increasing biodiesel yield from 74.6 to 90.5%. However, beyond 8 wt. % of catalyst dosage, the yield was reduced as a result of increasing the viscosity of the reaction mixture.

**Table 2-12:** Influence of catalyst dosage from previous investigations.

| Catalyst | Catalyst dosage (wt. %) | Optimum dosage (wt. %) | Conv.*/Yield** (%) | Ref. |
|---|---|---|---|---|
| KOH supported on palm shell activated carbon (KOH/AC) catalyst | 10.29 - 57.56 | 30.3 | 98.03** | [165] |
| BA (boiler ash) | 1, 3, 5 and 10 | 3 | 90* | [166] |
| KI/mesoporous silica | 2.5, 5 and 7.5 | 5 | 90* | [167] |

**2.11.4 Alcohol to oil molar ratio**

Theoretically, 3:1 represents the minimum molar ratio of alcohol to oil for complete conversion of triglyceride. However, because transesterification is a reversible reaction, an adequate amount of methanol should be available through the transesterification reaction to enhance the forward reaction. In addition, heterogeneous catalysed transesterification involves different phases, thus, the reaction rate is slow. Therefore, to achieve biodiesel production in shorter time, higher molar ratios of alcohol to oil are applied and investigated in many studies [168]. Table 2-13 demonstrates the influence of alcohol: oil molar ratio on biodiesel production.

**Table 2-13:** Impact of alcohol: oil molar ratio on biodiesel production.

| Alcohol type | Molar ratio range | Catalyst | Optimum value | Conv.*/ Yield** (%) | Ref. |
|---|---|---|---|---|---|
| methanol | 6:1-9:1 | palm oil mill fly ash supported calcium oxide | 12:1 | 98.30* 75.73** | [169] |
| methanol | 12:1-50:1 | 20-CeO$_2$/Li/SBA-15 | 40:1 | >98** | [170] |
| methanol | 6:1-12:1 | Sol-gel derived meso-porous hydrotalcites (HT) | 9:1 | 91.2* | [171] |
| methanol | 6:1, 9:1, 12:1, 15:1, 18:1 | KF/CaO | 12:1 | >90** | [172] |

## 2.11.5 Quality of the oil feedstock

The efficiency of the base catalysed transesterification process is affected by the quality of the feedstock, wherein the existence of water and/or free fatty acid (FFA) in the feedstock promotes the saponification reaction and in turn inhibits triglyceride (TG) conversion. Water causes the hydrolysis of triglyceride (TG) and results in free fatty acid (FFA) and glycerol (GL) as illustrated in equation (2-1), while the presence of FFA leads to soap formation as a consequence of the reaction of FFA with basic catalyst (see equation 2-2).

$$TG + 3H_2O = GL + 3FFA \qquad\qquad (2\text{-}1)$$

| R-COOH | + | NaOH | = | R-COONa | + | H$_2$O | (2-2) |
|---|---|---|---|---|---|---|---|
| Free fatty acid | | Sodium hydroxide | | Soap | | Water | |
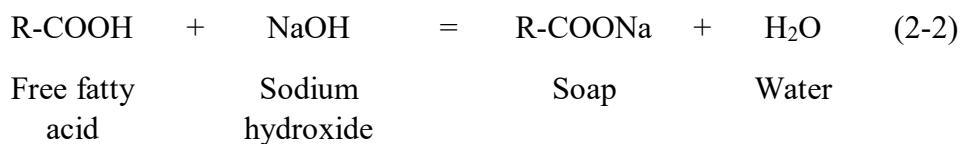
Soap interferes with the separation of fatty acid alkyl esters and thus reduces the FAMEs content [173]. Therefore, studying the effect of water and FFA content is essential. Yan et al. [174] have demonstrated the influence of FFA and water on the activity of the prepared $Zn_3La_1$ catalyst. Edible soybean oils with different concentrations of oleic acid and water were investigated to assess the impact of water and FFA on the reaction yield. The addition of FFA (oleic acid) resulted in shortening the reaction time required to reach a high FAME yield. For instance, the reaction time was decreased from 60 min to 20 min by addition of 5.20% FFA with a yield of 96.6%, which was maintained at 96.0% with further addition of 30.56% FFA. By contrast, water addition extended the reaction time by an additional 30 min with 3.12% addition of water (60 min of reaction time without water addition). Mutreja et al. [102] found the conversion was decreased from 97.6% to 96% and the reaction time was prolonged from 15 min to 20 min with increasing the FFA and water concentrations in used cotton seed oil from 0.2% FFA and 0.12 wt. % water to 0.8% FFA and 0.19 wt. % water, while increasing the water content from 1% to 2% resulted in decreasing the conversion from 95% to 90%. Hindryawati et al. [173] investigated the tolerance of $Li_2SiO_3$, $Na_2SiO_3$ and $K_2SiO_3$ catalysts to the addition of water and FFA. The recorded findings revealed that these catalysts can tolerate up to 1.25% free fatty acid and up to 1.75% water. Thus, the FFA and water content have a great influence on the transesterification reaction.

## 2.12 Kinetic studies of transesterification

The kinetics of transesterification are important for process design and for describing the rate of the chemical reaction [175]. Thus, researchers have investigated the reaction kinetics of transesterification and determined the kinetic parameters (reaction rate constant ($k$), frequency factor ($A$), activation energy ($Ea$)). Consequently, the relationship between

reaction temperature and time were studied for this purpose to understand their influence on the reaction rate. The combined contribution of chemical reaction and physical steps forms the heterogeneous reaction. Fig. 2.4 illustrates the steps of heterogeneously catalysed fluid reaction; these steps are summarised as follows [176]:

1) Diffusion of the starting materials (such as oil and alcohol) through the boundary layer to the catalyst surface.

2) Diffusion of the starting materials into the pores (pore diffusion).

3) Adsorption of the reactants on the inner surface of the pores.

4) Chemical reaction on the catalyst surface.

5) Desorption of the products from the catalyst surface.

6) Diffusion of the products out of the pores.

7) Diffusion of the products away from the catalyst through the boundary layer and into the fluid phase.

The surface reactions and methanol adsorption are reported as the rate determining steps for the heterogeneously catalysed reaction [96,177,178].
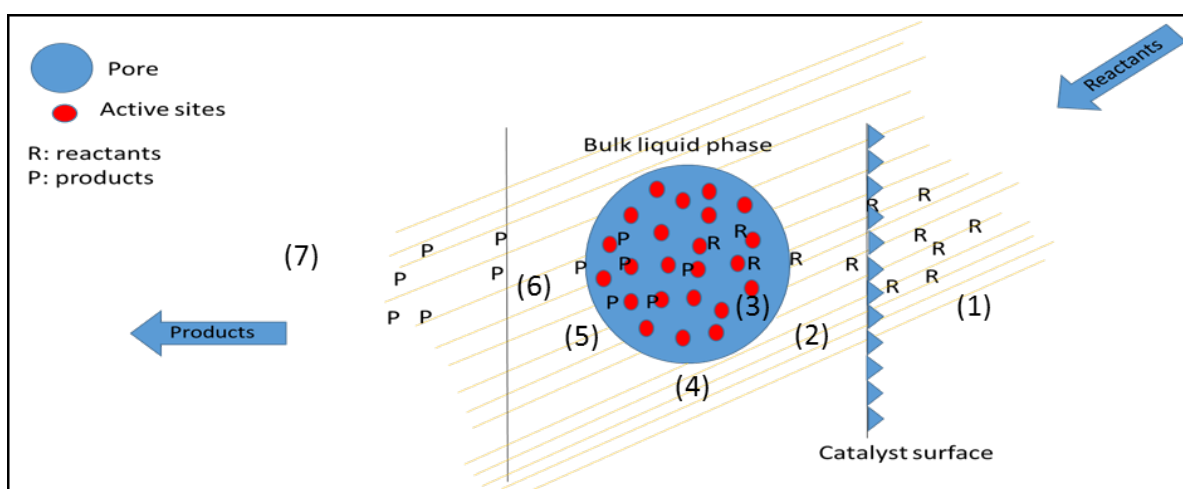


**Fig. 2.4.** Mechanism of the heterogeneous catalysed system.

Generally, the transesterification reaction is carried out by reacting vegetable oils or animal fats with a short chain of acyl acceptor in the presence of a catalyst. Thus, the overall reaction is expressed as follows:

$$A + 3B \overset{k1}{\underset{k2}{\leftrightarrow}} C + 3D \qquad (2-3)$$
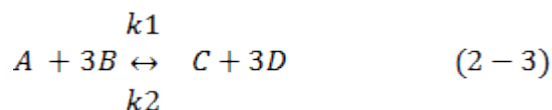
Where A is the oil; B is the alcohol; C is the glycerol, D is the fatty acid alkyl ester, $k1$ is the forward reaction rate constant and $k2$ is the reverse reaction rate constant. The step of rate determination begins with the three stepwise reversible reactions that are involved in the transesterification process. The reaction proceeds via the formation of the alkoxide species from the adsorption step of the proton in the hydroxyl group of alcohol by the catalyst surface. Then, the nucleophilic attack on the carbonyl carbon of triglyceride (TG) is started by alkoxide species to finally elaborate three molecules of fatty acid methyl esters (biodiesel) and one molecule of glycerol through the whole reaction cycle (see Fig. 2.5).
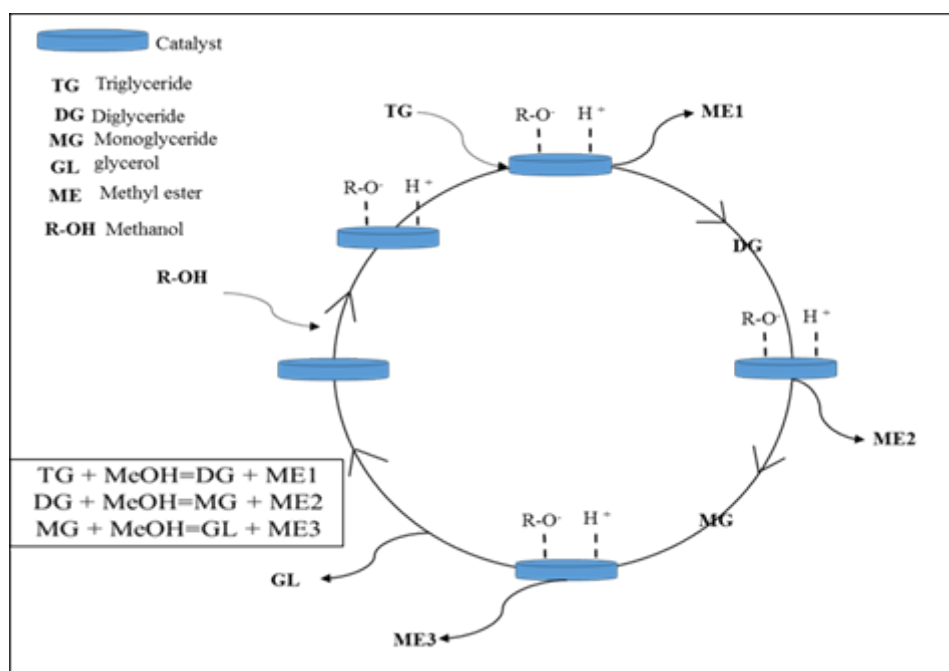


**Fig. 2.5.** The transesterification reaction scheme.

The transesterification reaction requires three moles of alcohol to react with one mole of oil according to Eq. (2-3). Transesterification is a reversible reaction, so excess alcohol is necessary to drive the forward reaction towards the formation of fatty acid alkyl esters [179]. Table 2-14 shows the kinetic order determined in some previous studies. Generally, the kinetic equation of the reaction can be described as below:

$$r = \frac{d[A]}{dt} = k_1[A][B] - k_2[C][D]^3$$

(2-4)

**Table 2-14:** The kinetic order of previous studies of heterogeneous catalysed transesterification.

| Catalyst | Feedstock | Kinetic order | Ref. |
|---|---|---|---|
| calcined snail shell | waste frying oil | First order | [180] |
| CaO | sunflower oil | Pseudo first order | [181] |
| CaO | waste cooking oil | Pseudo first order | [182] |
| Zr/CaO catalyst | Jatropha curcas oil | Pseudo first order | [183] |
| mesoporous alumina supported potassium (MAK) catalyst | canola oil | Pseudo first order | [184] |
| ZnO/TiO$_2$ catalyst | waste cooking oil | Pseudo first-order | [185] |
| zeolite Linde type A (zeolite LTA) | soybean and palm oils | Pseudo first order | [186] |

## 2.13 Optimization by Response Surface Methodology (RSM)

The traditional method for optimization is usually carried out by a one-dimensional manner so that different values of one parameter are experimentally carried out to obtain the optimum values. Therefore, finding the optimal values of many parameters is both cumbersome and inaccurate, since the interaction between the independent parameters is not considered. Conversely, statistical optimisation is a parsimonious method since chemicals and time are saved by keeping the number of experiments at the minimum rate. Response Surface

Methodology (RSM) is a cost effective method frequently used for optimization and experimental design [187].

**Table 2-15:** Previous studies of FAME production by Response Surface Methodology (RSM)

| RSM | Optimized Factor | Response factor | Ref. |
|---|---|---|---|
| CCD tool | Catalyst concentration, reaction time, oil: methanol molar ratio and reaction temperature. | Biodiesel yield | [189] |
| CCD tool | $X_{CL}$: precursor dosage $Ni(NO_3)_2 \cdot 6H_2O$, $X_{FR}$: flow rate of methanol, and $X_{CT}$: calcination temperature | Conversion of FFA | [190] |
| CCD tool | methanol to oil molar ratio ($x_1$), reaction time ($x_2$) and amount of catalyst ($x_3$) | biodiesel yield | [191] |
| BBD tool | reaction time, amount of catalyst, and methanol-to-oil molar ratio | FAME content | [192] |
| BBD tool | catalyst loading, ethanol to cottonseed oil molar ratio and reaction temperature | cottonseed oil conversion | [193] |
| BBD tool | methanol/oil molar ratio ($X_1$) amount of catalyst ($X_2$) and total reaction time ($X_3$) | *Jatropha curcas* oil conversion | [194] |

Response Surface Methodology (RSM) is a mathematical technique and a statistical analysis which is useful for the optimization of reaction parameters and allowing for a comprehensive understanding of correlations among the experimental parameters [188]. The response parameter (dependent variable, i.e. FAME conversion) is affected by several independent process parameters and this technique is useful to determine the most impactful parameter in a particular experimental design [187]. Central composite design (CCD) and Box-Behnken Design (BBD) are design tools of RSM. CCD and BBD tools have been applied widely for optimization of the transesterification reaction for efficient FAME production. These methods have proven its feasibility to predict the most significant parameters that greatly

affect the process of biodiesel production to achieve the maximum yield. In this work, the BBD tool will be applied to optimise three factors: catalyst dosage, methanol to waste canola oil ratio, and reaction temperature at fixed time of 3.5 h to predict the oil conversion to FAME. Table 2-15 shows previous optimization studies for biodiesel production using Response Surface Methodology (RSM).

## 2.14 Summary

This chapter shed light on many different aspects of the transesterification process such as the types of feedstock as well as catalytic and non-catalytic transesterification processing. A distinct advantage of biodiesel production is the sheer variety of various feedstocks that could be employed to synthesise biodiesel. Biodiesel feedstock can be categorized into three generations. The first generation is the edible or food grade oil that results in good quality biodiesel product, however, competition with human food increases its cost and limits its use. The second generation is non-edible oil which encompasses non-edible plant oil and waste domestic oil. The third generation is algae oil which offers an interesting substitute with the potential for providing renewable and sustainable fuel.

Subsequently, the transesterification process under the supercritical state was reviewed, where the reaction could be carried out without catalyst, but a high amount of alcohol as well as high pressure and temperature reaction conditions are required. Next, the most common transesterification process, the catalytic method, was discussed. The catalysts used in the catalytic transesterification process are broadly defined as homogeneous and heterogeneous catalysts. The homogeneous catalysts include base and acid catalysts, whose usage incurs some disadvantages related to post reaction processing, such as catalyst separation (as the catalyst is soluble) and the huge amount of wastewater generation for the neutralizing step

which increases the cost of the biodiesel production process. These disadvantages encouraged the development of insoluble solid catalysts to facilitate the separation process. This chapter then focused on the base solid catalytic process and the source of the solid catalyst. Mixed metal oxides which, a type of base catalyst, have demonstrated better stability and activity in the transesterification for FAME production in comparison with the bulk metal oxide. The effect of various factors on the transesterification process were discussed in detail. This chapter also discussed the kinetics of the triglyceride catalytic transesterification process. Finally, optimization by Response Surface Methodology (RSM) and its benefits in reducing experiment numbers and improving the accuracy of predictions of optimizing experimental conditions was discussed.

# CHAPTER 3

# Materials and Experimental Methods

## 3.1 Introduction

This chapter describes the materials, laboratory equipment and experimental methods utilized to carry out the research study. The used materials are provided in Section 3.2 of this chapter. The catalyst preparation and characterization are described in Sections 3.3 and 3.4. Section 3.5 details the experimental set-up and Section 3.6 illustrates the investigated parameters. The reusability is detailed in the Section 3.7. The analytical methods used to analyze the collected samples are discussed in Section 3.8.

## 3.2 Materials

### 3.2.1 Chemicals and oil feedstock for transesterfication reaction

In addition to anhydrous methanol (99.8%) which was purchased from Thermo Fisher Scientific Australia Pty Ltd, two different oil qualities were used as a feedstock canola oil which was obtained from local shopping Centre (Coles) in Australia and waste canola oil which was collected from local restaurant. The physico-chemical properties and fatty acid profile of the feedstock are tabulated in the Table 3-1.

### 3.2.2 Chemicals for catalyst preparation

The chemicals used for catalyst preparation were Titanium (II) oxide, Lithium nitrate ($LiNO_3$) and Zinc nitrate hexahydrate ($Zn(NO_3)_2.6H_2O$) which were purchased from Sigma-Aldrich Pty Ltd, and utilized without further purification. Waste chicken bone was collected from household environment.

### 3.2.3 Chemicals for analysis

For gas chromatography analysis (GC), the analytical standards (such as n-hexane (95%) as a solvent) were obtained from Sigma-Aldrich Pty Ltd, FAMEs mixture standard (C4 –C24), and methyl octanoate as internal standard to identify and quantify methyl ester conversion in the transesterification.

**Table 3-1:** The physico-chemical properties and fatty acid profile of the feedstock.

| Property | Fresh canola oil | Waste canola oil |
| --- | --- | --- |
| Saponification value (mgKOH/g) | 187 | 234 |
| Acid Value (mgKOH/g) | 0.072 | 3.67 |
| Specific gravity | 0.9457 | 0.9388 |
| Water content (wt. %) | 0.95 | 1.6 |
| Oleic acid (wt. %) | 56 | 21.9 |
| Linoleic acid (wt. %) | 26 | 54 |
| Linolenic acid (wt. %) | 10 | 6 |
| Palmitic acid (wt. %) | 4 | 8 |
| Stearic acid (wt. %) | 2 | 6.1 |
| Erucic acid (wt. %) | 2 | 4 |

For acid value analysis, chemicals used were potassium hydroxide, ethanol, isopropanol alcohol, and phenolphthalein indicator obtained from Ajax Finechem Pty Ltd, Chem Supply, Acros and Fisher, respectively.

Ethanol, ether, potassium hydroxide and HCL which obtained from Chem Supply, Merck, Ajax Finechem Pty Ltd and Thermo Fisher, respectively, were used to determine the saponification value.

To determine the basic strength, Hammett indicators were used which are Neutral red ($H_- =$ 6.8), bromothymol blue ($H_- = 7.2$), phenolphthalein ($H_- = 9.8$), 2, 4-dinitroaniline ($H_- = 15.0$) and 4-nitroaniline ($H_- = 18.4$) which purchased from Sigma-Aldrich Pty Ltd.

## 3.3 Catalyst Preparation

The method that was adopted in the catalyst preparation was the wet impregnation method. Briefly, the method involves mixing a designed weight of the metal precursors with deionized water followed by mixing for a certain period of time at room temperature. Then, the resulted slurry was dried in the oven and the obtained dried samples were thermally treated in the muffle air furnace to produce the oxides.

## 3.3.1 Lithium based titanium dioxide catalyst (Li/TiO$_2$)

Lithium impregnated TiO$_2$ catalysts for transesterification reactions were prepared by a wet impregnation method. In a typical catalyst preparation procedure, the required amount of lithium nitrate (LiNO$_3$) was suspended in deionized water using ultrasonic bath, and titanium dioxide was slowly added into the aqueous solution. The resulted slurry was mixed for 4 h at room temperature using magnetic mixer, and then evaporated to dryness by hot plate (at 50 °C for 30 min. then the temperature was risen to 70 °C for another 30 min) and heated overnight at 120 ºC and finally calcined at 450, 600 and 750 ºC for 4 h under air flow in muffle furnace. Similarly, a series of catalysts with different amounts of LiNO$_3$ (20, 30, 40 wt. %) were prepared in order to get the final lithium concentration in the range of 20- 40 wt. %. The obtained samples were calcined at different temperatures (450, 600, and 750 °C) and denoted as x-LT-y where, x symbolizes lithium amounts and y symbolizes calcination

temperature, for example 30LT600 means 30 wt. % of lithium loaded on $TiO_2$ and calcined at 600 ºC. Fig. 3.1 show the preparation procedure.
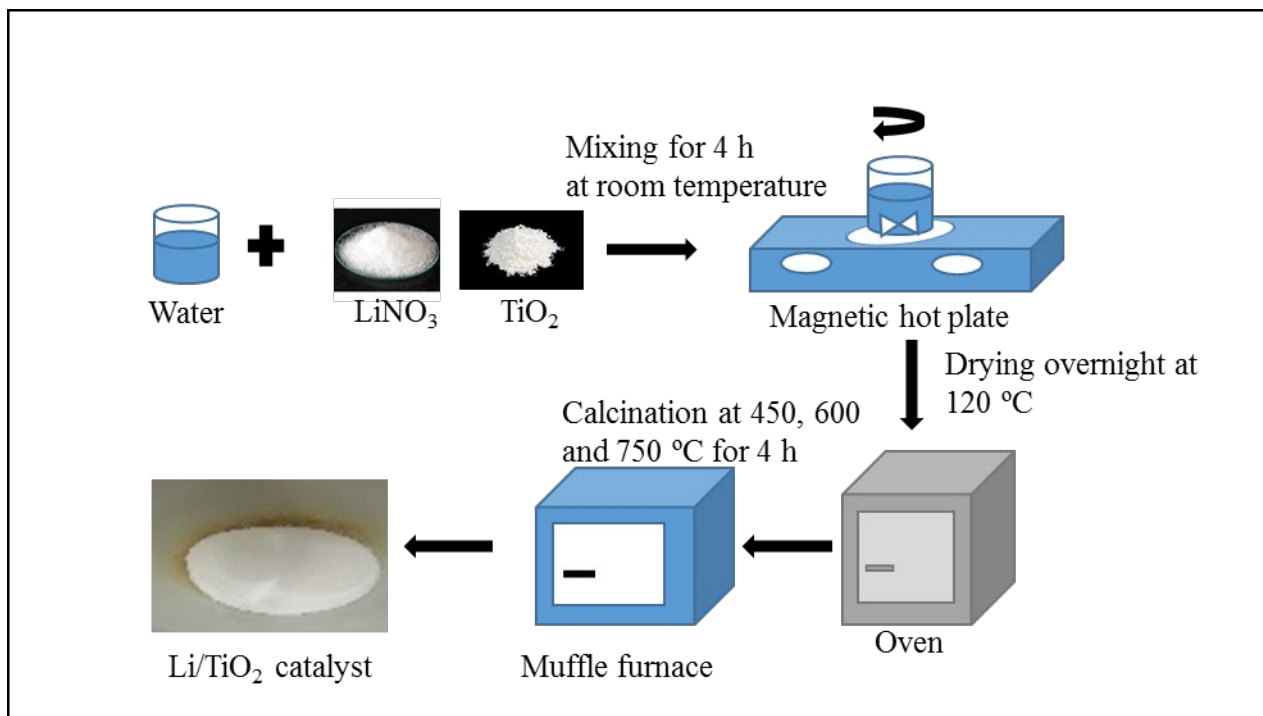


**Fig. 3.1**. The $Li/TiO_2$ catalyst preparation procedure.

### 3.3.2 Lithium chicken bone-based catalyst (Li-Cb)

The preparation method of chicken bone was adopted from reported method Znad & Frangeskides [195]. The waste chicken bones were boiled at 200 ºC to remove the attached organic materials (meat, collagen and fat) away. Subsequently, the chicken bones (Cb) were washed thoroughly with ultra-pure water ($H_2O$) and allowed to dry in the oven at 75 ºC overnight. The Cb then finely pulverized by a mortar and pestle. The obtained Cb powder was then sieved to get particle size ≤150 μm and stored in a clean glass container in the desiccator to avoid atmospheric moisture. The lithium ion impregnated on chicken bones (Li-Cb) were prepared by a wet impregnation method (see Fig. 3.2). A specific amount of chicken bone (Cb) of 7 g was suspended in distillated water using ultrasonic bath, and various

amounts (0 - 3 g) of lithium nitrate (LiNO$_3$) were slowly added into the aqueous solution. The resulted slurry was homogenized for 4 h at room temperature using a magnetic mixer, and then it was slowly evaporated to dryness on hot plate at 100 ºC overnight and finally calcined at different temperature (750 to 900 ºC) for 4 h under air flow in muffle furnace. The obtained samples were denoted as x-Li-Cb-y where, x represents lithium nitrate amounts (g) and y refers to calcination temperature, for example 1Li-Cb900 means 1 g of lithium nitrate loaded on Cb and calcined at 900 ºC.
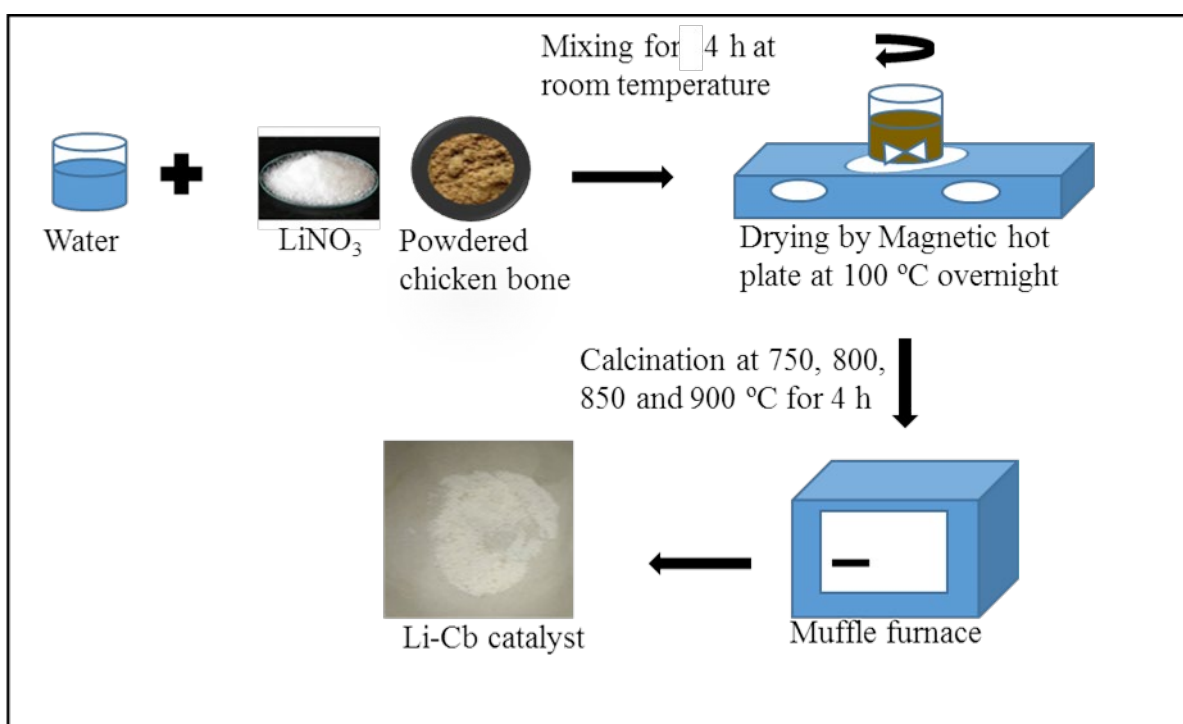


**Fig. 3.2**. The Li-Cb catalyst preparation procedure.

### 3.3.3 Mixed oxide (lithium/ zinc) based chicken bone catalyst (Li/Zn-Cb)

Three catalysts based on chicken bone were prepared by wet impregnation method, Lithium-based chicken bone (Li-Cb), Zinc-based chicken bone (Zn-Cb) and Lithium/ Zinc-based chicken bone (Li/Zn-Cb). The waste chicken bone was pre-treated according to method as

described elsewhere [195]. Then, Li-Cb, Zn-Cb and Li/Zn-Cb were synthesized. In brief, the required amount of lithium nitrate and zinc nitrate hexahydrate individually (Li and Zn) or combined (Li/Zn) were suspended in deionized water using ultrasonic bath, then 7 g of chicken bone powder (Cb) was slowly added into the aqueous solution. The resulted slurry was mixed for 4 h at room temperature using magnetic stirrer (500 rpm), and then evaporated to dryness by hotplate and heated overnight at 100 ºC, and finally calcined at 850 ºC for 4 hours under air flow in muffle furnace. The preparation method is shown in Fig. 3.3.
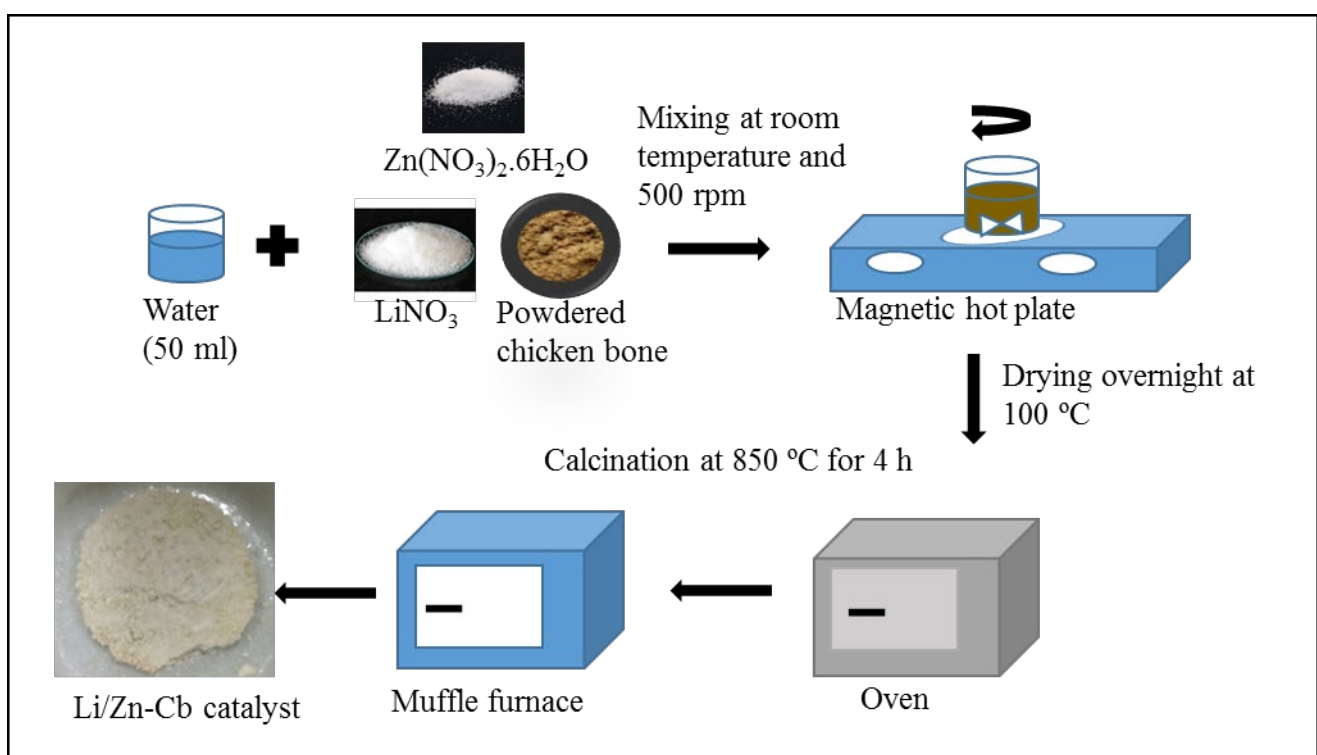


**Fig. 3.3.** The Li/Zn-Cb catalyst preparation procedure.

### 3.4 Catalyst characterization

The prepared catalysts were characterized by several techniques to investigate the texture properties of the catalyst. These techniques are FTIR, XRD, TGA/DSC, FE-SEM, Surface area, and the basicity of catalyst.

### 3.4.1 Fourier Transform-Infrared (FTIR)

The functional groups of the prepared catalysts were determined using Fourier-transformed infrared (FTIR) spectroscopy (shown in Fig. 3.4). Each sample of a catalyst as a powder was placed in the sample holder and pressed for direct analysis. The spectra were obtained via (Perkin Elmer spectrum 100) FT-IR spectrometer in the wavelength range from 400 to 4000 $cm^{-1}$ and 4 scans were carried out for each sample.
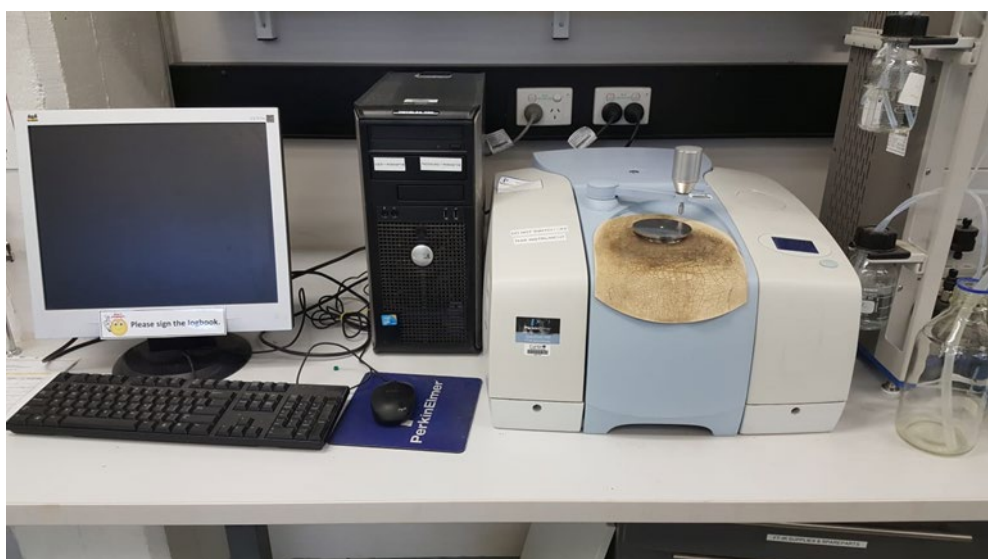


**Fig. 3.4.** Fourier-transformed infrared (FTIR) spectroscopy**.**

### 3.4.2 X-ray diffraction analysis (XRD)

The crystallography of the synthesized catalyst samples was identified by XRD. The X-ray diffraction analysis was performed on a Bruker D8 X-ray diffractometer (Bruker AXS, Germany), with a copper K alpha ($\lambda= 1.5418$ $^0A$) radiation source (40kV & 40mA) with a Lynx Eye detector. The scan parameters used were: $2\Theta$ scan range from 10-80 degree and total scan time of 1hr.

### 3.4.3 Thermo gravimetric/ differential scanning calorimetry analysis (TGA/DSC)

Uncalcined sample was analyzed by the thermo gravimetric (TGA) analyzer to investigate the thermal transition of the prepared catalyst. The analysis was performed using METTLER TOLEDO TGA/DSC 1 STAR$^e$ System under the Argon flow rate of 60 ml/min over the temperature range of 35 to 1000 ºC at a ramping rate of 10 ºC/min. Prepared catalysts were weighted and placed into an alumina pans that were automatically analyzed in sequence.

### 3.4.4 Field emission scanning electron microscope analysis (FE-SEM)

Field emission scanning electron microscope (FE-SEM) measurements were recorded with Zeiss Neon 40EsB FESEM with an Oxford Instruments Inca x-act SDD x-ray detector and Inca software for $LiTiO_2$ while for Li-Cb and Li/Zn-Cb catalysts, the FE-SEM measurements were recorded with MIRA3 TESCAN with an Oxford Instruments Inca x-act SDD x-ray detector and Inca software.

### 3.4.5 Surface area analysis

The surface area of samples was measured by $N_2$ adsorption- desorption isotherm using the BRUNAUER- EMMER- TELLER (BET) surface area method with Micromeritics, Tristar II Surface area and Porosity analyzer (Fig. 3.5). Before measurements, the moisture and volatile impurities were removed by degassing all samples at 200 °C overnight. The $N_2$ desorption isotherm using Barrett Joyner Halenda (BJH) method was used to determine the pore size of the catalysts.

**Fig. 3.5**. Micromeritics, Tristar II Surface area and Porosity analyzer.

### 3.4.6 The basicity of catalyst analysis

The basicity of the catalyst was analysed by Hammett indicator method to identify the basic strength of the prepared catalyst. The method is outlined by shaking about 25 mg of a catalyst with 5 mL of Hammett indicator solution and left for 2 h to equilibrate. Then the change of the catalyst color was noted.

### 3.5 Experimental set-up

The experiments were carried out in a three- necked round bottom flask of 100 ml connected to a magnetic stirrer and a condenser as shown in Fig. 3.6a. Water bath was used to control the temperature through the reaction where the flask was immersed in it. Fig. 3.6b shows the lower glycerol layer and top FAME layer produced from fresh canola oil, while Fig. 3.6c illustrates the biodiesel sample from the waste canola oil after separating the catalyst. Fig. 3.7

shows the flow diagram of the transesterfication process. Firstly, the catalyst and methanol were mixed together for 40 min under heating then when the mixture reached the suitable temperature (40-60 °C), a weighted amount of preheated oil (at the required temperature) was added. After the reaction duration was completed, the samples were transferred to the separation step by a centrifuge to isolate the solid catalyst and then the liquid mixture was left overnight for further separation. The excess methanol was evaporated and recovered by a rotary evaporator under vacuum.
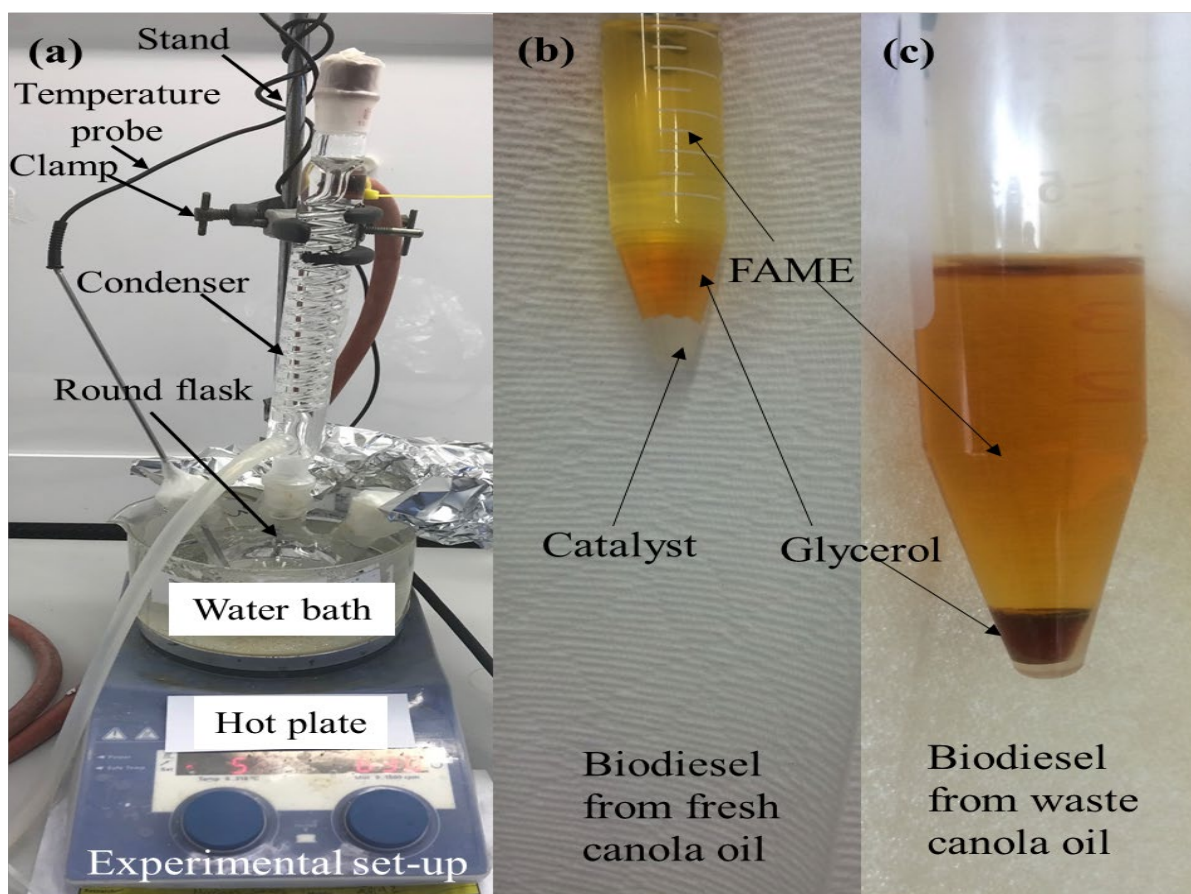


**Fig. 3.6**. (a) The experimental set-up; (b) FAME sample from fresh canola oil; (c) FAME from waste canola oil
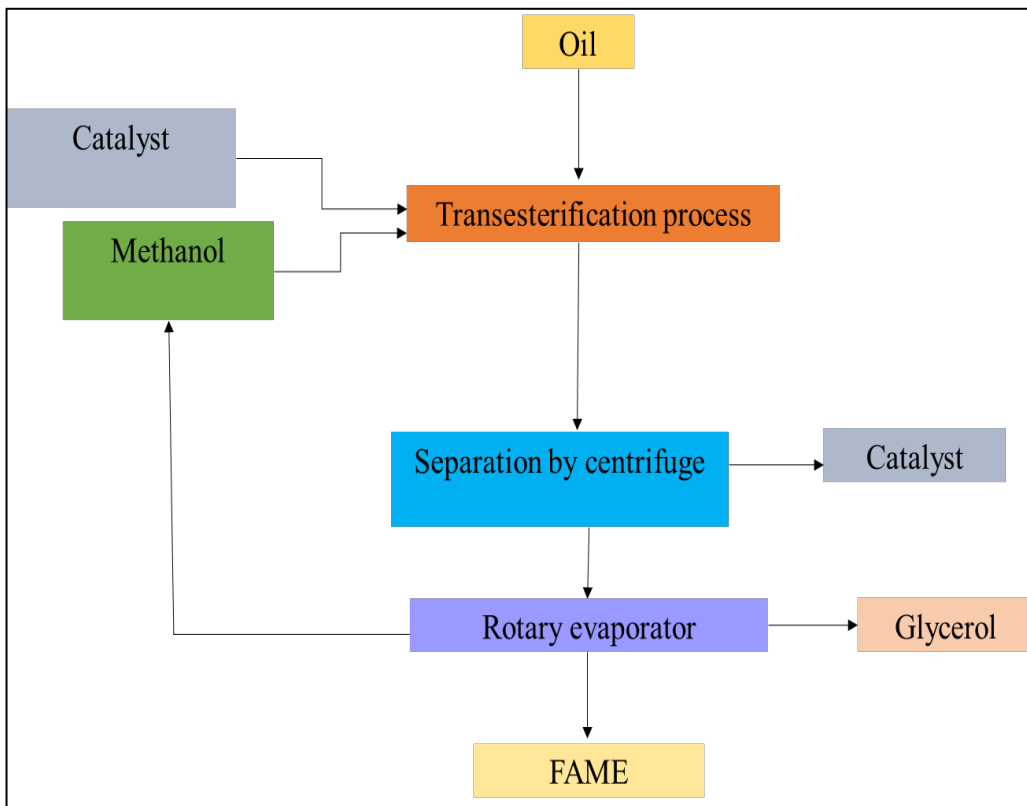
**Fig. 3.7**. The transesterification process flow diagram.

## 3.6 Factors investigated

### 3.6.1 Catalyst dosage

The influence of catalyst dosage on the transesterification reaction was studied for each catalyst. For lithium-based titanium dioxide catalyst (Li/TiO$_2$), the catalyst dosage of 1, 2, 3, 4, 5, 6, 7 wt. % based on oil weight was investigated. In case of lithium chicken bone-based catalyst (Li-Cb), catalyst dosage of 1, 3, 4, and 5 wt. % were studied to assess the effective amount of catalyst on the transesterification conversion. The impact of mixed oxide (lithium/ zinc) based chicken bone (Li/Zn-Cb) catalyst dosage on the transesterification efficiency in the reaction medium was studied (1, 2, 3, 4, 5 wt. %) with respect to the oil weight.

### 3.6.2 Methanol: oil molar ratio

The transesterfication is a reversible reaction where excess alcohol needed to drive the reaction towards the FAME production. A wide range of MeOH:oil molar ratio from 6:1 to 28:1 has been investigated in this work using different catalysts (Li/TiO$_2$, Li-Cb, Li/Zn-Cb).

### 3.6.3 Transesterfication time

Adequate reaction time offers enough contact between reactants and active sites of the catalyst to obtain the highest conversion, therefore, the influence of wide range of transesterfication time of 1 – 5 h on the FAME production will be investigated in this study.

### 3.6.4 Transesterfication temperature

The influence of reaction temperature was studied because of its high impact on the FAMEs production. The reaction was carried out at the atmospheric pressure, thus exceeding the methanol boiling point will reduce the required amount of methanol needed for maximum conversion. A wide range of temperature was selected in this study (35 – 75 °C) to investigate the transesterfication and FAME formation. The following table (Table 3-2) summarizes the parameters investigated using different catalyst.

**Table 3-2:** The investigated parameters employing various catalysts

| Catalyst | Catalyst dosage (Wt. %) | MeOH: oil molar ratio | Reaction time (h) | Reaction temperature range (°C) |
|---|---|---|---|---|
| Li/TiO$_2$ | 1, 2, 3, 4, 5, 6, 7 | 9:1-28:1 | 1- 5 | 35, 45, 55, 65, 75 |
| Li-Cb | 1, 3, 4, and 5 | 12:1-20:1 | 1 - 3.5 | 40, 50 and 60 |
| Li/Zn-Cb | 1, 2, 3, 4, 5 | 6:1 to 20:1 | 1 - 4 | 40, 45, 50, 55, 60 and 65 |

**3.7 Reusability**

The reusability of Li/TiO$_2$ was studied according to the following procedure: the catalyst was filtered to separate it from the reaction solution then washed with methanol for three times and once with hexane and left to dry overnight at 120 ºC. Then, the catalyst used for the following transesterification reaction at the selected optimal conditions (24:1 MeOH:oil, 5% of catalyst, 65 ºC reaction temperature and 3 h of reaction time). The reusability of the Li-Cb and Li/Zn-Cb catalysts was carried out by separation the solid catalyst and washing them with hexane to remove the undesired and attached organic molecules then dried in the oven at 75 ºC overnight. The catalyst reactivation was conducted by calcination at 850°C for 1 h in case of Li-Cb and 1.5 h for Li/Zn-Cb then the catalyst was ready to apply again for the next reaction cycles.

**3.8     Analytical methods**

**3.8.1   Determining the acid value (AV) of feedstock**

The acid value was calculated by the titration method according to EN 14104. In order to calculate the acid value 1 g of oil sample was dissolved in a 10 ml of isopropanol alcohol. The obtained solution was titrated at room temperature (25 ºC) by a standardized solution of ethanoic potassium hydroxide (0.1 M KOH) and using phenolphthalein as an indicator. When the solution color changed from light yellow to pink, the end point recorded. The oil acid value was then calculated according to the Eq. (3-1):

$$Acid\ value\,(AV) = \frac{V \times C \times M}{m} \times 100\% \qquad (3-1)$$

Where, $V$ is the volume of KOH solution required for the titration; $C$ is the molarity of the KOH solution; $M$ is the molecular weight of KOH (56.1 g/gmol); $m$ is the mass of sample (g).

### 3.8.2 Determining the saponification value (SV)

The saponification value is the number of milligrams of potassium hydroxide consumed to saponify one gram of fat or oil [196]. The procedure of estimation was described by weighing 1 g of oil in a tared flask then 10 ml of the fat solvent (ethanol/ether) was added to dissolve the oil. To the obtained solution, about 25 ml of 0.5 N of ethanoic KOH was added. Then the content in the flask was heated under refluxing for 30 minutes in a bath of boiling water. After cooling down the mixture, two drops of phenolphthalein indicator were added to the mixture. Finally, the mixture was titrated with 0.5 N of HCL and when the mixture color changed from pink to colorless, the endpoint was recorded. The above procedure was repeated but without oil for the blank test. The saponification value was calculated using Eqs. (3-2), and (3-3):

$$Saponification\ value\ (SV) = \frac{N \times M \times V}{m} \qquad (3-2)$$

$$V = V_b - V_t \qquad (3-3)$$

Where, $N$ is the normality of KOH, $M$ is the molecular weight of KOH (g/mol), $V$ is the volume of KOH consumed by 1g fat (ml), $V_b$ is volume of HCL used for the Blank titration, $V_t$ is volume of HCL used for the test titration and $m$ is the oil weight (1 g)

### 3.8.3 Determining the conversion to FAMEs

The FAMEs were determined and analyzed via a gas chromatograph (GC) (Agilent Technologies 7890B) as shown in Fig. 3.8. The GC analysis was carried out with a mass spectroscopy detector (5977A MSD) and a FAME-Wax capillary column (30m, 0.25mmID, 0.25μm, a fused-silica column coated with 0.25μm Cross bond polyethylene glycol film).

The analysis approach was according to EN-14103: Determination of Total FAME and Linolenic Acid Methyl Esters in Biodiesel. The method is outlined as weighing approximately 250 mg of liquid sample in a 10 mL vial, then add 5 mL of internal standard (methyl octanoate, 10 mg / mL) solution using a pipette and the hexane was the solvent. The FAMEs content and conversion were calculated according to the Eqs. (3-4) and (3-5), respectively:

$$\text{FAMEs content (\%)} = \frac{\sum A - A_s}{A_s} \times \frac{C_s \times V_s}{m} \times 100 \tag{3-4}$$

$$\text{Conversion to FAMEs (\%)} = \frac{\sum A - A_s}{A_s} \times \frac{C_s \times V_s}{m} \times \frac{mass\,of\,biodiesel}{mass\,of\,oil} \times 100 \tag{3-5}$$

Where $\Sigma A$ is a sum of the areas under all peaks from C4:0 to C24:1; AS is an area under the peak of methyl octanoate used as the internal standard; $C_S$ is the methyl octanoate solution concentration (mg/ mL); $V_S$ is the internal standard solution volume (mL); and $m$ is a sample weight (mg).



**Fig. 3.8**. Agilent Technologies 7890B (GC).

Prior to the FAME samples analysis, a commercial standard FAME mixture (C4-C24) was allowed to run through the GC in order to identify the order and retention times of the fatty acid methyl esters peaks which are usually found in FAME samples. The instrument parameters are provided in Table 3-3 and the GC-MS peaks are shown in Fig. 3.9. The fatty acid profile of the used feedstocks (canola oil and waste canola oil) was also determined by Gas Chromatograph (GC) and shown in Table 3-1 in section 3.2.1.
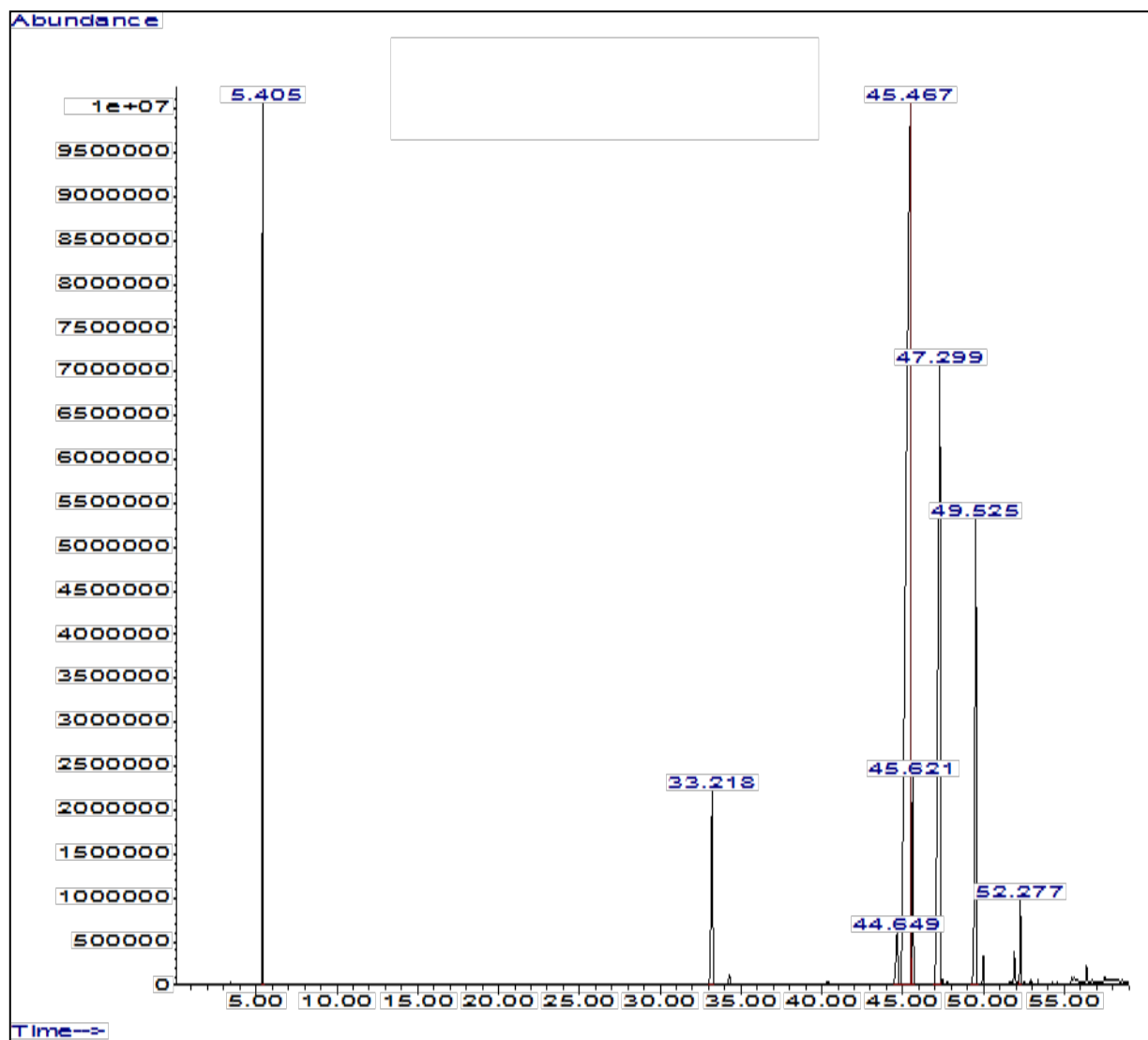


**Fig. 3.9**. The GC-MS peaks.

**Table 3-3:** The GC-MS instrument parameters.

| Gas chromatography | Agilent Technologies 7890B | | |
|---|---|---|---|
| Detector | mass spectroscopy detector 5977A MSD | | |
| Column flow | 1ml/min | | |
| Split ratio | 50:1 | | |
| Oven program | Temp (C) | Rate (C/min) | Hold (min) |
| | 80 | 5 | 0 |
| | 100 | 5 | 3 |
| | 140 | 5 | 10 |
| | 160 | 5 | 10 |
| | 180 | 5 | 3 |
| | 230 | 5 | 3 |
| Column | FAME-Wax capillary column (30m, 0.25mmID, 0.25μm) | | |
| Carrier gas | Helium | | |
| Injection volume | 1 μL | | |

## 3.9 Experimental Design for Optimisation by RSM

The optimization of biodiesel production process was performed by Box Behnken Design (BBD) method of Response surface methodology (RSM) and the interaction between three independent factors were investigated. The biodiesel production process is significantly influenced by the reaction temperature ($X_1$), methanol to waste canola oil molar ratio ($X_2$) and catalyst dosage ($X_3$), thus, they were chosen for optimization. The synergistic relationship between the input variables and the response variable was examined by employing a matrix of three levels and three parameters. 15 experiments were conducted by varying the reaction temperature from 40 to 65 ºC with a central point of 52.5, methanol to waste canola oil molar ratio from 6:1-20:1with a central point of 13:1, and catalyst dosage 1 to 5 wt. % with a central point 3. The range of these factors were chosen based on our

previous investigation that was carried out in the laboratory. The conversion to FAMEs (%) was selected as the response variable. In this study, JMP statistical discovery TM software from SAS (version 13.1.0) was adopted for BBD experimental design, regression analysis and 3D response surface graphs plots.

## 3.10 Ultrasound assisted transesterfication

Ultrasonic cleaner model FXPl 4M (300 watts of ultrasonic power and the chamber is provided by the sonic energy and the piezoelectric transducers bonded to the tank bottom with a frequency of 40 kHz) was used for the ultrasound assisted Li/Zn-Cb transesterification reaction. A heater (Ratek thermoregulatory) was attached to the bath to keep the desired reaction temperature constant. The batch reactor of 50 ml round-bottom flask with three necks was connected with a condenser to keep methanol amount constant through the reaction, and thermometer probe to monitor the reaction temperature. Firstly, the mixture of calculated amount of methanol and catalyst were stirred for 40 min at room temperature on the magnetic mixer before moving the reactor and was immersed in the bath sonication. Then, the pre-heated oil at ≈ 60 ℃ was transferred to the mixture and the mixing was continued by sonication irradiation for different times (0.5- 3 h). The catalyst dosage was investigated by varying the dosage from 1 to 4 wt. /wt. % based on the oil weight while the MeOH: oil molar ratio and the reaction temperature were kept constant at 18:1 and 60 °C, respectively. The withdrawn sample was centrifuged at 4500 rpm for 20 min to separate the solid catalyst. The top layer, which is rich with methyl esters, was isolated for further FAME analysis. Fig. 3.10 shows the sonication experimental set-up.
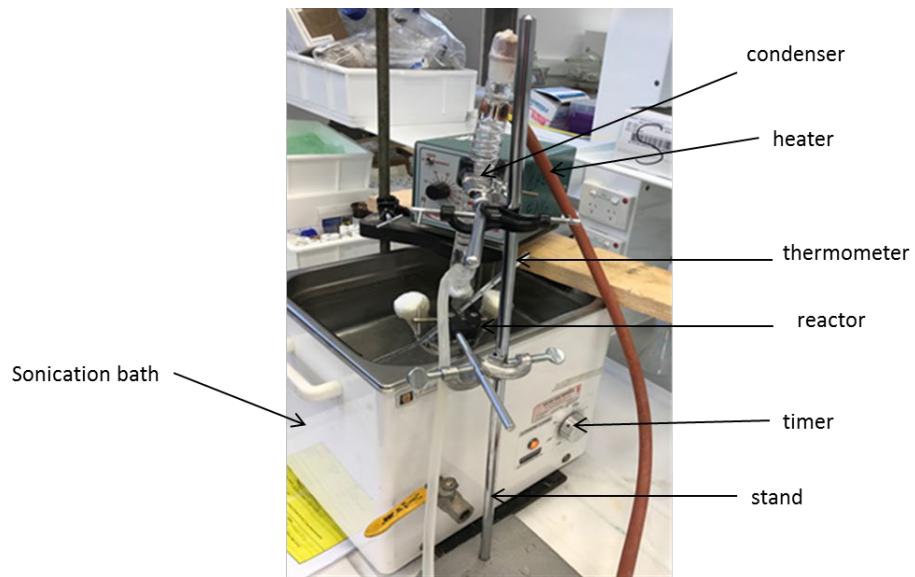
**Fig.** 3.10. The ultrasound assisted transesterfication set-up.

# CHAPTER 4

# Biodiesel production from canola oil using novel Li/TiO$_2$ as a heterogeneous catalyst prepared via impregnation method

## 4.1 Introduction

In recent years, increasing global consumption of fossil based fuel results in the environmental issues associated with the emission of greenhouse gases such as NOx, SOx, CO, $CO_2$ and shortage in the conventional fossil fuel sources [197]. This problem has promoted researchers to take steps to substitute the fossil fuels with a renewable and sustainable fuel. Biodiesel, which is chemically a term of the mono-alkyl esters of long chain fatty acids and is mainly synthesized by transesterification of vegetable oils or animal fats with alcohol (methanol or ethanol), has appeared as an alternative, biodegradable, renewable, and non toxic fuel [8]. Conventionally, homogeneous catalysts such as sodium hydroxide (NaOH) are widely used in industrial processes for biodiesel production. However, the product of these catalysts should be washed and purified to remove the soluble catalyst and to agree with the European standards for the biodiesel specifications. Thus, the separation and purification of the product which increase the process cost and affect the environment are the drawbacks of homogenous catalysts. To solve these problems, researchers have extensively focused on replacing homogeneous catalysts with different types of heteroge

neous (solid) catalysts which are insoluble and recyclable.

Eliminating the additional purification steps and the ability to reuse the catalyst several times result in reducing the synthesis cost of biodiesel and environment concerns [126]. Currently, various heterogeneous catalysts such as mixed oxides, alkaline-earth metals oxides, alkali metals supported on zeolite, alumina and solid acid catalysts have been reported at variable operating conditions. Among a great variety of solid catalyst, $TiO_2$ has been utilized widely as photo catalyst. Separate studies have documented the use of $TiO_2$ and Lithium oxides as catalyst for biodiesel production, as compile in Table 4-1. However, to the best of our knowledge, no study has been reported biodiesel synthesis utilizing Li corporate with titanium oxide catalysts.

**Table 4-1:** $TiO_2$ and Lithium oxides as catalyst for biodiesel production

| Catalyst type | Preparation method | Feedstock | Operating conditions | Yield/ conversion (%) | Ref. |
|---|---|---|---|---|---|
| Ca0.9Li0.6Zr0.9 O3 | nitrate-b-alanine solution combustion method | soybean oil | Ethanol/oil= 12:1, Temp.=50ºC, t=30min, cat%=10 | 60 | [198] |
| Potassium titanate 20%K/TiTH | $TiO_2$ was impregnated with $KNO_3$ after being hydrothermally treated | canola oil | MR=36:1, cat%=6, t=2 h, temp.=65ºC | ~100 | [47] |
| Potassium titanate | hydrothermal synthesis method | safflower oil | MR=1:1, Cat%=3, temp.=50ºC | 100 | [46] |
| $LiALO_2$ | The solid-state reaction | soybean oil | MR=24:1, cat%=8,temp.=65ºC, t=2 h | 97.5 | [163] |
| Mesostructured Sr and Ti mixed oixdes MST-SGC MST-EISA | 1.sol-gel combustion (SGC) method. 2.evaporation-induced self - assembly (EISA) method. | palm kernel oil | Temp (SGC)=170ºC, temp(EISA)= 150ºC, MR=20:1, cat%=10, t=3 h | 99.9 | [99] |
| Alkali metal (Li, Na, K) supported rice husk | Wet impregnation method | used cooking oil | MR= 9:1, cat%=3, t=1 h, temp.=65ºC | 96.5-98.2 | [173] |
| 5-Li/MgO-250 | Impregnation method | animal (mutton) fat | MR=12:1, cat%=5, t=40 min, temp.=65ºC | 99 | [199] |
| $TiO_2$–MgO mixed oxides (MT-1-923) | sol-gel method | waste cooking oil | MR=50:1, cat%=10, t=6 h, temp.=433K | 92.3 | [200] |

Xie et al. [201] have reported the transesterification of soybean oil in the presence of Lithium-Doped ZnO Catalysts. Kumar and Ali [197] have demonstrated the catalytic activity of Li, Na, and K impregnated on CaO for the transesterification of used cotton seed oil. Recently, Castro et al. [109] have investigated the significant effect of the supporting material of the catalyst and they found lithium-based mixed oxides have been strongly affected by the supporting materials. However, these catalysts exhibited weak stability due to the losing

active sites from the catalyst into the solution. In fact, enhancing the catalyst stability leads to improve the catalyst performance for increasing the biodiesel production. Hence, the development of a heterogeneous catalyst with a high stability, and ability to produce FAME under mild temperature and atmospheric pressure, are of great interest for industrial scales. Generally, the reaction temperature could be controlled by incorporating alkali earth metals in catalysts, which results in enhancing the operating conditions [202].

Plant oils have attracted a considerable attention as an alternative fuel source which is exposed to some chemical modification methods like transesterification (alcoholysis), pyrolysis (thermal cracking) and emulsification. However, Transesterification has a prominent position in the synthesis of higher quality biofuel from vegetable oils in the presence of a catalyst. The process involves the formation of methoxide ions ($CH_3O-M^+$) from the proton adsorption ($H^+$) in the methanol's hydroxyl group by the basic sites (i.e. M: metal cations, Li and Ti) on the catalyst's surface then these ions attack (nucleophilic attack) the carbonyl groups in the triglycerides (TG).

Nucleophilic attack leads to form three molecules of fatty acid methyl esters (biodiesel) and one molecule of glycerol through a three steps of alkoxy species interchange as shown in Scheme 4-1. In this study, Li-based $TiO_2$ catalyst as a solid catalyst has been adopted for biodiesel production from canola oil. The influence of calcination temperature and lithium loading amounts were investigated in details and the reaction kinetics was studied. Moreover, the reaction parameters such as methanol/oil ratio, catalyst amount, and reaction temperature and time have been optimized. Furthermore, the reusability and the alkali metal leaching were studied.
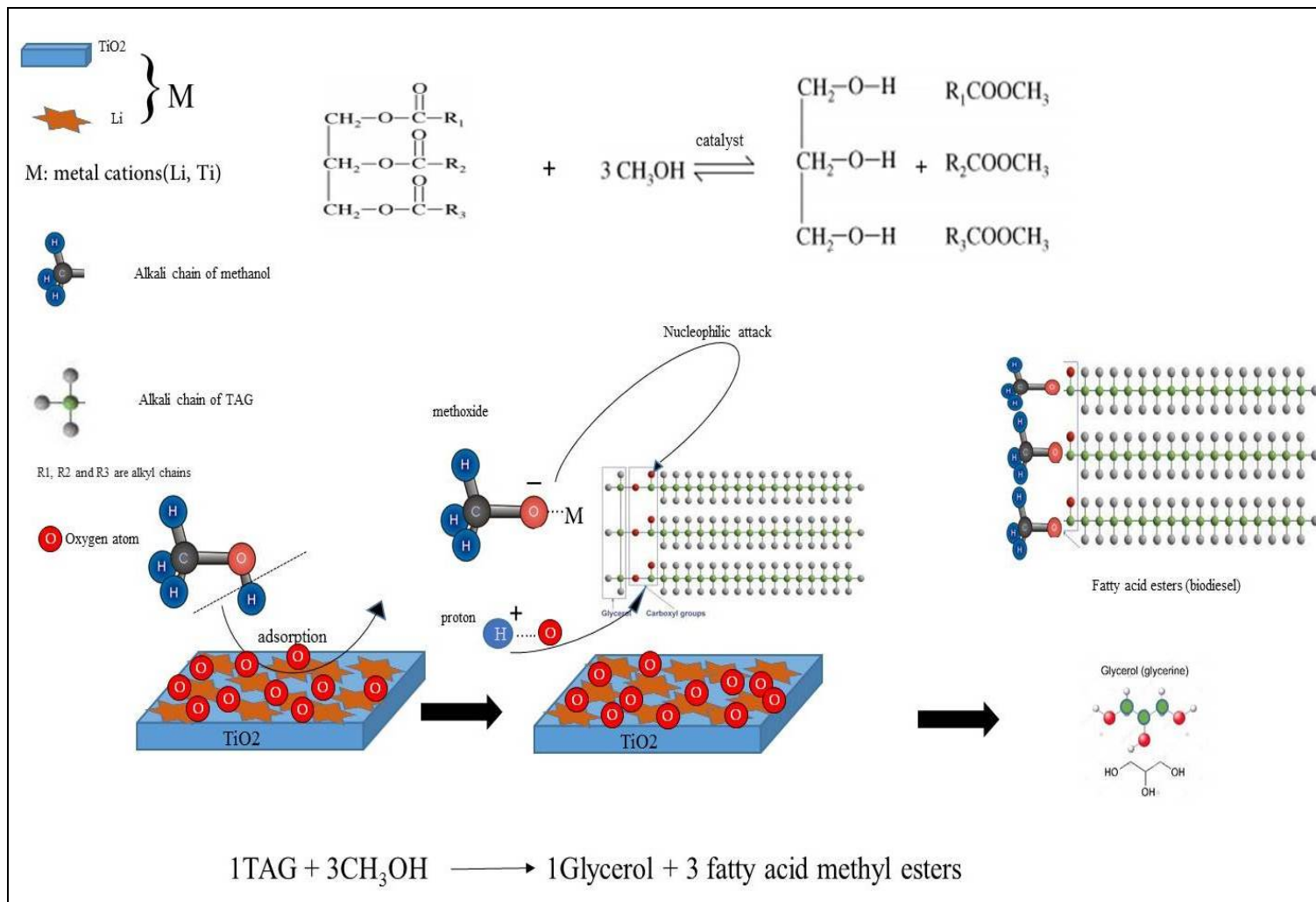
**Scheme 4.1.** The mechanism of transesterification process

## 4.2 Materials and methods

In Chapter 3, the experimental set-up, procedure, analytical methods and characterisations are described. Section 3.2.1 describes transesterfication chemicals and feedstock. Sections 3.2.2 and 3.2.3 give chemicals for catalyst preparation and analysis. Section 3.3.2 provides the preparation method of catalyst (Li/TiO$_2$). Sections 3.4.1-3.4.6 provide the catalyst characterizations. Details of the experimental set-up and transesterfication process are provided in Section 3.5. The investigated transesterfication parameters are fully described in Sections 3.6.1-3.6.4 and the ranges of catalyst dosage (wt. %), MeOH: oil molar ratio, reaction time (h) , and reaction temperature (ºC ) were 1- 7, 9:1-28:1, 1-5, and 35-75, respectively. Section 3.7 is regarding catalyst reusability. The analytical procedures and conversion to FAMEs estimation are given in Sections 3-8.1- 3.8.3.

## 4.3 Results and Discussion

### 4.3.1 X-ray diffraction and surface area analysis

The XRD patterns of the titanium-based catalysts at different LiNO3 loading is shown in Fig. 4.1a. The X-ray diffraction peaks of TiO$_2$ were sharp and intense at 2θ of 25.41°, 37.93°, 48.14°, 53.86°, 55.05° and 62.57° which mainly correspond to the anatase phase with appearance of small peaks of rutile at 2θ of 68.36°, 69.97° and 74.95°. New diffraction peaks were observed when the LiNO$_3$ was added (samples were calcined at 600 ºC) which are assigned to the Li$_2$TiO$_3$ phase at 2θ of 18.60°, 36.29°, 43.47°, 57.77° and 63.14°. Li$_2$O diffraction peaks were not detected for Li loaded samples. The finding is consistent with findings of past studies by many researchers [109,199,201], where lithium was used with different supports such as MgO, Mg(Al)O and ZnO.

Furthermore, since the calcination temperature impacts the structure of catalyst and the catalytic activity, the catalyst with different calcination temperatures was characterized by

XRD, asdifferent calcination temperatures was characterized by XRD, as illustrated in Fig. 4.1(b). Since the catalyst with 30% LiNO$_3$ content gave the highest conversion (78% refer Fig. 4.6), this amount was fixed for further XRD characterization at different calcination temperatures. The calcination at low temperature (450 °C) showed a low crystallization intensity of Li$_2$TiO$_3$ phase while the intensity was increased at calcination temperature of 600 °C (without affecting the TiO$_2$ structure). However, at 750 °C of calcination the intensity of TiO$_2$ crystalline phases reduced. In addition, the diffraction lines at 2θ of 18.60°, 36.29°, 43.47°, 57.77° and 63.14° were shifted to produce a new phase which was assigned to the LiTiO$_4$. These results could be attributed to the incidence of interaction between metals which led to alteration in the crystalline structure [203].

Table 4-2 presents the results of surface area, pore volume and pore size of catalyst with different loading amounts of lithium and calcination temperatures. It is revealed from Table 4-2 that the surface area of pure TiO$_2$ decreased with increase of Lithium from 20 to 40 loading wt. %.

However, unexpected increase in the surface area of catalyst was noticed with loading 30 wt% of lithium, comparing with other two catalysts (20 and 40 wt. %), as shown in Table 4-2. This finding reveals that lithium was combined with the supporting materials and penetrated through the surface of supporting material (TiO$_2$), which led to an increment of the surface area [204]. However, the surface area reduced from 9.25 m$^2$/g to 3.06 m$^2$/g with increasing of the calcination temperatures from 450 to 750 °C respectively (Table 4-2). Based on the results, increasing the calcination temperature induces phase crystallization changing and sintering process, which dramatically reduces the surface area and pore volume [203]. Kaur and Ali [199] and Goncalvesa et al. [198] have also noticed these changes of Li addition on the morphological properties of magnesium and calcium oxides, respectively. Moreover,

the average pore size (~11 nm) of prepared samples was found in the mesoporous range (2-50 nm) which is larger than triglyceride molecule (~0.6nm) to diffuse through the catalyst [182].
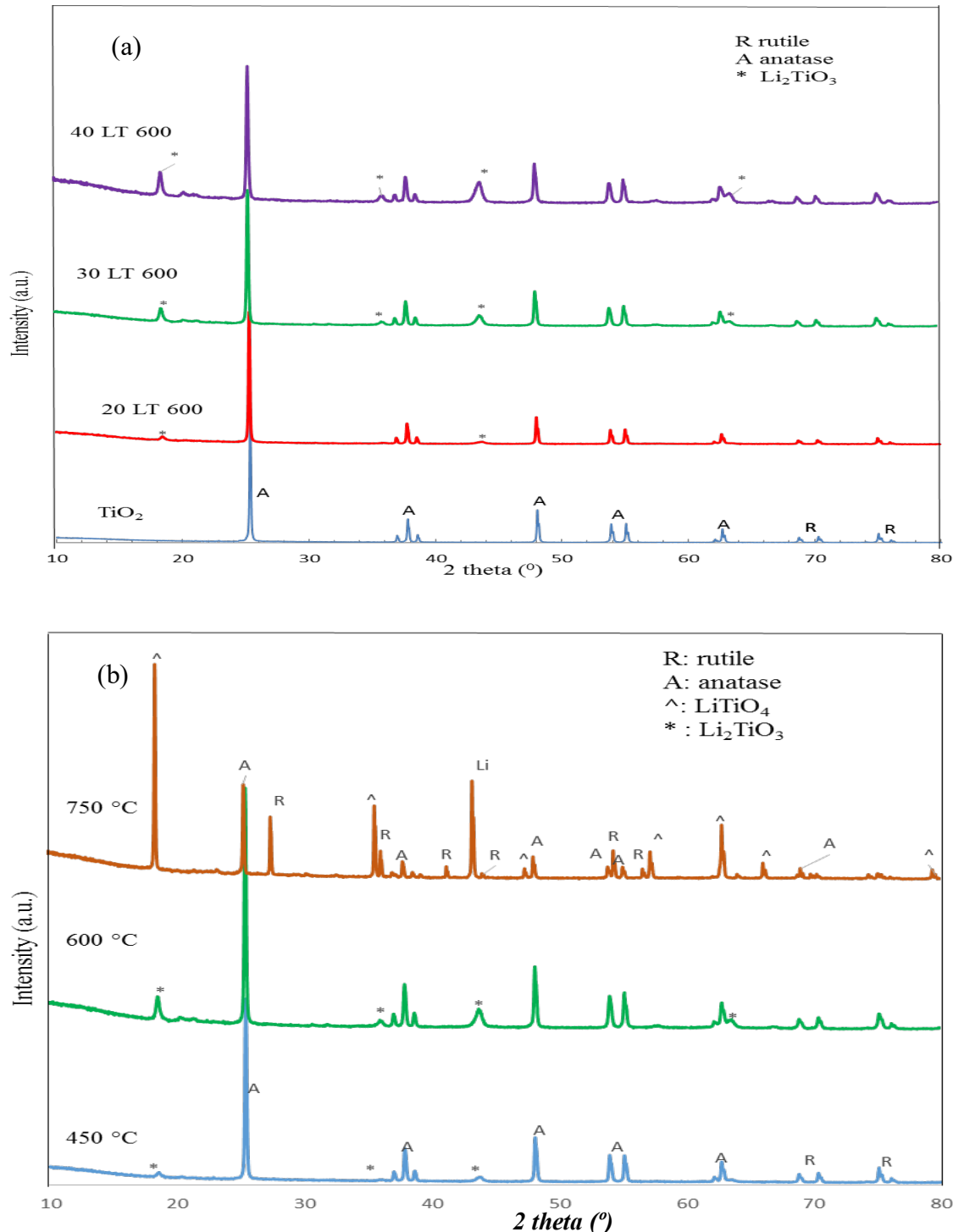


**Fig. 4.1.** XRD patterns of the catalysts: (a) different $LiNO_3$ loading calcined at 600 °C; (b) 30LT at different calcinations temperatures.

**Table 4-2:** Results of BET surface area, pore size and pore volume for various Li loading amounts and calcination temperatures.

| S. No. | Catalyst type | BET surface area $(m^2/g)\pm SD$ | Pore size(nm) | Pore volume $(cm^3/g)$ |
|--------|---------------|----------------------------------|---------------|------------------------|
| 1. | $TiO_2$ | 10±0.1 | 7.32 | 0.018 |
| 2. | 20LT600 | 5.57±0.1 | 12.87 | 0.011 |
| 3. | 30LT600 | 7.63±0.08 | 11.94 | 0.02 |
| 4. | 40LT600 | 5.53±0.2 | 13.04 | 0.011 |
| 5. | 30LT450 | 9.25±0.09 | 9.72 | 0.024 |
| 6. | 30LT750 | 3.06±0.09 | 6.45 | 0.006 |

[1]**SD**: standard deviation

### 4.3.2 FT-IR analysis

The chemical groups of the prepared catalyst were investigated by employing FTIR. Fig. 4.2a and b present the FTIR spectra of the catalysts prepared with different lithium amounts loading and at different calcination temperature. For pure $TiO_2$, the spectrum at 729.1cm$^{-1}$ was characterized to the Ti-O vibration. As depicted in Fig. 4.2a, the spectrum at the reign 400-860 cm$^{-1}$ are attributed to the presence of M$^+$-O bond structure [202]. The band at 866 cm$^{-1}$ corresponds to the formation of mixed metal oxides ($Li_2TiO_3$)which was undetectable for pure $TiO_2$ and noticeable for catalysts possessing Li. These results are analogous with XRD data where $Li_2TiO_3$ formation was observed. The sharp spectrum at 1440 cm$^{-1}$ and 1505 cm$^{-1}$are recognized to the C=O bond from carbonates which is attributed to the adsorption of $CO_2$ from the ambient atmosphere and the split peak is an evidence of the presence of $CO_2$ as it is a common feature in carbonate compounds [46]. The C=O peaks were remarkable for Li samples since Li ion is sensitive to $CO_2$ at high temperature [198]. Moreover, a broad spectrum which is shown at around 3200 cm$^{-1}$, is associated to the O-H stretching vibration mode of water species [18]. The FTIR spectrum for the catalysts at different calcination temperature (Fig. 4.2b) shows appearance of a new peak at 1131 cm$^{-1}$ for 750 °C calcinate

catalyst due to the formation of LiTiO$_4$. In 30LT450 sample the peaks appeared at 1645cm$^{-1}$ and 1347 cm$^{-1}$ due to $\delta$OH bending vibration and N-O bond vibration of LiNO$_3$ respectively were vanished as the temperature increased in case of 30LT600 and 30LT750 because of the loss of water from the catalyst structure and decomposing of LiNO$_3$. The FTIR findings indicate that the impregnation of Li metal on TiO$_2$ was successfully linked.
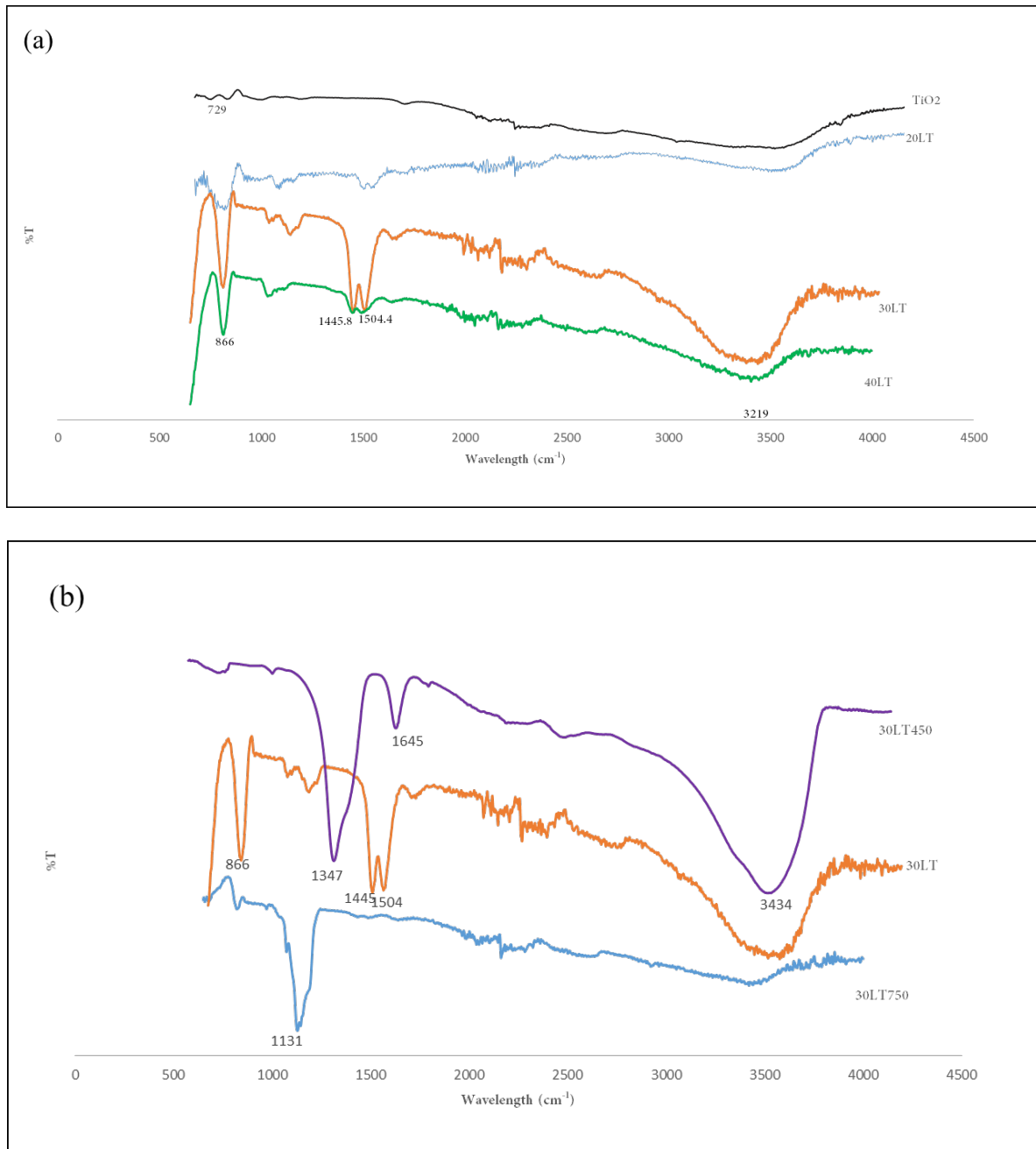


**Fig. 4.2.** FT-IR spectra of (a) different Li impregnated amount; (b) different calcination temperatures.

### 4.3.3 TGA/DSC analysis

Fig. 4.3 illustrates the thermogravimetric curves of Li/TiO$_2$. From Fig. 4.3, it is apparent that two stages of mass loss were observed for 30LT sample. In first stage, a little weight loss, around 100 °C, which was correspond with endothermic peak in DSC curve at same temperature, which were attributed to the escape of adsorbed water species.

While, the second stage occurred at 600 °C due to the thermal decomposition of LiNO3 that associates with endothermic process observed in the DSC curve. Xie et al. [201] have also reported an endothermic signal at 600 °C for LiNO$_3$ decomposition. DSC curve shown an endothermic peak between 200 and 300 °C correspond to no weight loss in TGA curve which probably could be assigned to the interference between LiNO$_3$ and TiO$_2$. Moreover, no weight loss was noticed above 600 °C on the TGA profile which means the decomposition process was completed. Consequently, from this analysis, 600 °C was considered to be the consistent temperature to calcine 30LT catalyst.
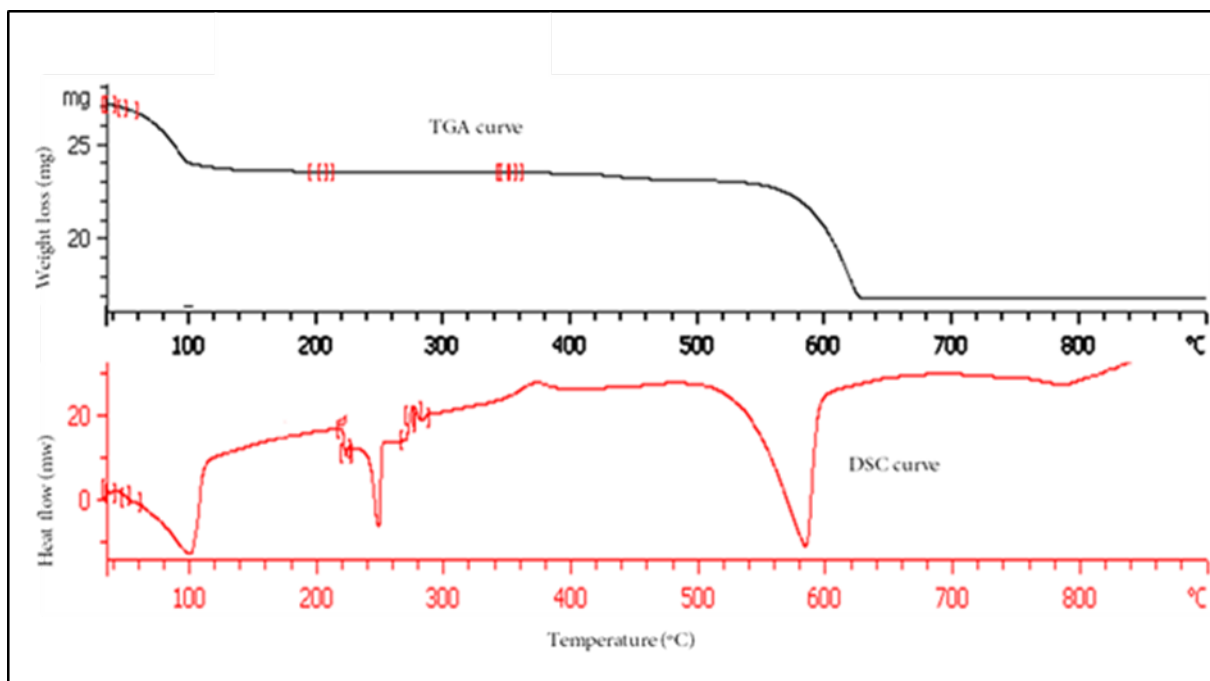


**Fig. 4.3.** Thermogravimetric TGA/DSC profile of 30LT.

### 4.3.4 FE-SEM analysis

The FE-SEM was used to study the changes in morphology of prepared catalysts at different amounts of lithium loading and calcination temperatures. The FS-EM image of pure $TiO_2$ particles is originally spherical in form with a relatively smooth surface as shown in Fig. 4.4a. Fig. 4.4(b-d) shows the effect of lithium loading on the morphology of $TiO_2$ at 20, 30, and 40 wt %. The FE-SEM images of the surface of the synthesized catalysts exposed an obvious transformation of the spherical particles of the $TiO_2$ into assorted particle shapes between round and angled corner particles with inhomogeneous size distribution. With increasing addition of lithium (40 wt% of $LiNO_3$), the catalyst particles became like molten with a dense appearance.
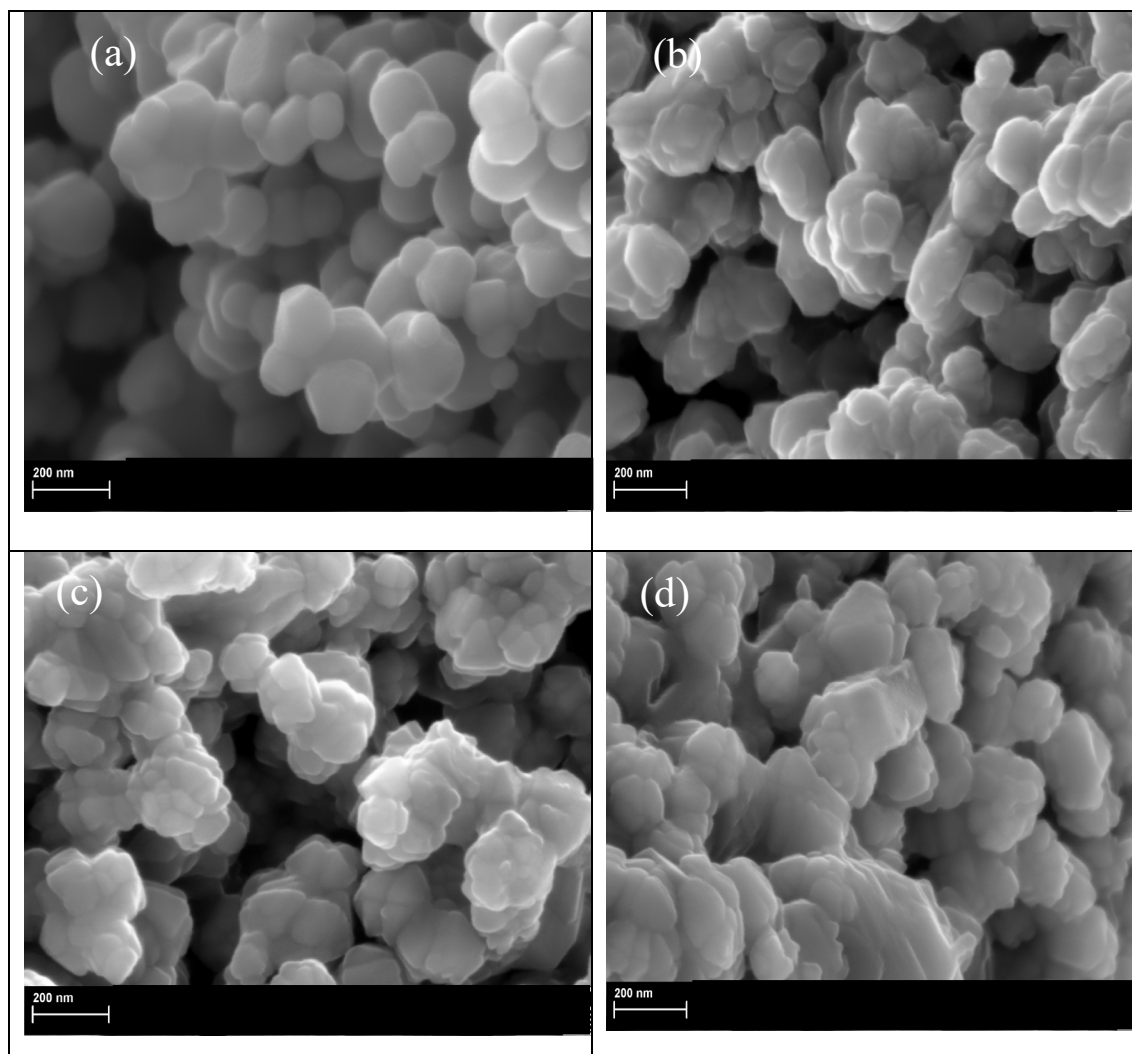
**Fig. 4.4.** FE-SEM micrographs of (a) TiO$_2$; (b) 20LT600; (c) 30LT600; (b) 40LT600.

Fig. 4.5(a-c) shows the FE-SEM images of the synthesized samples at different calcination temperatures (450, 600, and 750 °C). Increasing the temperature from 450 to 600 °C resulted in changing the particle size with emergence of agglomerations and at high temperature (750 °C), it turned to smooth large particles whichwas attributed to small surface area as a consequence of sintering. These results are in agreement with the results discussed before using XRD and BET analysis.
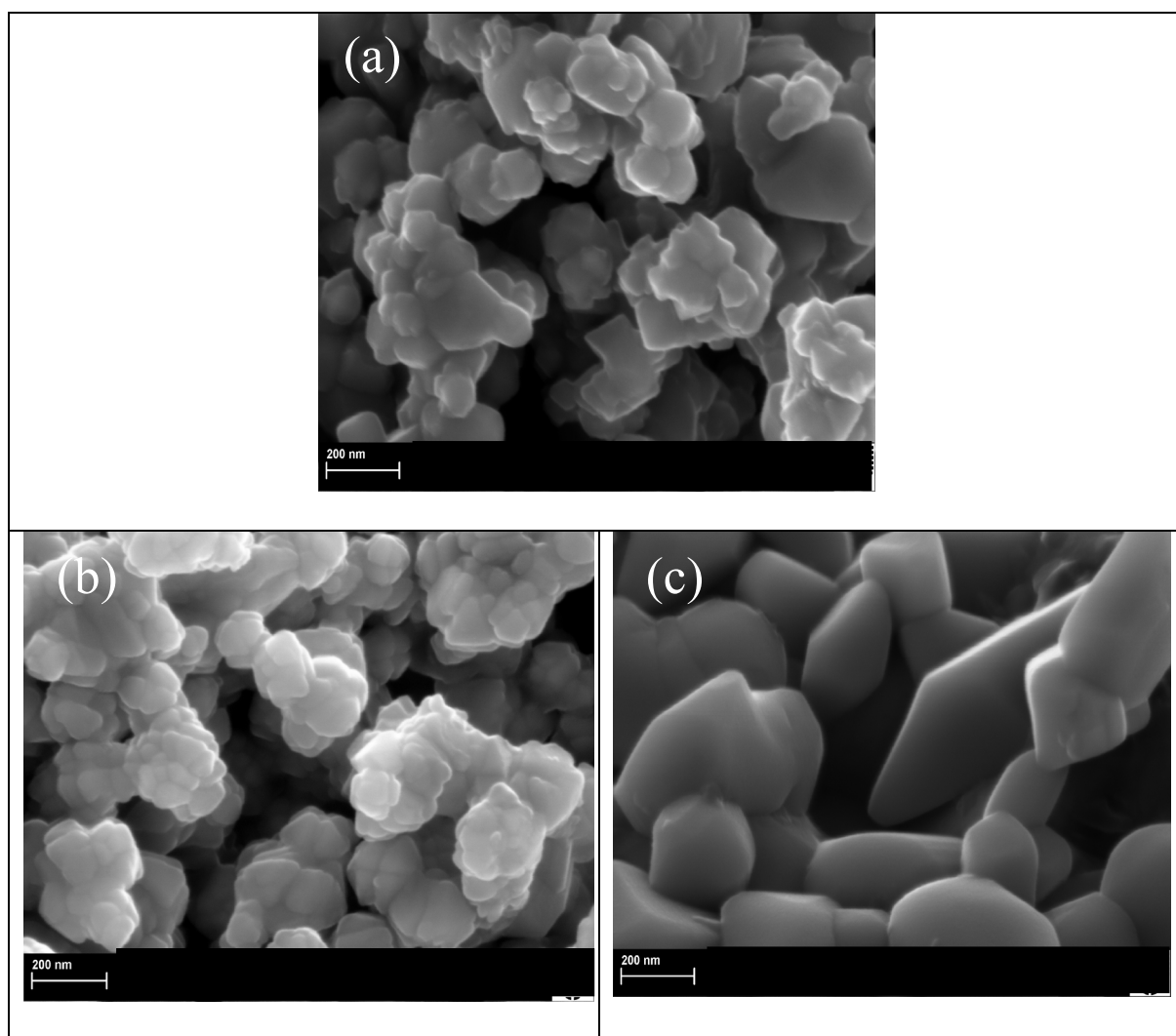


**Fig. 4.5.** FE-SEM micrographs of (a) 30LT450; (b) 30LT600; (c) 30LT750.

### 4.3.5 Effect of the Li to TiO₂ percentage weight ratio

In order to verify the influence of impregnated amount of lithium ion on the activity of the catalyst to obtain the highest conversion to FAMEs, three different concentrations of lithium were tested in respect with the $TiO_2$ weight (wt. %). Fig. 4.6 has shown that impregnation with 30 wt % $LiNO_3$ exhibited the highest conversion under the reaction conditions of 12:1 MeOH:oil ratio, for reaction time of 3 h, at reaction temperature 65 °C and a 5% of catalyst. The high surface area of 30LT that calcined at 600 °C could be the reason of the high catalytic activity [204].
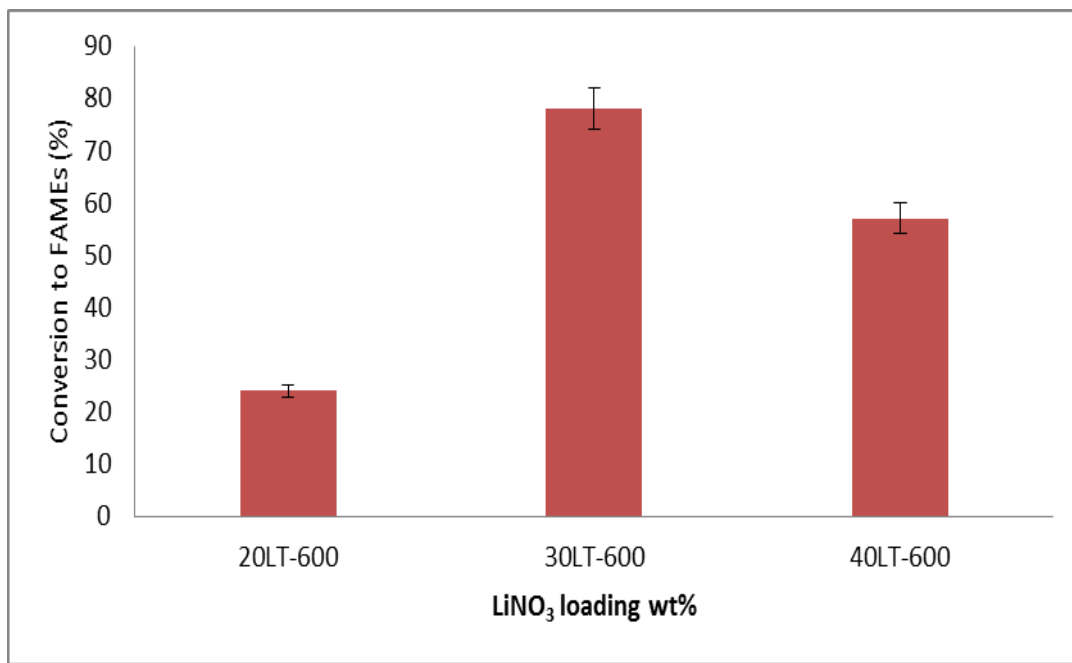


**Fig. 4.6.** Effect of impregnated lithium ion on the FAME production

### 4.3.6 Effect of the calcination temperature

Fig. 4.7 depicts the results for the effect of calcination temperature on the performance of 30LT catalyst. This study has found that the FAME conversion increases with the increase of temperature up to 600 °C then the conversion goes down upon increasing the calcination temperature. The finding suggests that $Li_2TiO_3$ phase which was observed in the 450 and 600 °C calcined catalyst samples as mentioned in XRD analysis together with $TiO_2$ phases might

be the reason of increasing the conversion. The calcination at low temperature (450 °C) showed a low crystallization intensity of $Li_2TiO_3$ phase while the intensity was increased at calcination temperature of 600 °C (without affecting the $TiO_2$ structure) as shown in Fig. 4.1. While increasing heating up to 750 °C caused decreasing $TiO_2$ phase intensity and emergence of $LiTiO_4$ phase which could be the reason after losing the activity of catalyst. These results were supported by XRD and BET analysis too. It seems that $TiO_2$ and $Li_2TiO_3$ phases have mainly affected the catalyst's efficiency. Consequently, 600 °C was a suitable calcination temperature for the prepared catalyst as supported by TGA/DSC analysis.
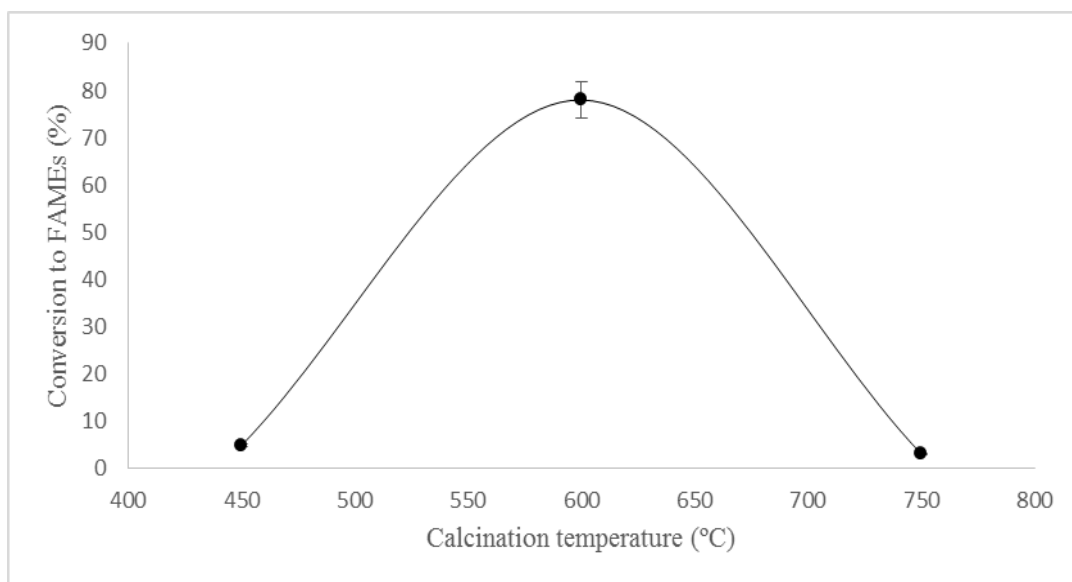


**Fig. 4.7.** Effect of calcination temperature on the FAME production.

### 4.3.7 Effect of transesterification conditions

To evaluate the efficiency of the prepared catalyst, it was applied to the canola oil transesterification under various reaction parameters. Since the loading amount of 30wt. % and calcination temperature at 600 ºC gave the highest production value, all investigations were conducted with 30LT catalyst calcined at 600 ºC.

**4.3.7.1 Effect of Methanol to oil molar ratio**

The influence of Methanol to oil ratio was studied at the reaction conditions of 65ºC, for 3 hours reaction time and 5 wt. % catalyst. Transesterification is reversible reaction so excess amount of methanol is required to drive the reaction towards biodiesel formation. Thus, the reaction was carried out by varying the MeOH:oil ratio from 9:1 to 28:1 to assess the optimum value of methanol. Fig. 4.8a shows increasing the methanol to oil ratio increases the ester content. However, the excess amount of methanol could lead to reduce the yield as a result of dissolving of glycerol (by-product) and shifting the reaction towards the reactants [127]. Therefore, the optimum ratio of methanol to oil was 24:1.

**4.3.7.2 Effect of Catalyst amount**

The effect of catalyst dosage was investigated on the activity of 30LT600 by changing the loading amounts of catalyst to the reactor based on the oil amount. The reaction was carried out under 24:1 methanol:oil ratio at 65 ºC for 3 hours. Fig. 4.8b shows with increasing the amount of catalyst, the ester content was increased and beyond 5wt. %, the conversion was remained same. Hence, 5wt% was seemed to be reasonable. It is apparent from this figure that the reaction reached to equilibrium state [45] at 5wt. % and beyond of catalyst.

**4.3.7.3 Effect of Reaction temperature**

The reaction temperature has a significant effect on carrying out the transesterification reaction. Fig. 4.8c, shows the influence of reaction temperature on the performance of catalyst from 35 to 75 ºC at 24:1 methanol:oil ratio with catalyst amount of 5% and a reaction time for 3 h.

As it can be seen, increasing the temperature is favourable condition for FAMEs content. Referring to the kinetic performance, increasing reaction temperature enhances the reaction

rate leading to raise the molecular collision and decline the activation energy limitation [202]. However, after 65 ℃ the conversion was reduced due to the possibility of evaporating the methanol resulting in reducing the availability of methanol for the reaction [205]. Consequently, the reaction temperature at 65 ℃ was chosen to carry out the rest experiments.
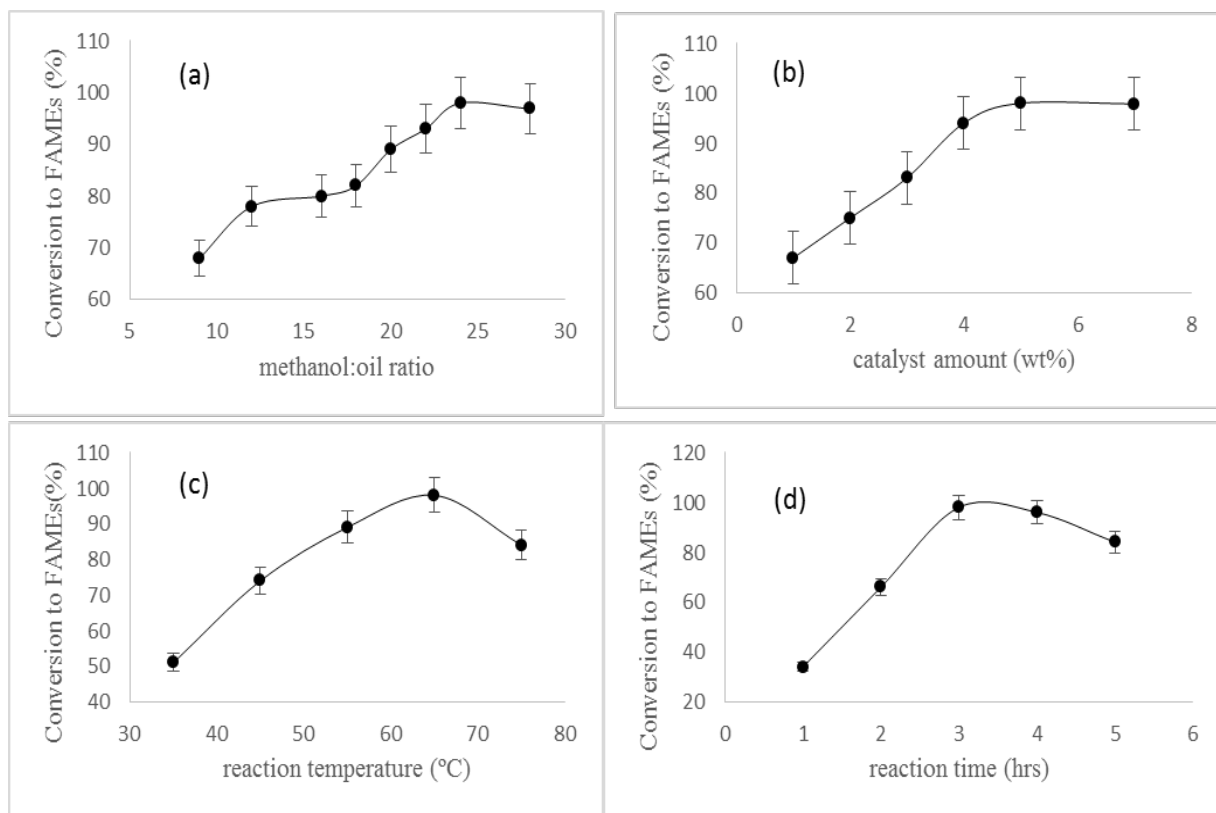


**Fig. 4.8.** Effect of (a) methanol: oil ratio (b) catalyst amount (wt. %) (c) reaction temperature (d) reaction time on the ester content.

### 4.3.7.4 Effect of reaction time

One of the important variables in the biodiesel production is a reaction time. As transesterification is equilibrium reaction, thus adequate time is required to reach equilibrium. In addition, a well contact time between reactants is necessary so that reagents can reach the active sites of catalyst and the conversion is occurred [160] The effect of reaction time is shown in the Fig. 4.8d where the other parameters were remained constant as follow: 24:1 methanol:oil molar ratio, 5%wt of catalyst and a reaction temperature of 65 ℃.

As it is cleared from Fig. 4.8d, the ester content was increased with increasing the reaction time up to 3 hours and achieved the highest conversion, then the conversion was reduced with time. This behaviour might be explained by the possibility of occurring reversible reaction [206, 207].

### 4.3.7.5 Kinetic studies

In order to understand the relationship between the reaction time and temperature and, their influences on the transesterification reaction, the kinetics of biodiesel production process were investigated. The order of the reaction was varied to find the model that fit best to the reaction using regression coefficient ($R^2$).Since the transesterification is a reversible reaction, excess amount of methanol is needed to shift the reaction towards esters formation. Therefore, the reverse reaction could be neglected and the reaction rate constants could be independent on the methanol concentration. Furthermore, ignoring the intermediate reactions could be assumed and considering the transesterification reaction occurs in one step. To verify this hypothesis, firstly the zero order was assumed and the equation as follows:

$$\frac{dx}{dt} = K_{Me} \qquad (4\text{-}1)$$

Where, *[Me]* is concentration of FAMEs, $K_{Me}$ is the rate constant, *x* is the ester content. The rate constant was obtained by drawing the ester content (*x*) against the reaction time (*t*).

The second model which could be considered for transesterification is a pseudo-first order reaction rate and the equation is expressed as below:

$$r = \frac{d[TG]}{dt} = \frac{d[Me]}{dt} = k'[TG][ROH]^3 \qquad (4-2)$$

Where *r* and *k'* are the reaction rate and reaction rate constant, respectively, [*TG*], [*Me*] and [*ROH*] are the triglyceride, methyl esters and methanol concentration , respectively and t is the reaction time. As the assumptions of the reaction are occurring in the triglyceride

molecule and the methanol is in excess, the above Eq. (4-2) could be re-written as follows [208]:

$$r = -\frac{d[TG]}{dt} = k[TG] \qquad\qquad (4-3)$$

Where $k = k'[ROH]^3$

By Re-arrearage the above equation and integrate both sides (taking on the account when the initial time $(t) = 0$, $[TG] = [TG]_o$ and when $t = t$, $[TG] = [TG]$), the equation could be expressed as follows:

$$-\frac{d[TG]}{[TG]} = k\,dt \qquad\qquad (4-4)$$

$$-\ln\frac{[TG]}{[TG]_0} = kt \qquad\qquad (4-5)$$

Mass balance equation is as below,

$$\frac{[TG]}{[TG]_0} = (1 - X_{Me}) \qquad\qquad (4-6)$$

Where $X_{Me}$ is the ester content (conversion to FAMEs).

So from substituting the Eq. (4-5) in Eq.(4-6), the rate reaction constants could be calculated by fitting the ester content and reaction time to the below equation:

$$-\ln(1 - X_{Me}) = kt \qquad\qquad (4-7)$$

In addition, because the transesterification reaction was conducted at different reaction temperatures, the activation energy was determined through applying Arrhenius equation to investigate the effect of temperature on the particular reaction rate [182, 185, 209] as shown below:

$$k = Ae^{\frac{-Ea}{RT}} \qquad\qquad (4-8)$$

After simplifying the above equation, we obtain the following equation:

$$\ln k = \ln A - \frac{Ea}{RT} \qquad\qquad (4-9)$$

Where $Ea$ is the activation energy (kJ/mol), $R$ is the universal gas constant (8.314 kJmol$^{-1}$K$^{-1}$), $k$ is the reaction rate constant (h$^{-1}$), $A$ is a frequency factor (h$^{-1}$) and $T$ is the reaction temperature (K). From plotting the (*ln k*) vs. (*1/T*), the intercept corresponds to (*ln A*) and the slope represents ($\frac{Ea}{R}$).

The experimental data were conducted to the Eqs. (4-2 and 4-8) and shown a good agreement with a zero order model. Table 4-3 demonstrates that the values of correlation coefficients $R^2$ indicated a better fit of zero order model for canola oil transesterification as well the increment in the temperature and duration of reaction, increase ester content in both models. Table (4-4) also presents the reaction rate constants ($k$) and $R^2$ values with reaction temperatures represents that the reaction rate constants increase with increasing the reaction temperatures.

**Table 4-3:** Reaction temperatures, rate constants and $R^2$ values of canola oil transesterification by 30LT600 catalyst

| Temperature ($^o$C ) | Rate constant ($k$) | | $R^2$ | |
|---|---|---|---|---|
| | Zero order | Pseudo first order | Zero order | Pseudo first order |
| 45 | 0.2368 | 0.3714 | 0.8862 | 0.7727 |
| 55 | 0.3289 | 0.7077 | 0.9341 | 0.8025 |
| 65 | 0.3456 | 0.9577 | 0.9422 | 0.8061 |

The findings suggest that increasing the temperatures promote the molecules collision and thus decreasing the mass transfer limitation. The activation energy, which is defined as the minimum quantity of energy needed for activating atoms or molecules to undergo a chemical reaction, (*Ea*) was calculated and it was found to be 39.366 and 16.461 kJ/mol for Pseudo

first order and zero order models respectively. The findings provide evidence that the normal conditions of temperature and pressure could be employed to carry out the reaction.

### 4.3.8 Reusability of catalyst

The reusability is one of the important characters of the heterogeneous catalysts. To study the possibility of regenerating the catalyst, after the completion of reaction, the catalyst was separated by filtration and washed three times with methanol and once with hexane then dried overnight at 120°C after that, it was directly subjected to the transesterification reaction under the optimum conditions (24:1 MeOH:oil, 5% of catalyst, 65ºC reaction temperature and 3 h of reaction time). Fig. 4.9 shows the conversion to FAMEs was gradually declined with increasing the number of reuse recycle.
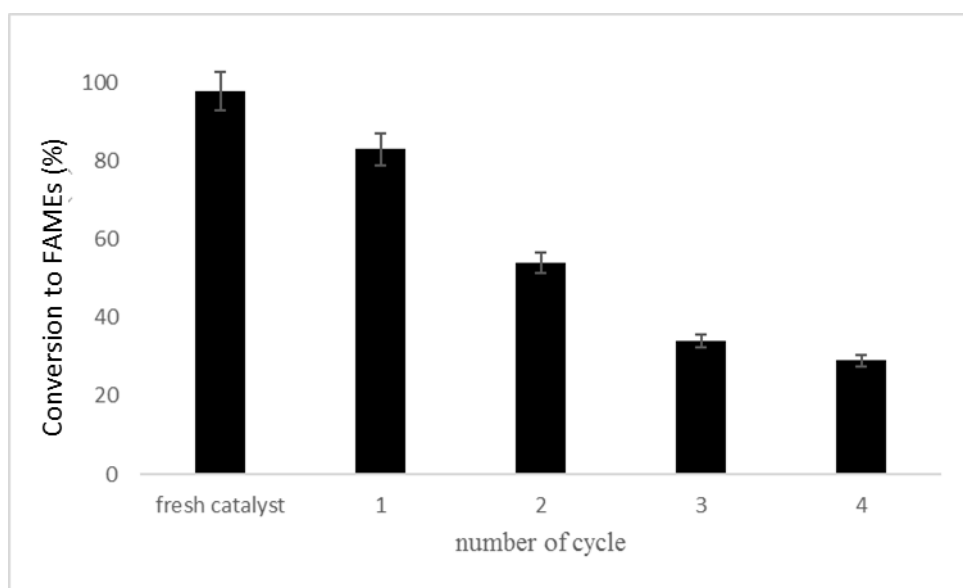


**Fig. 4.9.** Reusability of 30LT600 catalyst under the optimum reaction conditions.

The decreasing catalyst efficiency might be due to leaching of $Li^+$ ion from catalyst surface or diffusion of canola oil and FAME molecules into the catalyst by blockage the catalyst pores and remain persist even after washing the catalyst with organic solvents. Therefore, to evaluate the catalyst deactivation due to the blocking of pores by organic material, TG/DSC

analysis was done. Fig. 4.10 presents TG/DSC result for the fourth reuse of catalyst, as it can be observed that the stages of decomposition are similar to the fresh one except appearing of an exothermic peak at 300ºC which corresponds to the decomposition of residual organic material. Thus, the accessibility of the reactants to the active sites was hindered due to the blockage of catalyst pores which led to decline the ester content. However the deactivation of catalyst due to pores filling can be resolved and it is suggested to regenerate the catalyst for every consecutive cycle of usage, via recalcitrant it at 300 for 2 h, which would remove all the materials blocked in the catalyst pores. Moreover, to assess the losing of catalyst activity as the leaching of $Li^+$ ion and the catalyst stability, the catalyst was reacted with methanol under the optimum conditions (without oil) then the methanol was decanted and has been reacted with oil in the absence of catalyst.
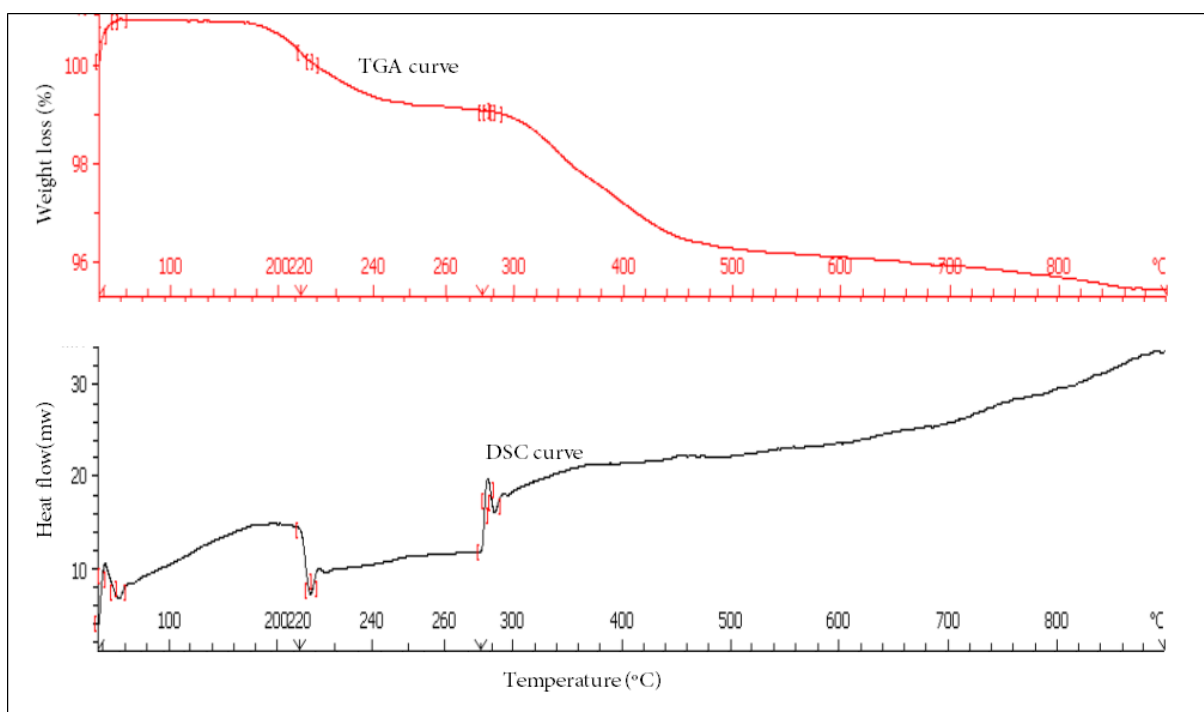


**Fig. 4.10.** TGA/DSC analysis of 4th used of 30LT600.

The latter experiment revealed there is just 26% of ester content, which revealed that, there was leaching but the leached $Li^+$ ions have insignificantly contributed to prompt the

homogeneous reaction, hence, the catalyst deactivation was mainly by pore-filling with organic moieties rather than by leached ions.

### 4.3.9 Investigation the performance of 30LT600 for waste and fresh oil

The biodiesel production from fresh edible oil is always being criticized; hence finding the alternate feedstocks is introduced and tested by many researchers. Consequently usage of waste cooking oil was proposed as feedstocks for biodiesel production [210-212], which possess many advantages such as, it reduces the harmful environmental impacts caused by the disposal of used cooking oils directly into drainage which causes severe blockage too and on the other hand biodiesel production from used cooking oil significantly reduced the total production cost of biodiesel [213]. However, the optimum condition for biodiesel production from fresh oil and used oil are unpredictable, thus here in this research the same optimum conditions were used to compare the capability of ester content for used or waste cooking oil. It was found that the catalyst can be used for biodiesel production from waste cooking oil with 91.73% ester content.

### 4.4 Summary

The purpose of the current study was to enhance the activity of $TiO_2$ for biodiesel production by inclusion of Lithium ions onto it using impregnation method and evaluate the efficiency of prepared catalyst under mild reaction conditions. A series of $LiNO_3/TiO_2$ catalysts were synthesized at different calcination temperatures which were investigated and conducted for the transesterification process using canola oil for biodiesel production. The study showed that addition of lithium has improved the $TiO_2$ reactivity towards biodiesel production which could be attributed to enhance the surface properties of $TiO_2$. However, 30 wt. %, of $LiNO_3$ and 600 ºC of calcination temperature has shown the highest activity for FAMEs formation

due to the formation of $Li_2TiO_4$. The obtained 30LT600 catalyst exhibited high catalytic performance for biodiesel production under the optimum transesterification conditions of 24:1 methanol:oil ratio, with 5% catalyst dosage, for the reaction time of 3 hours at 65 ºC of reaction temperature and up to 98% conversion to FAMEs was achieved for fresh canola oil. The kinetics of reaction provided evidence that the normal conditions of temperature and pressure could be employed to carry out the transesterification process by 30LT600. The synthesized catalyst was used for transesterification process of waste cooking oil also and obtained 91.73% of conversion to FAMEs. The catalyst reusability studies showed that the activity of catalyst decreased upon successive runs of used mainly due to pore-filling by organic materials, i.e. triglyceride and glycerol as approved by TGA/ DSC analysis and also because of $Li^+$ leaching.

# CHAPTER 5

# Development of a lithium based chicken bone (Li-Cb) composite

# as an efficient catalyst for biodiesel production

## 5.1 Introduction

Energy scarcity is one of the most important global issues challenging the developed world. The rapid growth of population and increasing the demand for energy to meet the high standards of human life in the developed era has drawn the attention to explore new sources of energy. The conventional sources of energy could be classified into three major types: petroleum, natural gas and coal, which are facing the risk of depletion in the near future as well as causing the ecological issues. The emission gases from the conventional fuels are threatening to the environment and contributing to the global warming and climate change [214]. Biodiesel, which is chemically defined as mono-alkyl fatty acid esters, has appeared as a promising fuel candidate [61]. It is a biodegradable, non-toxic and renewable fuel, moreover, it could be used directly or blended with fossil based fuel in diesel engines [215].

Biodiesel is produced via catalytic transesterification process between methanol or ethanol and oil (vegetable oil or animal fat). Previously, the homogeneous (acid/base) catalysts (e.g. KOH, NaOH, HCL and $H_2SO_4$) were widely utilised for biodiesel production. These catalysts performed well in terms of reaction time and operating conditions. However, for the case of alkali (base) catalysts the presence of water or free fatty acid in the feedstock causes formation of soap which consumes the catalyst and negatively affects the yield, while the acid catalysts have relatively slower reaction rate [216].

Moreover, washing and purification of the crude product are required to separate trace concentrations of unreacted triacylglycerols, partially reacted diacylglycerols and monoacylglycerols, glycerol and methanol, which result in wastewater and increase the production cost of biodiesel [59,217]. Heterogeneous catalysts have gained a significant interest. They can be simply separated from the reaction mixture and reused which in turn simplifies the biodiesel process and eliminates the downstream processing steps. Moreover,

heterogeneous catalysts are environmental friendly in nature and have attracted researchers' attention [218].

The reaction mechanisms of heterogeneous and homogeneous catalysts are similar. The mechanism of catalytic transesterification reaction is described by the disassociation of catalyst and methanol to release $CH_3O$ (methoxide anion) from the reaction of methanol ($CH_3OH$) and a hydroxide ion ($OH^-$). The carbonyl carbon of the triglyceride is attacked by the anion ($CH_3O$) in three steps to produce a mole of methyl ester along with di-glyceride and/or mono-glyceride in the first and second step. Finally, after the third step, three moles of methyl ester and a mole of glycerol are formed [219]. Solid or heterogeneous catalysts could be obtained from various sources such as biomass and waste substances.

In order to reduce the biodiesel production cost and avoiding accumulation of wastes in the environment, other green and sustainable sources of heterogeneous catalyst for biodiesel production have been suggested and investigated such as eggshells, seashells and stones (limestone) [128]. Moreover, animal bones which consist of organic (30%) and inorganic compounds (70%), are available frequently and can be a good source for calcium and phosphorus oxide [220]. Table 5-1 summarized some investigations for biodiesel production from nature sources.

In this chapter, chicken bone (Cb) was applied as catalyst after loaded with lithium nitrate to investigate the potential of lithium based chicken bone (Li-Cb) catalyst for biodiesel production from canola oil as a cost effective and efficient heterogeneous catalyst for biodiesel production. The impact of lithium impregnating amounts and calcination temperature were investigated and the reaction kinetics was studied in details. In addition, the reaction conditions and the reusability have been also addressed.

**Table 5-1:** Modified waste materials derived catalyst for FAMEs production.

| Type of the catalyst | Feedstock | Reaction conditions | Conv.[**]/yield[*](%) | Ref. |
|---|---|---|---|---|
| 30%CaO-CeO$_2$/HAP-650 (HAP[***] from pig bone) | Refined palm oil | Cat. dosage=11 wt.%  methanol:oil molar ratio =9:1, temp.=65 ºC, time=3 h | 91.8%[*] | [221] |
| C900 (Chicken bone) | Waste cooking oil | catalyst loading= 5.0 g methanol:oil molar ratio=15:1, temperature= 65 ºC, time= 4 h | 89.3%[*] | [127] |
| Waste animal bones calcined at 800 ºC | Palm oil | catalyst dosage=20 wt.%, 18:1 methanol:oil molar ratio=, stirring 200 rpm, temperature=65ºC, time= 4 h | 96.8%[**] | [134] |
| calcined waste chicken bone at 800 °C for 5 h | Waste cooking oil | catalyst dosage=3.0 wt%, methanol:oil ratio= 3:1, temperature= 80 °C, time=3h | 96.3%[*] | [128] |
| Waste shells of mollusk and egg 800 ºC for 4 h | palm olein oil | catalyst amount= 10 wt.%, methanol/oil molar ratio = 12:1, temperature = 60 ºC, time= 2 h | > 95%[*] | [222] |
| ostrich-eggshell derived CaO | waste cooking oil | Catalyst=1.5 wt.%, methanol/oil molar ratio = 12:1, temperature=65 ºC time= 2 h, speed=250 rpm | 96%[*] and 94%[*] for calcined ostrich- and calcined chicken-eggshells | [217] |
| 2%Li doped egg shell derived CaO | Nahor oil (*M. ferrea* Linn) | catalyst amount=5 wt.%, methanol:oil ratio= 10:1, temp.=65 °C, time=4 h | 94%[**] | [104] |
| acid-treated quail eggshell catalysts (Qes-2 h) | palm oil | oil/catalyst weight ratio= 2/0.03, methanol/oil molar ratio= 12/1, temp.= 65 ºC | 98%[**] | [131] |
| 2 g LiNO$_3$/Chicken bone calcined at 850 ºC (2Li-Cb850) | Fresh and used canola oil | catalyst amount=4 wt.%, methanol:oil ratio= 18:1, temp.=60 °C, time=3 h | 96.6%[*](fresh oil) 94.9%[*](used oil) | this study |

[***]HAP: hydroxyapatite Ca$_5$(PO4)$_3$(OH)

## 5.2 Materials and methods

Chapter 3 fully described the experimental set-up, procedure, analytical methods and characterisations. Transesterfication chemicals and feedstock are provided in Section 3.2.1.

Chemicals for catalyst preparation and analysis are given in Sections 3.2.2 and 3.2.3. Preparation method of catalyst (Li-Cb) is described in Section 3.3.2. Sections 3.4.1-3.4.6 provide the catalyst characterizations. The experimental set-up and transesterfication process are detailed in Section 3.5. The investigated transesterfication parameters are fully described in Sections 3.6.1-3.6.4 and the ranges of catalyst dosage (wt. %), MeOH: oil molar ratio, reaction time (h) , and reaction temperature (ºC) were 1- 5, 12:1-20:1, 1 - 3.5, and 40- 60, respectively. Regarding catalyst reusability please refer to Sections 3.7. Sections 3-8.1- 3.8.3 describe the analytical procedures and conversion to FAMEs estimation.

## 5.3 Results and Discussion

### 5.3.1 Surface area analysis and the basicity

The surface area of the catalyst is one of the important parameters that can significantly affect the catalyst activity. Table 5-2 presents the BET surface area and basic strength of chicken bone and Li loaded chicken bone samples. The obtained surface area in this investigation did not show a trend, with the increase of the lithium amount in the catalyst. This might have happened either due to the blocking of pores after lithium insertion resulting in reduction of the surface area [223] or lithium was combined with the supporting materials which led to increase the surface area [204]. However, the impregnation of different amount of lithium on the chicken bone did not show any significant changes on the surface area of the prepared catalysts. Moreover,

the surface area is reduced from $8.62m^2/g$ to $2.58m^2/g$ with increase of the calcination temperatures from 750 to 900 °C, respectively (Table 5-2). Based on the results, phase crystallization changing and sintering process were induced accordingly with increasing the calcination temperature and led to significant reduction of the surface area [203]. The basic strength was measured as described previously in Section 3.4.6. The prepared catalysts retained higher basic strength than the raw chicken bone. As can be seen from Table 5-2, increasing the loaded amount of lithium from (0 to 2 g) resulted in increasing the basic strength from $7.2 < H\_ < 9.8$ to $15.0 < H\_ < 18.4$. However, the basicity was decreased beyond 2 g of loaded amount of lithium whereas 3Li-Cb850 sample with 3 g of loaded lithium showed less basic strength ($9.8 < H\_ < 15.0$) which reflected in lower FAME content. The reason is the overloaded amount of lithium covered the basic sites of catalyst and hindered the reactants from access the catalyst active sites. This could explain the decreasing of catalytic activity [224,225]

**Table 5-2:** Results of BET surface area (S.A) and basic strength of the synthesized catalysts.

| S. No. | Catalyst type | BET S.A ($m^2/g$) ± SD[1] | Basic strength (H\_) |
|---|---|---|---|
| 1. | 0Li-Cb850 | 4.68± 0.001 | $7.2 < H\_ < 9.8$ |
| 2. | 1Li-Cb850 | 5.92± 0.001 | $9.8 < H\_ < 15.0$ |
| 3. | 2Li-Cb850 | 4.00± 0.13 | $15.0 < H\_ < 18.4$ |
| 4. | 3Li-Cb850 | 5.02± 0.10 | $9.8 < H\_ < 15.0$ |
| 5. | 2Li-Cb750 | 8.62± 0.10 | $6.8 < H\_ < 7.2$ |
| 6. | 2Li-Cb800 | 3.97± 0.05 | $9.8 < H\_ < 15.0$ |
| 7. | 2Li-Cb900 | 2.58± 0.11 | $9.8 < H\_ < 15.0$ |

[1]SD: standard deviation

**5.3.2 FT-IR analysis**

The functional groups of the synthesized catalysts were identified using Fourier-transformed infrared (FT-IR) spectroscopy. The spectra of calcined chicken bone (0Li-Cb850) and lithium-based chicken bone samples (1Li-Cb850, 2Li-Cb850, 3Li-Cb850) are presented in Fig. 5.1. The transmittance mode in FT-IR analysis exhibits the presence of carbonate group at around 1410-1455 $cm^{-1}$ and 872 $cm^{-1}$, hydroxide group at around 3500 $cm^{-1}$, which is quite similar to Kong et al. [226], while phosphate group at 1011- 1075 $cm^{-1}$ and at around 962 $cm^{-1}$ as illustrated in Fig. 5.1a. The samples with Li ion loading show new characteristic IR peaks at around 2014-2287 $cm^{-1}$ which are missed in chicken bone FT-IR and could be ascribed to the formation of a new phase of $Li_3(PO)_4$ compound. The FT-IR patterns with regard to calcination temperature are shown in Fig. 5.1b. As can be seen there is no big difference between the patterns. However, the peak of carbonate group became weaker with increasing the calcination temperature of the samples from 750 to 900 °C.

### 5.3.3 TGA/DSC analysis of Li based chicken bone catalyst

Fig. 5.2 shows the TGA/DSC analysis of pre-calcined 2Li-Cb. As can be seen there are some weight loss stages in TGA curve along with endothermic peaks in DSC curve. Adsorbed water and organic materials were removed from the parent catalyst below 600 °C, while the endothermic peaks at 600 °C and 800 °C are attributed to the decomposition and interfering of $LiNO_3$ with inorganic residue of chicken bone (hydroxyapatite). Furthermore, TGA curve is almost constant above 850 °C, which reflected that the decomposition process has completed and the later temperature 850 °C was selected as the consistent temperature for calcination [131].

### 5.3.4 X-ray diffraction and FE-SEM

Powder X-ray diffraction patterns for (0Li-Cb850, 1Li-Cb850, 2Li-Cb850, 3Li-Cb850) are presented in Fig. 5.3. The XRD patterns of chicken bone (0Li-Cb850) showed that hydroxyapatite is the major component which acts as a base material [127].
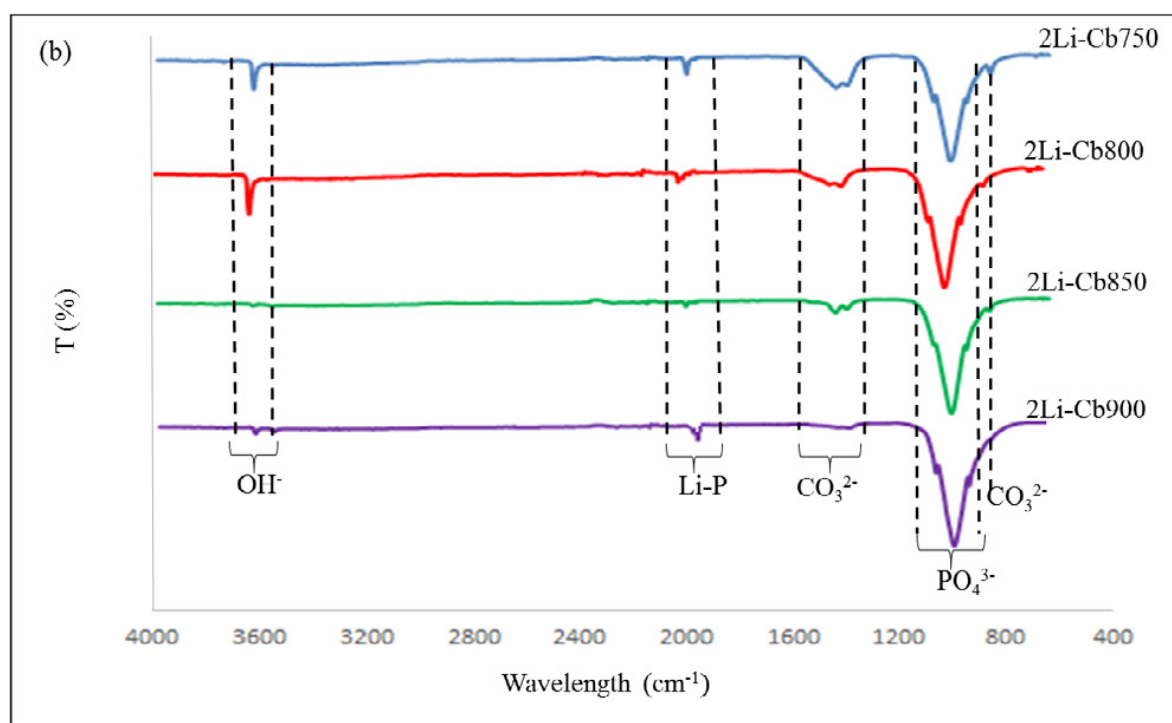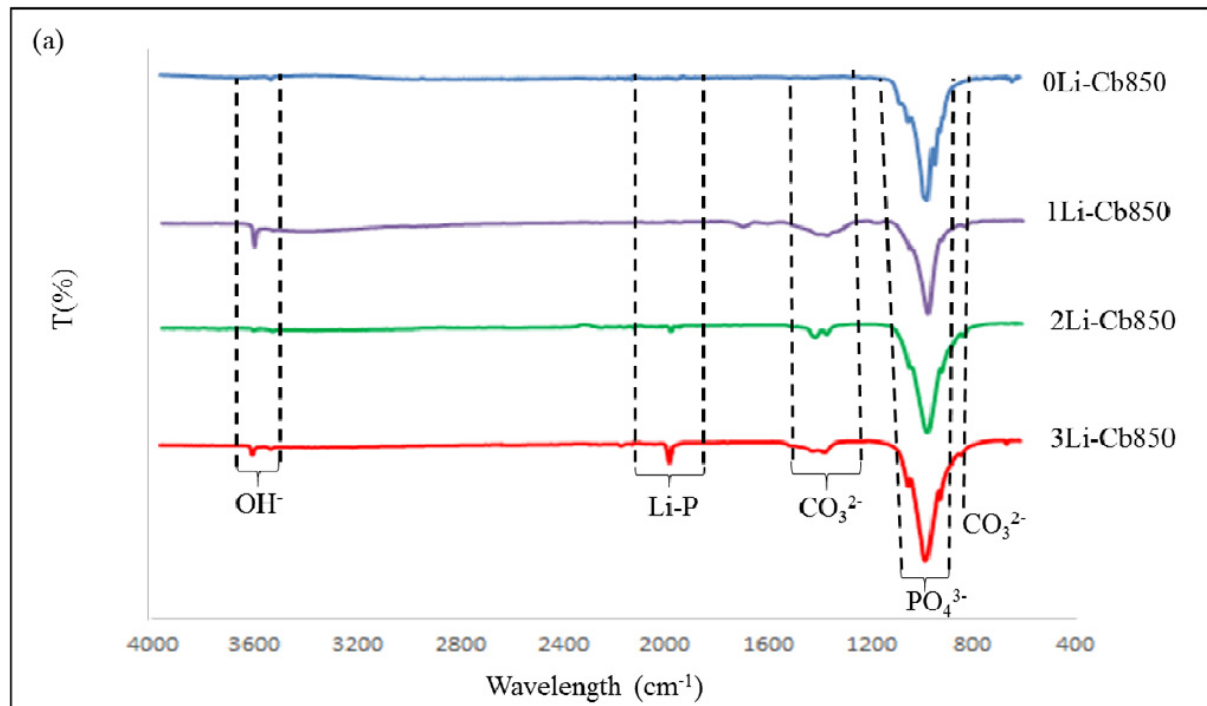
**Fig. 5.1**. FT-IR spectra of (a) different Li impregnated amount; (b) different calcination temperatures.
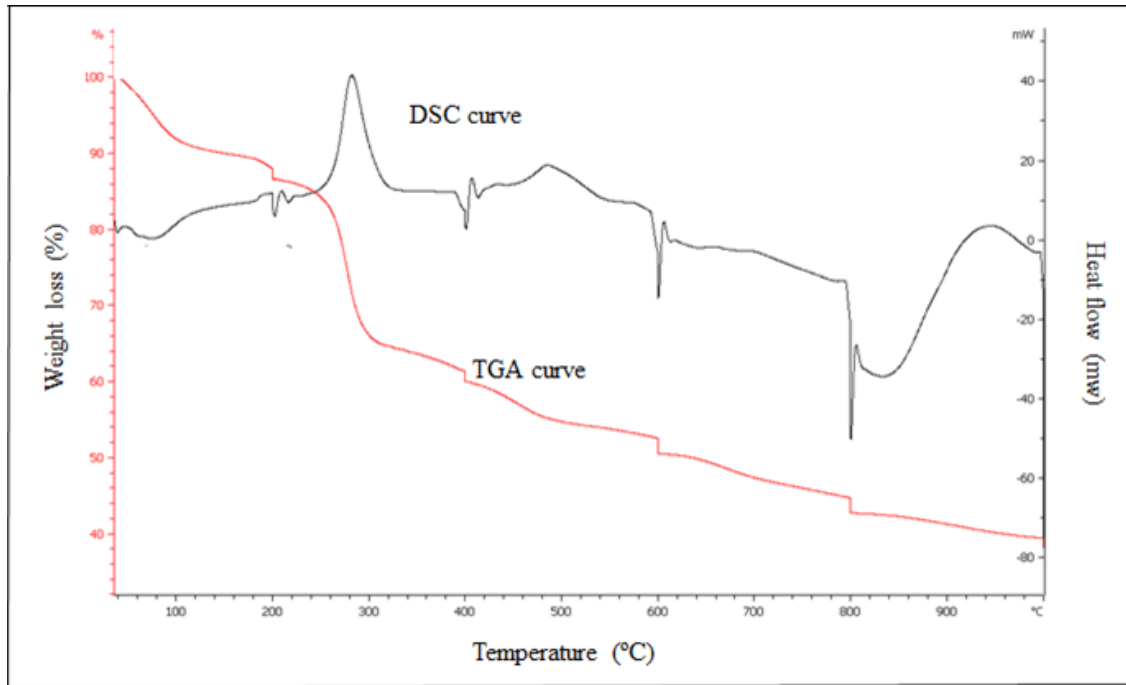


**Fig. 5.2.** TGA/DSC analysis of pre-calcined 2Li-Cb.

In addition, new peaks have been observed for (1Li-Cb850, 2Li-Cb850, 3Li-Cb850) at $2\theta$ of 16.95º, 22.36º, 23.2º, 24.83º, 34.78º, 36.41º, 36.49º, and 61.06º which can be attributed to the lithiophosphate as a result of combination of lithium with the chicken bone. Furthermore, XRD shows CaO peaks at $2\theta$ of 32.93º, 37.41º, 53.95º, 64.29º and 67.39º where its crystallization has been enhanced by insertion of Li to the chicken bone structure. However, the intensity of CaO peak was decreased by increasing the amount of lithium above 2 g. Fig. 5.4 shows the micro-structural (FE-SEM) images of chicken bone (0Li-Cb850) and 2Li Cb850 catalyst indicating the formation of rod-like grains when Li was loaded on the chicken bone (Fig. 5.4b) while the latter without Li addition (Fig. 5.4a) has dense small spherical grains.
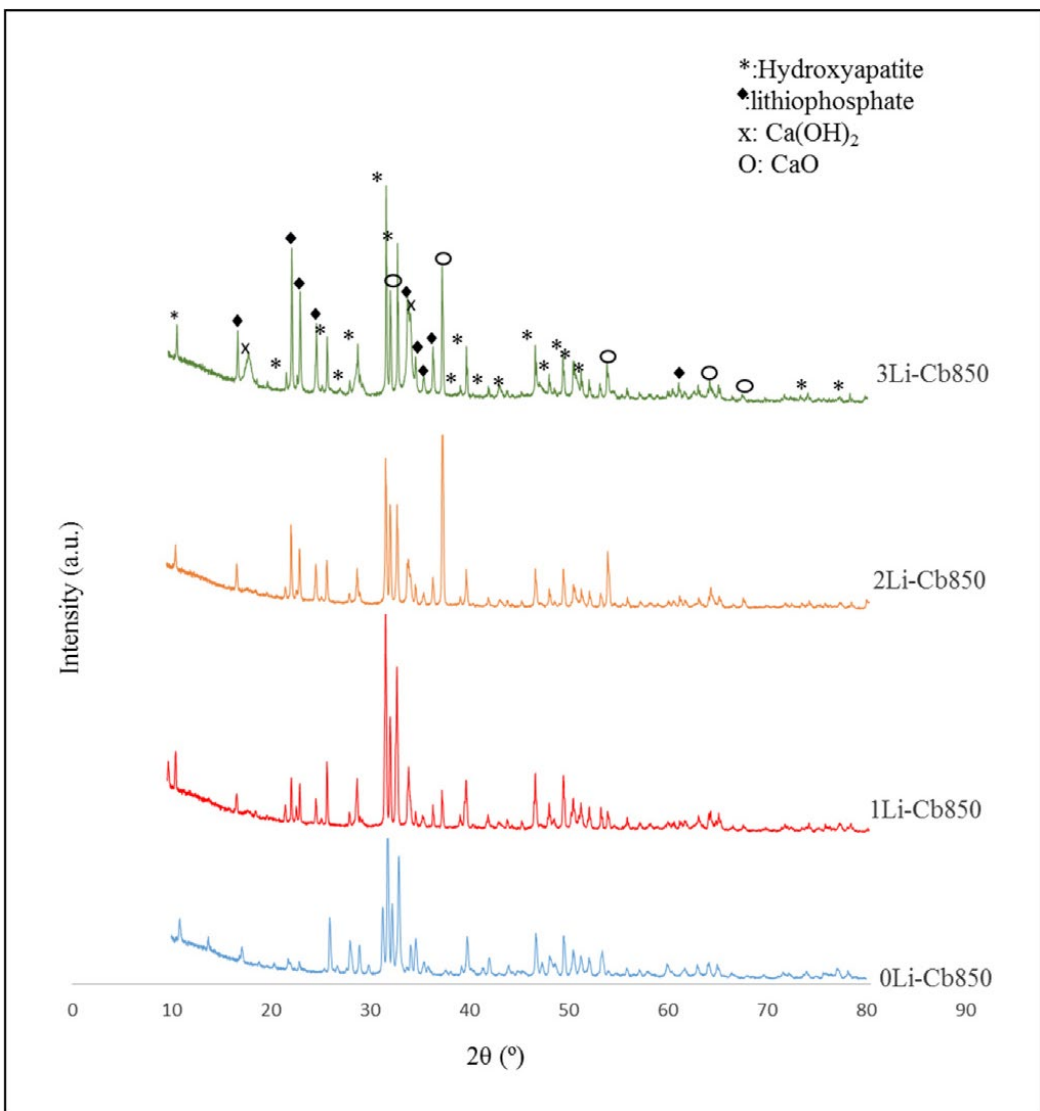
**Fig. 5.3**. XRD analysis for xLi-Cb850, (x -lithium nitrate amount; 0-3g).
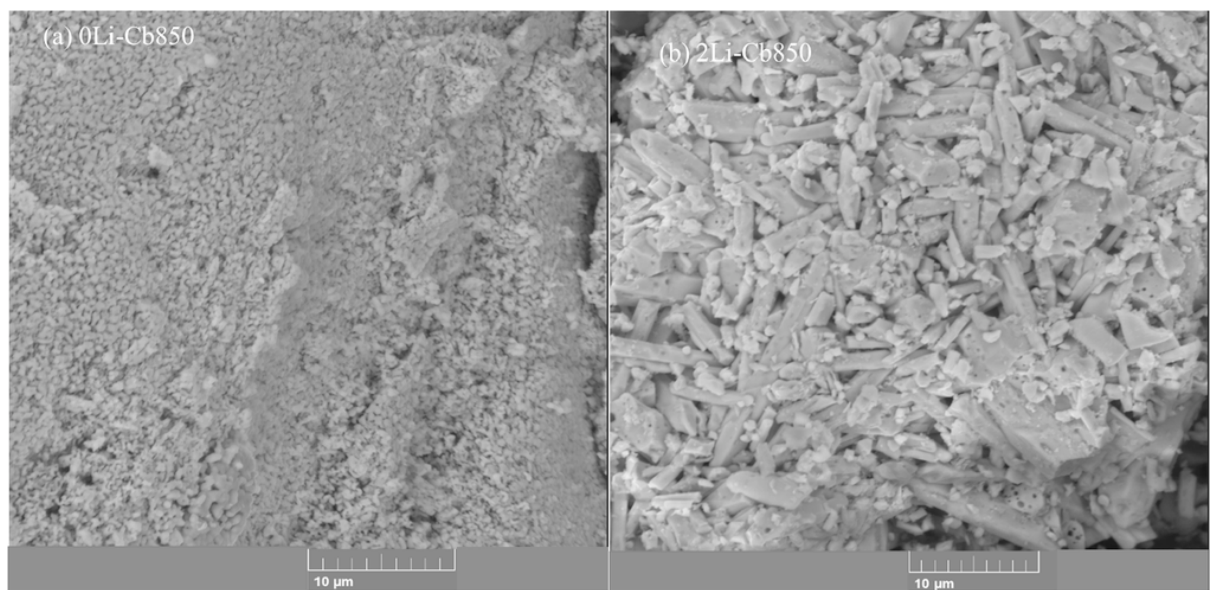


**Fig. 5.4.** FE-SEM analysis of (a) 0Li-Cb850; (b) 2Li-Cb850.

## 5.3.5 Impact of Li loading on chicken bone and reaction time

Fig. 5.5 shows the influence of different transesterification time (1-3.5 h) on the FAME content for different Li loaded catalyst (0Li-Cb850, 1Li-Cb850, 2Li-Cb850, 3Li-Cb850) calcinated at 850 °C. The results show that the highest FAME content is for the 2 g of lithium nitrate (2Li-Cb850) at 3 h of reaction time, which could be crediting to the higher basicity of 2Li-Cb850 (Table 5-3). The possible reason for the decreasing of catalyst activity with increasing the lithium amount is the lithium penetration through the Cb in different ways depending on the uptake level of Cb towards lithium. The lithium was well dispersed on the surface of Cb at low concentration of lithium nitrate, but at higher concentration of lithium nitrate the lithium ions deposited on the surface of Cb and blocks the active sites [203]. Thus, 2Li-Cb850 was chosen for further investigation.
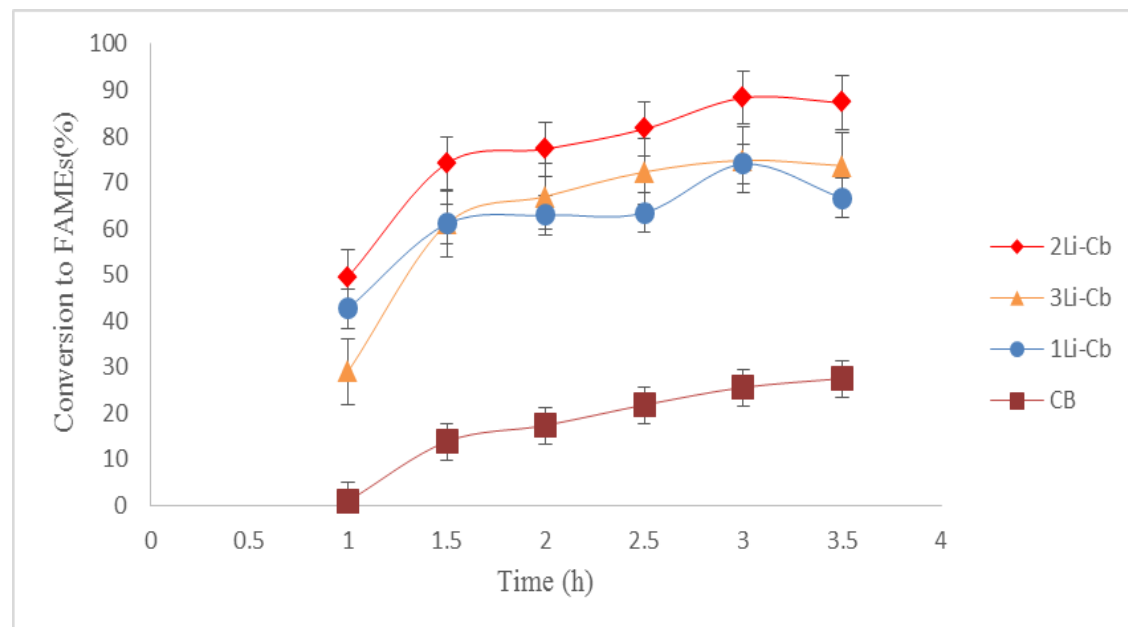


**Fig. 5.5.** The effect of different amounts of lithium nitrate loaded on chicken bone calcined at 850 ºC.

## 5.3.6 Impact of calcination temperature

The calcination temperatures of catalyst were investigated to optimize the synthesis of catalyst for higher FAME content and consequently four different temperatures (750 ºC, 800 ºC, 850 ºC and 900 ºC) were tested and the results are illustrated in Fig. 5.6. The FAME content is increased with increasing the calcination temperature from 750 ºC to 850 ºC then lowered down at 900 °C. The surface area and basicity of the catalyst could be affected by calcination temperatures, which consequently affect the catalyst efficiency. The reduction in the FAME content with further increasing in the calcination temperature up to 900 °C is due to occurrence of sintering of the catalyst [134].

## 5.3.7 Transesterification reaction condition

## 5.3.7.1 Impact of reaction time

Fig. 5.5 depicts the impact of reaction time on transesterification reaction of canola oil in the presence of 2Li-Cb850 catalyst. The duration of reaction time was varied from 1 to 3.5 h and the samples were withdrawn every 30 min at 3% catalyst loading and 60 °C of reaction temperature and 12:1 of methanol:oil molar ratio. The FAME content was increased with extending the reaction time and achieved the highest content at 3 h of reaction time then it was remained almost constant afterward. This behavior could be explained as the reaction reached to the equilibrium state as discussed by Wang et al. [227] earlier
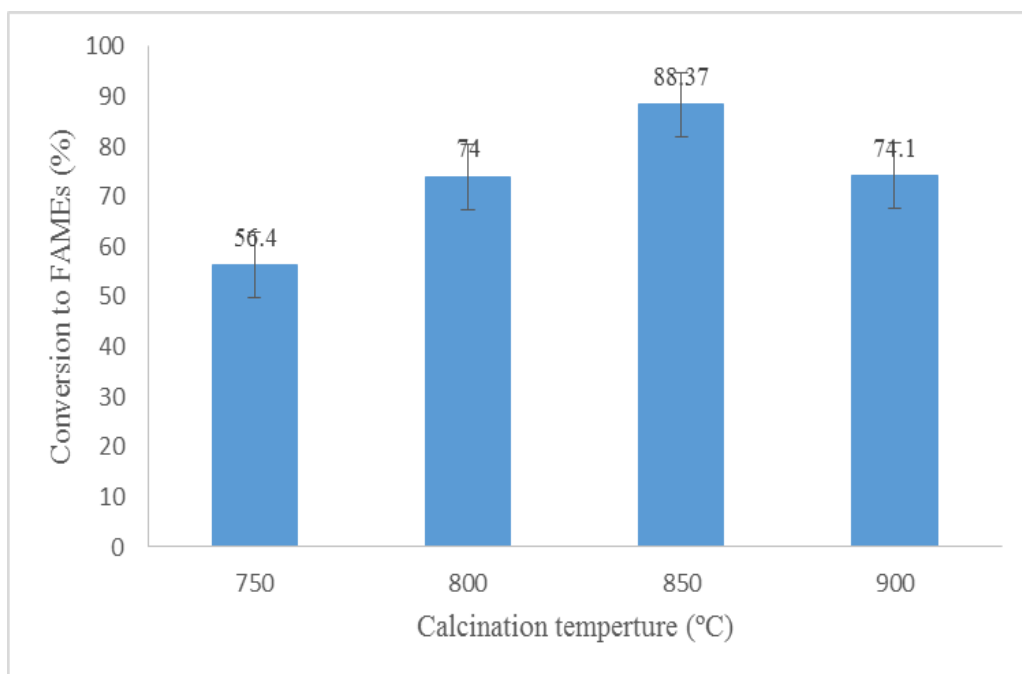
**Fig. 5.6**. The effect of different calcination temperature for 2Li-Cb.

**5.3.7.2 Impact of catalyst dosage**

The influence of catalyst dosage was studied on the transesterification of canola oil at 60 °C and 12:1 of methanol to oil ratio using the 1, 3, 4, and 5wt % of 2Li-Cb850 catalyst. Fig. 5.7 shows with low amount of catalyst, the FAME content was low (62.6%) which was attributed to the lack of the active sites in the reaction medium [223] and beyond 4wt %, the content was decreased due to the formation of soap resulting from increasing the viscosity of the reactants which suppressed the reaction [182]. Hence, 3wt % of the catalyst dosage was the optimum value for the reaction and for optimizing the other reaction parameters.
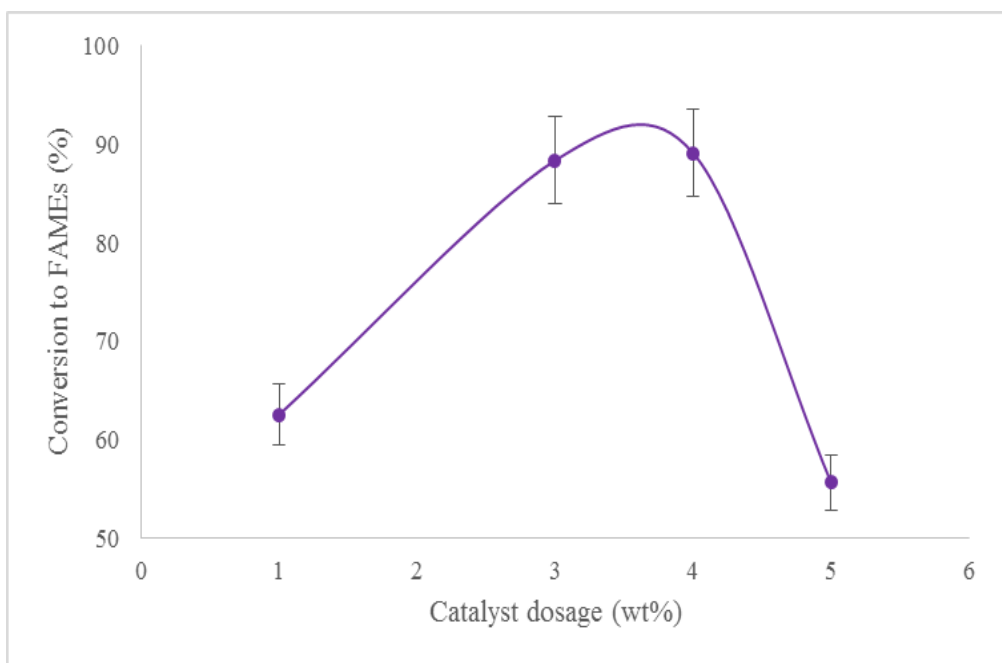
**Fig. 5.7**. The impact of catalyst dosage on transesterification.


### 5.3.7.3 Impact of methanol: oil molar ratio

The transesterification is a reversible reaction so, excess amount of methanol is employed to shift the reaction forward and enhance the FAME content. However, increasing the methanol:oil ratio beyond the optimal ratio will not increase the conversion, but will increase cost for excess methanol recovery [228]. As indicated in Fig. 5.8, the FAME content increased with increasing the methanol:oil ratio within the range of 12:1 (89.1%) to 18:1 (98.3%). While the highest ratio (20:1) had the lowest FAME content (69.8%) because excessive methanol diluted the reaction between the catalyst and reactant and shifting the reaction towards the reactants [217,229]. Therefore, 18:1 is the appropriate methanol/oil ratio for this reaction.
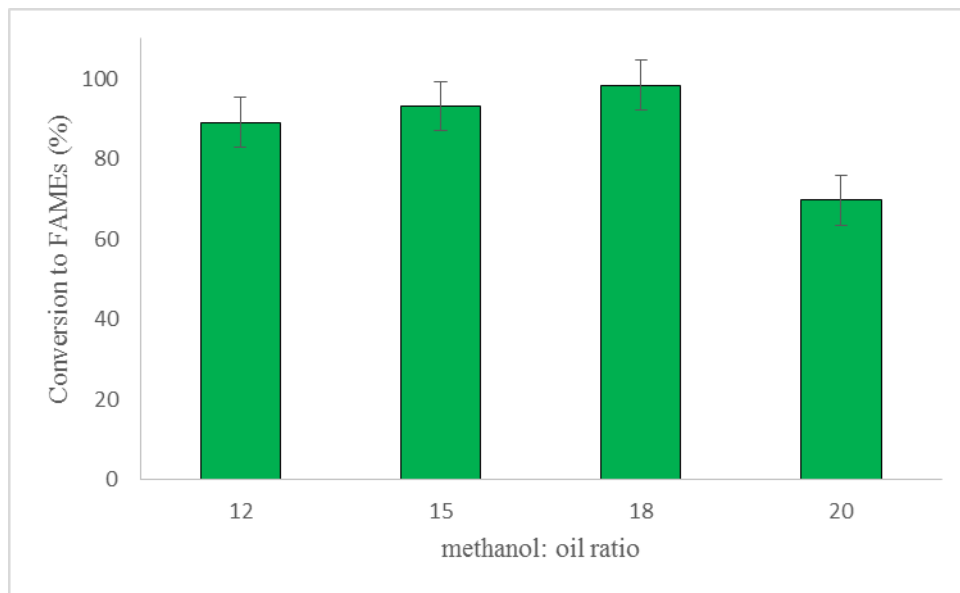
**Fig. 5.8**. The impact of methanol: oil molar ratio on transesterification.

### 5.3.7.4 Impact of reaction temperature

Fig. 5.9 illustrates the impact of reaction temperature on the transesterification at different reaction time. The reaction was carried out at 18:1 of methanol:oil molar ratio, 3% of catalyst dosage and reaction time duration in range from 1 to 3.5 h. The reaction temperature was studied at 40, 50 and 60 °C. The highest FAME content of 96.6% was achieved at 60 °C and stabilized at 3 h. According to the kinetic study, raising the molecular collision and declining the activation energy limitation could have occurred with increasing the reaction temperature as a result of enhancing the reaction rate [230].

### 5.3.8 Reusability

It was shown in Fig. 5.10 that the FAME content of 96.6, 90.5, 86.1, 84.7 and 82% were obtained for five consecutive cycles of the canola oil transesterification using regenerated 2Li-Cb850. Indicating that the catalyst could be reusable at least 5 times with a 6e15% FAME drop from the 96.6% FAME obtained over fresh catalyst. The

decay in the synthesized catalyst activity after each cycle could be attributed to the settling of the reaction product and by product (biodiesel and glycerol) or un-reacted oil deeply on the active sites of the catalyst surface which resulted in obstruction the reactants access to the active basic sites [231]. However, the FAME content by reused catalyst was quite high along the five consecutive cycles which means this catalyst could attain its activity for more than five cycles before losing its activity.
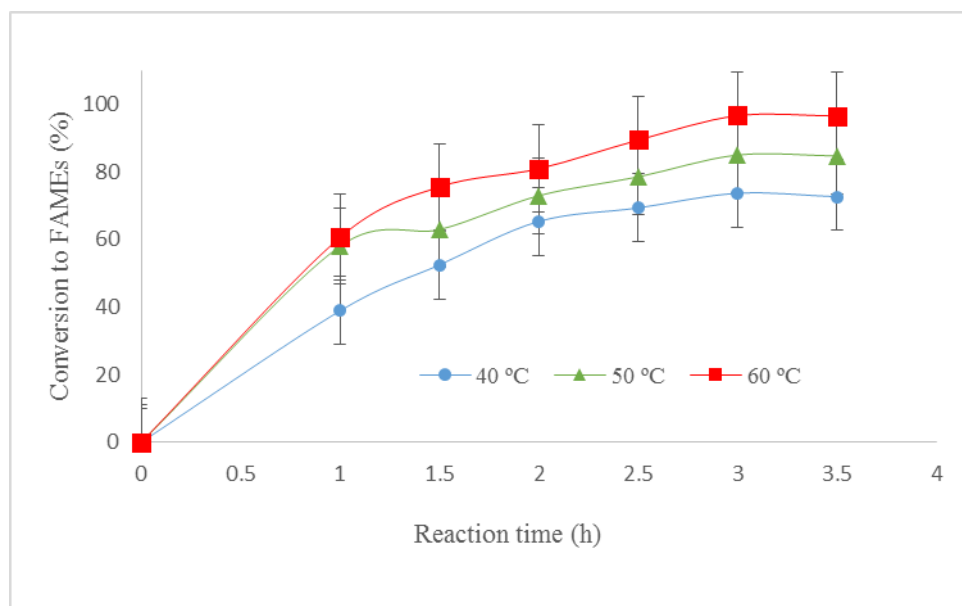


**Fig. 5.9**. The impact of reaction temperature on transesterification.
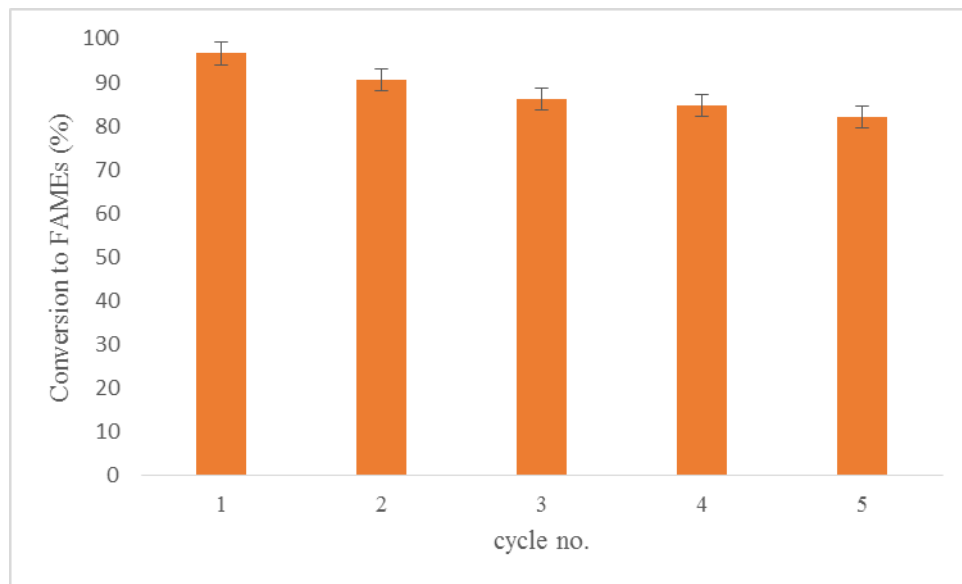


**Fig. 5.10**. Reusability of 2Li-Cb850 catalyst.

101

**5.3.9 Transesterification of waste and fresh canola oil**

Production of biodiesel from food grade oils is the main obstruction in the marketing of biodiesel due to the high cost of edible oil. Hence, replacement of fresh oil with lower cost oil is a substantial solution for a cost effective biodiesel production. Waste cooking oil is being produced in huge amount every year across the world. Waste cooking oil could cause several problems such as blocking the drains and contaminating the aquatic habitat [210-212]. On the other hand, waste cooking oil could be adapted as a feedstock for biodiesel synthesis at lower cost.

Consequently, to figure out the ability of 2Li-Cb850 catalyst for FAMEs production from waste canola oil, experiment was conducted under the same optimum conditions applied for transesterification of fresh canola oil (60 °C reaction temperature, methanol:oil ratio of 18:1, 3% of catalyst loading for 3 h of reaction time).

The FAME content produced under the same aforementioned conditions and using the catalyst 2Li-Cb850 was 94.9% and 96.6% for used and fresh canola oil, respectively, Fig. 5.11. In this study, the difference in the obtained FAME contents was mainly due to the different acid values of both fresh and waste canola oil used. The acid value of fresh and waste canola oil was 0.072 mgKOH $g^{-1}$ and 3.67 mgKOH $g^{-1}$, respectively. It's worth mentioned here, that different type of oils have different physico-chemical properties which lead to different performance using the same catalyst and under the same conditions. The presence of water or free fatty acid decreases the reaction rate and/or prolong the reaction time to reach the highest conversion or yield [163, 232, 233].
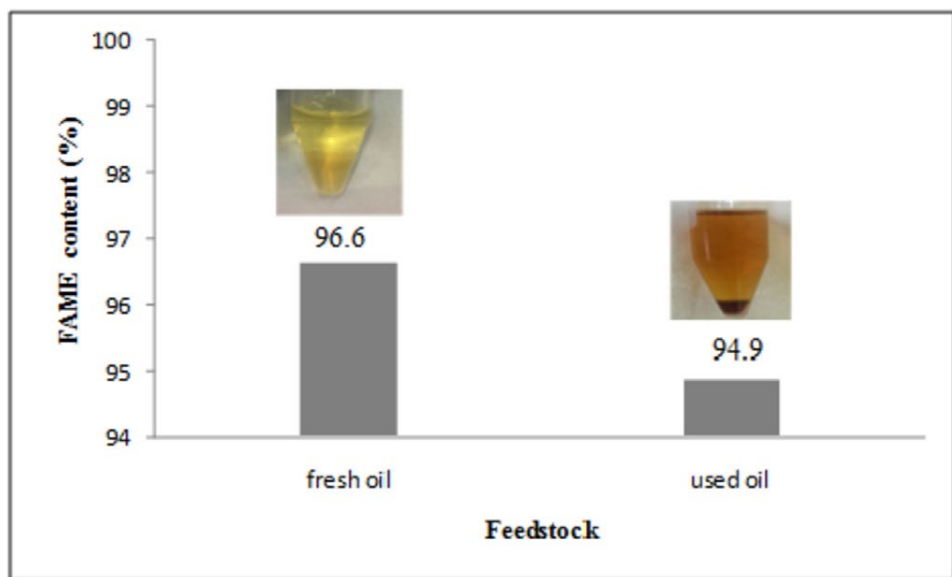
**Fig. 5.11.** Investigation the potential of 2Li-Cb850 catalyst to produce FAMEs from fresh and used canola oil.

### 5.3.10 Kinetic studies

In order to understand the transesterification kinetic of the Li based chicken bone catalyst at different reaction time and temperatures. Zero and pseudo first order kinetic models (as represented by Eqs.4-1 and 4-7, respectively) were fitted to the experimental results.

The assumptions considered for these two models (Eqs.4-1 and 4-7) are: (i) Using excess methanol in the reaction to accelerate the forward reaction to displace the equilibrium towards the FAMEs formation and reduce the extension of the reverse reaction due to the fact that the reaction rate constants are independent on the concentration of methanol. (ii) By assuming that the intermediate reactions are much faster than this one, the transesterification process could be considered as a single step [180].

$$\frac{dx}{dt} = K_{Me} \qquad\qquad (4\text{-}1)$$

$$-\ln(1 - X_{Me}) = kt \qquad\qquad (4-7)$$

Where $K_{Me}$ and $k$ are the reaction rate constants for the zero and first order, respectively, x is the conversion to FAMEs, and t is the reaction time. The rate constant ($K_{Me}$) was obtained by drawing the conversion to FAMEs ($X_{Me}$) against the reaction time ($t$) (Fig. 5.12a), while $k$ was evaluated by drawing (-ln(1- $X_{Me}$) vs. $t$) as shown in Fig. 5.12b.
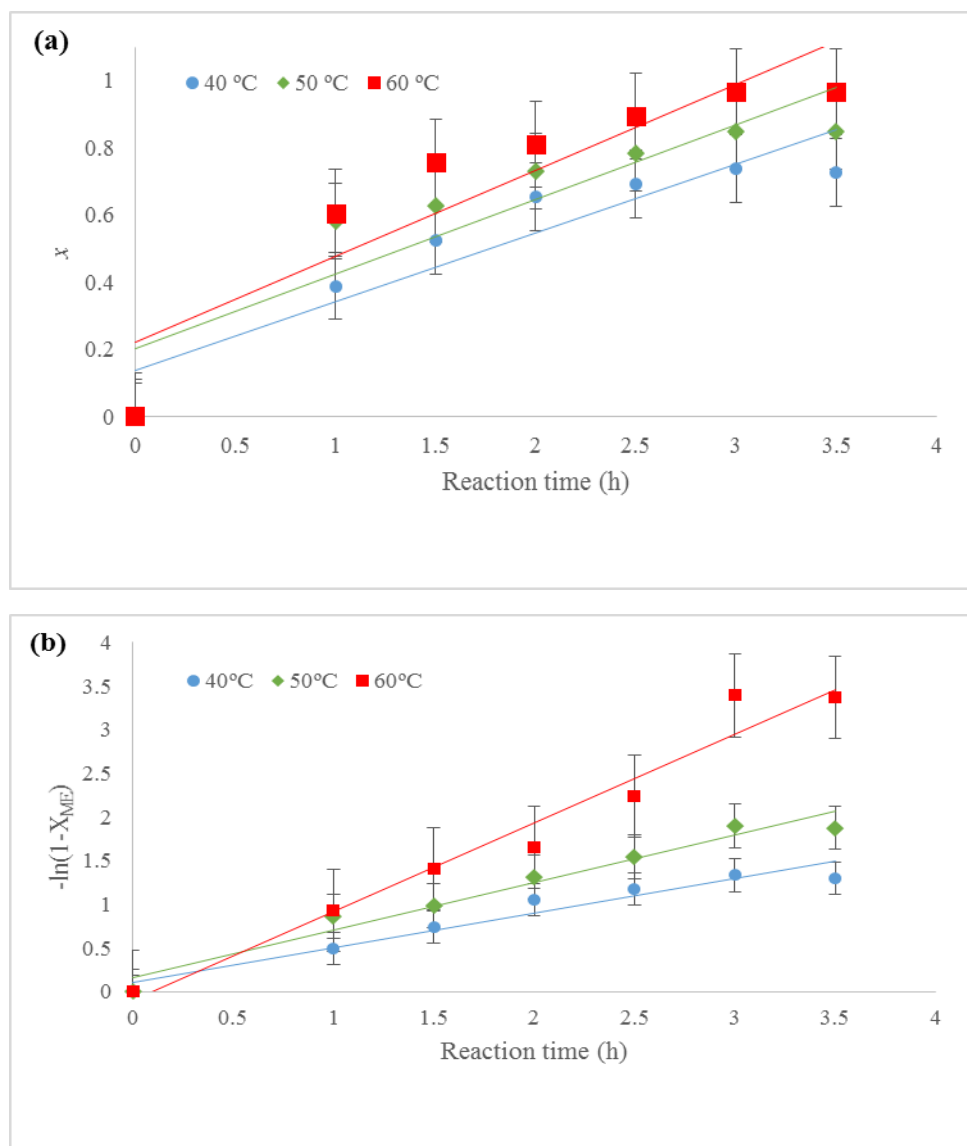


**Fig. 5.12**. Fitting the kinetic models, (a) Zero order model, (b) 1st pseudo order model for transesterification of canola oil.

The obtained results summarized in Table 5-3 suggest that pseudo first order model is the best fit for canola oil transesterification. Table 5-3 also reveals that the reaction rate constants increase with increasing the reaction temperatures. These results could be discussed as the collision of molecules has been promoted by increasing the reaction temperatures and resulted in declining the limitation of mass transfer.

**Table 5-3:** Reaction temperatures, rate constants and $R^2$ values of canola oil transesterification by 2Li-Cb850 catalyst.

| Temperature (ºC) | Rate constant (K) | | | $R^2$ | |
| --- | --- | --- | --- | --- | --- |
| | Zero order | Pseudo first order | | Zero order | Pseudo first order |
| 40 | 0.21 | 0.40 | | 0.87 | 0.94 |
| 50 | 0.22 | 0.54 | | 0.81 | 0.96 |
| 60 | 0.26 | 1.02 | | 0.83 | 0.96 |

Moreover, since different reaction temperatures have been investigated for the transesterification reaction, determining the activation energy was substantial to study the impact of these temperatures on the reaction rate [180,182,209]. The values of activation energy (*Ea*) and frequency factor (*A*) can be estimated by fitting the experimental results at different temperatures using Arrhenius equation, Eq. (4-9).

$$\ln k = \ln A - \frac{Ea}{RT} \qquad (4-9)$$

Where *Ea, R, k, A, T* are the activation energy (kJ mol$^{-1}$), the universal gas constant (8.314 J mol$^{-1}$K$^{-1}$), the reaction rate constant (h$^{-1}$), a frequency factor (h$^{-1}$) and the reaction temperature (K), respectively. The slope and intercept of the graph between *lnk* and *1/T* (Fig. 5.13) give the values of activation energy and frequency factor. The estimated values for *Ea* and *A* were 16.93 kJ/mol and $2.49 \times 10^6$ h$^{-1}$, respectively. The activation energy for the transesterification of canola oil applying the catalyst (2Li-

Cb850) was lower than the activation energy obtained for base catalyzed transesterification reaction, i.e. 33.6- 84 kJ/mol [182,209], indicates that the transesterification is much easier to carry out under the catalyst (2Li-Cb850) than the regular base catalyst.
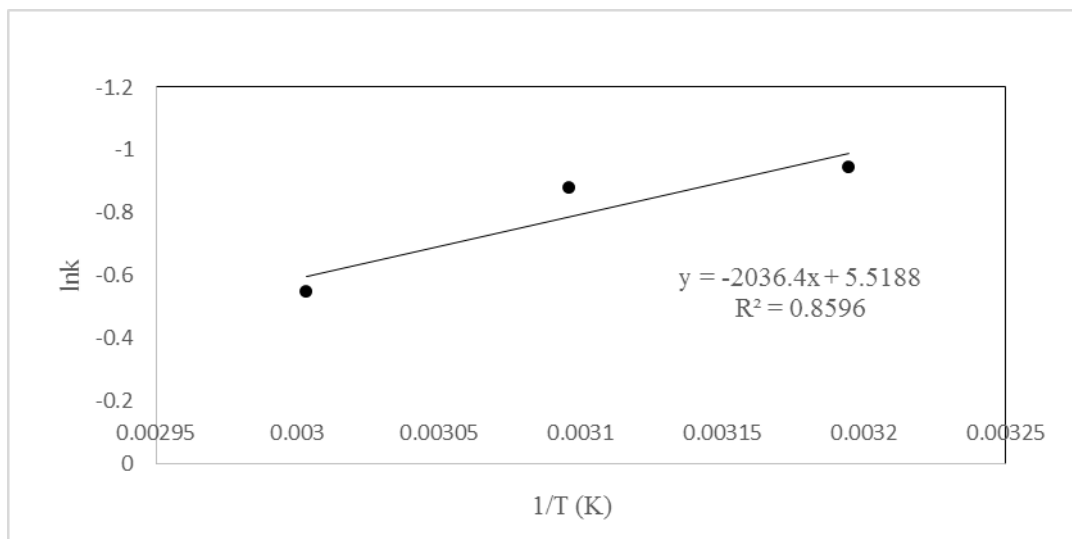


**Fig. 5.13.** The activation energy of pseudo 1st order model.

## 5.4 Summary

The activity of lithium based chicken bone (Li-Cb) composite as a solid catalyst for biodiesel production was investigated in this research. The impregnation method was employed to integrate Li ions on the chicken bone and the efficiency of modified catalyst was evaluated at mild temperature and pressure (60 °C and 1 atm.). The 2 g of LiNO3 loaded on chicken bone (Cb) and calcined at 850 °C (2Li-Cb850) catalyst revealed to be an efficient catalyst for the transesterification process of canola oil for the production of biodiesel. The main reason of the catalyst reactivity could be attributed to the enhancement of the basicity of chicken bone by addition of lithium. The prepared (2Li-Cb850) catalyst was employed for transesterification of fresh and waste canola oil and the FAME content was 96.6% and 94.9%, respectively. The

reusability study revealed good activity for 5 successive runs under the above optimum conditions conducted with fresh canola oil. In addition, the results of the kinetic model were best represented by the pseudo first order model with 0.58 $h^{-1}$ rate constant at 60 °C, and the associated frequency factor and activation energy were 2.49 × $10^6$ $h^{-1}$ and 16.93 kJ/mol, respectively.

# CHAPTER 6

# Transesterfication of waste canola oil by lithium/zinc composite supported on waste chicken bone as an effective catalyst

**6.1 Introduction**

Depletion of fossil fuel reserves, high price of crude oil, environment issues and energy security have inspired the researchers to find a renewable and sustainable alternative fuel [18]. Biodiesel can be considered as a promising and potential source of energy as it is biodegradable, bio-renewable and nontoxic fuel. Biodiesel is a fatty acid alkyl esters and the catalytic transesterification is the common method for biodiesel production [17]. The process comprises of the reaction between vegetable oils or animal fats with short chain of alcohol such as methanol and ethanol in the presence of homogeneous or heterogeneous catalysts [234].

Sodium hydroxide, potassium hydroxide or alkoxides are examples of homogeneous basic catalysts, which are widely used in industrial scale processes owing to the faster transesterification reaction rate comparing to the acid catalysts [235]. However, the difficulties in the catalyst retrieval and generation of waste water in the downstream separation and purification processes are the major drawbacks in the base-catalyzed transesterification processes [102]. Besides, the feedstock quality has a significant effect on the efficiency of the homogeneous alkali-catalyzed process whereas the high content of water and free fatty acids in the oil stocks results in the soaps formation, which in turn cause emulsification, thereby obstructing the product separation and reducing the product yield [6]. To overcome these problems, replacing the homogeneous catalysts by the heterogeneous catalysts is an attractive solution that could reduce the production cost and produce biodiesel in a more environmentally friendly method [59].

Mixed metal oxides, alkali-doped metal oxides and hydrotalcites are heterogeneous catalysts that have been developed for biodiesel production [103, 236-238]. The heterogeneous catalysts have economic and environmental advantages in comparison

with the soluble catalysts such as easy separation from the product mixture and then recycle for the next run of transesterification reaction [239]. The heterogeneous catalysts could by fabricated also from waste or natural materials such as animal bones [134, 240], birds egg, seashells, ashes and rocks [241-244], these have been employed as a solid catalyst for biodiesel production. These green catalysts are eco-friendly and contribute to reduce the biodiesel cost [245]. For instance, Obadiah et al. [134] have investigated the potential of animal bone for biodiesel production from palm oil. Chen et al. [240] prepared a novel solid catalyst, $K_2CO_3$ loaded onto calcined pig bone. The catalyst contains 30% wt. of $K_2CO_3$ loading and calcined at 600 ºC exhibited a high catalytic activity (yield of 96.4%) under the optimal reaction conditions (reaction time of 1.5 h, catalyst loading of 8% wt. and methanol/ palm oil molar ratio of 9:1).

There is a wide spectrum of feedstock that could be used in biodiesel production such as edible and non-edible oils. However, the conflict regarding the food vs the fuel has drawn attention towards using the non-edible oils such as waste cooking oil. The feedstock shares almost 70-95% of the total biodiesel production cost [246]. There are many advantages of utilizing waste oils for biodiesel synthesising: (i) abundantly available, (ii) inexpensive feedstock, and (iii) environmental benefits [40], which could contribute to reduce the cost of biodiesel. Singh et al., [112] demonstrated the biodiesel production from waste frying oil via a novel ß-potassium dizirconate (ß-$K_2Zr_2O_5$) catalyst. Conversion to FAMEs was noticed to be 96.85% at the molar ratio of methanol: oil of 10:1, 4 wt% of catalyst dosage, and reaction time of 2 h at 65 ºC. The biodiesel derived from waste sunflower oil was synthesised by zeolite based catalyst by Al-Jammal et al. [247]. The KOH/TZT (treated zeolitic tuff, TZT) catalyst showed the highest biodiesel yield of 96.7% at the optimum reaction conditions ( 2 h

reaction time, 50 ºC, methanol:oil molar ratio of 11.5:1, stirring speed of 800 rpm, and 335 mm particle size).

Nowadays, the idea of producing biodiesel economically from waste material as a catalyst and waste feedstock is an attractive subject. Agrawal et al. [248] have produced biodiesel form used frying oil by exoskeleton of mollusk as a solid catalyst and resulted in the yield of 92% and conversion of 97.8%. Nair et al. [249] obtained biodiesel yield of >89% and conversion of >97% from waste frying oil after 3 h of reaction time in the presence of 3.0 g of calcium oxide derived from mereterix as a catalyst and methanol:oil molar ratio of 6.03:1. Conventionally, the transesterfication is conducted by the mechanical stirring which needs a longer reaction time to allow the immiscible reactants (oil and methanol) to mix together which put high energy on the process and results in an expensive process. Thus, some techniques have been incorporated to accelerate the reaction and increasing the yield, and saving energy. Ultrasound technique is a felicitous method to form fine emulsions by providing the process an intense mixing of oil and methanol [140,249, 250]. Maghami et al[251] compared the biodiesel production from ultrasonic and conventional process of waste fish oil transesterfication. The results showed that reaction time of ultrasonic method was half the reaction time of the conventional method to reach 87% of FAMEs content at the optimum conditions of 1% of catalyst (KOH), 55 °C of reaction temperature, and 6:1 of alcohol to oil molar ratio.

To the best of the authors' knowledge, no research has been carried out on the influence of loading the chicken bones with zinc or a mixture of zinc and lithium on the biodiesel production using waste cooking oil. Therefore, in this study, the feasibility of loading the waste chicken bone (Cb) with Zn, Li, and Li/Zn for transesterification of waste canola oil will be investigated under different operating

conditions of catalyst dosages, methanol:oil ratio, reaction time and temperature. The reaction kinetics and the catalyst reusability have been also investigated. In addition, ultrasound effect was investigated and the results were compared with the conventional process.

## 6.2 Materials and methods

The experimental set-up, analysis and process procedure are detailed in Chapter 3, specifically transesterfication reactants, preparation and characterization of the applied catalyst, feedstock analysis and sampling. The performance of the applied catalyst (Li/Zn-Cb) was investigated under different conditions: catalyst dosing (1 - 5 %), MeOH:oil ratio (6:1 - 20:1), reaction temperature (40 – 65 °C), reaction time ( 0 - 4 h). The ultrasound experiments were given in Section

## 6.3 Results and Discussion
### 6.3.1 Influence of metal concentrations

Influence of different metals (Zn and Li) and their concentrations on the performance of the chicken bones powder (Cb) have been investigated for transesterification of waste canola oil (WCO) at MeOH:Oil ratio=18:1; 60 ºC; 4% catalyst dosing, and 3 h of reaction duration. The results demonstrated in Table (6-1), show that incorporating the Cb with equal ratios of Li and Zn (Li/Zn-Cb$_2$) enhanced the conversion to FAMEs more than 4 folds to 96 %, which could be attributed to the improving the texture properties of the catalyst as proved by the characterization studies. Therefore, in the following sections, the characterization and performance of Li/Zn-Cb$_2$ will be further investigated under different conditions.

**Table 6-1:** The influence of metals (Li, Zn) concentration on the catalyst activity

| Catalyst | Li:Zn:Cb wt. ratio | Conversion (%) |
|----------|--------------------|----------------|
| Cb | 0:0:7 | 23 |
| Li-Cb | 2:0:7 | 94 |
| Zn-Cb | 0:2:7 | 50 |
| Li/Zn-Cb$_1$ | 1:2:7 | 84 |
| Li/Zn-Cb$_2$ | 2:2:7 | 96 |
| Li/Zn-Cb$_3$ | 2:1:7 | 77 |

## 6.3.2 X-ray diffraction and surface area analysis

The XRD diffraction peaks of chicken bone (Cb) and the metal ion chicken bone based catalysts (Zn-Cb, Li-Cb and Li/Zn-Cb$_2$) are shown in Fig. (6.1). As can be seen that Li/Zn-Cb$_2$ catalyst comprises the diffraction peaks of lithiophosphate at 2 theta of 16.95º, 22.36º, 23.2º, 24.83º, 34.78º, 36.41º, 36.49º, and 61.06º which were noticed also in Li-Cb catalyst. ZnO diffraction peaks at 2 theta of 34.48º, 36.26º, 46.68º, 56.57º, 62.95º, 67.98º and 69.04º were noticed in Zn-Cb catalyst. In addition, the diffraction peaks of calcium zinc oxide phosphate hydroxide were observed at 2 theta of 71.63º, 73.99º, 75.6º, 77.13º and 78.22º as a result of the interaction of the chicken bone with $Zn(NO_3)_2.6H_2O$. Insertion of zinc ion has enhanced the diffraction peaks of lithiophosphate and hydroxyapatite which could be the reason of higher activity of Li/Zn-Cb$_2$. Moreover, the diffraction peaks of metals nitrates ($Zn(NO_3)_2.6H_2O$ and $LiNO_3$ were not observed in the patterns of all the prepared catalysts which could be attributed to the uniform dispersion of the metal ions throughout the surface of chicken bone [252]. The results of surface area, pore volume and pore size of the chicken bone derived catalysts are tabulated in Table (6-2). It is revealed from Table (6-2) that the surface area of the chicken bone (Cb) decreased by inserting lithium or/ and zinc ion into its structure. This is might be owing to the covering the chicken bone's pores with the metal compound [240].
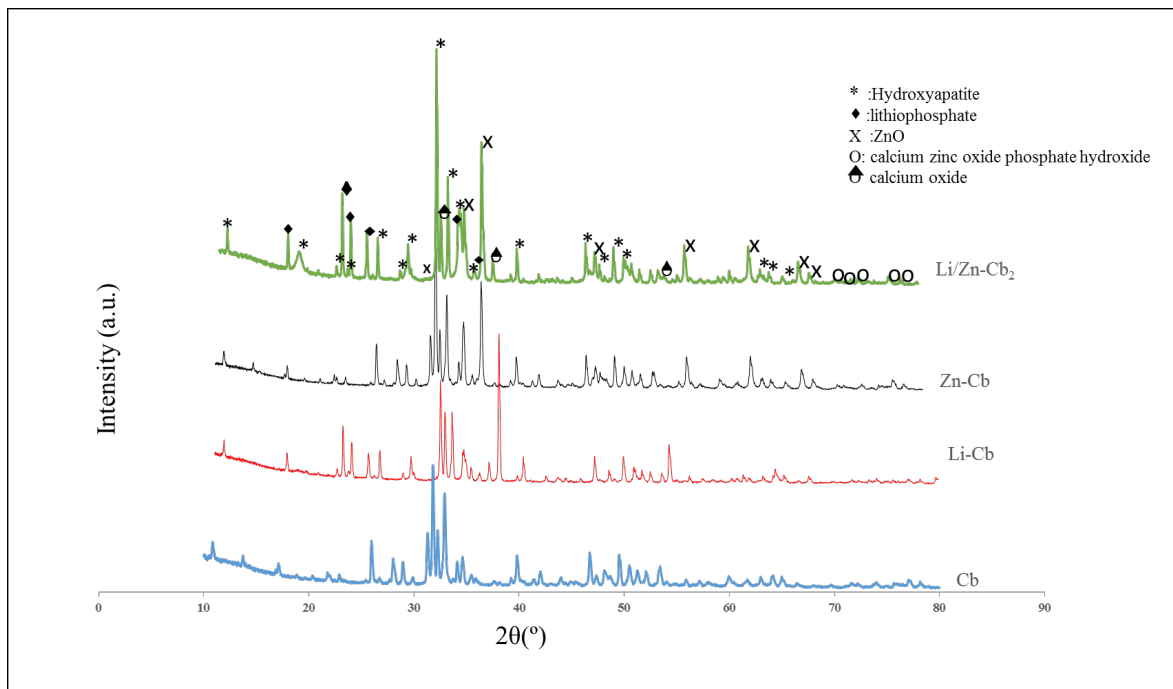
**Fig. 6.1**. XRD data of catalysts based chicken bone.

The lower surface area was observed for Li/Zn-Cb$_2$ catalyst, which could be attributed to the high interaction between the metal ions (Li and Zn) and the support (Cb) which in turn enhanced the conversion to FAMEs. Moreover, the prepared samples comprised pore sizes from ~6 to ~13 nm which are within the mesoporous range (2-50 nm) and larger than the triglyceride molecule (~0.6 nm) which ease its diffusion through the catalyst porous [182].

**Table 6-2:** The BET surface areas, Pore size and Pore volume of the prepared catalysts

| Catalyst | Surface area $S_{BET}$ (m$^2$/g) ± SD[1] | Pore size (nm) | Pore volume (cm$^3$/g) |
|---|---|---|---|
| Cb | 4.68±0.001 | 6.29 | 0.0070 |
| Li-Cb | 4.00± 0.13 | 10.73 | 0.0013 |
| Zn-Cb | 3.96±0.11 | 12.75 | 0.0089 |
| Li/Zn-Cb$_2$ | 3.22±0.001 | 9.08 | 0.0025 |

[1]SD: standard deviation

113

### 6.3.3 FE-SEM analysis

Typical FE-SEM images of the prepared catalysts are shown in Fig. 6.2. It was identified that the particles of raw calcined chicken bone have a dense and spherical structure (Fig. 6.2a), while for the particles of zinc based chicken bone (Zn-Cb) catalyst, bright and round shape and densely packed structure appeared over chicken bone particles (Fig. 6.2c) [253]. Moreover, the FE-SEM image for the catalyst with lithium ion (Li-Cb) (Fig. 6.2b) shows rod-like particles, while with lithium/zinc ion (Li/Zn-Cb$_2$) clearly shows homogeneously distributed zinc ions onto the surface of multi-faces rod structure of Li-Cb (Fig. 6.2d).
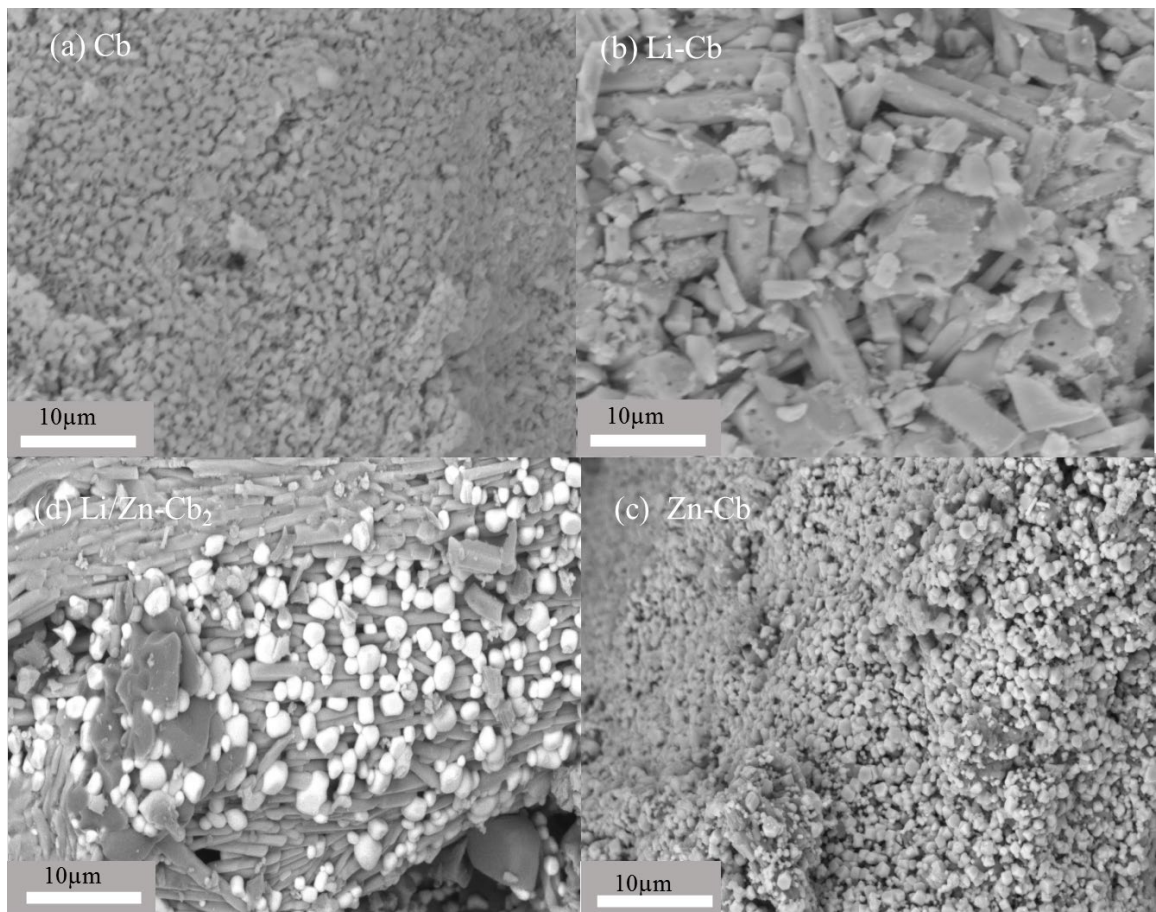


**Fig. 6.2**. FE-SEM micrographs of (a) raw chicken bone (Cb); (b) Lithium chicken bone (Li-Cb); (c) Zinc chicken bone (Zn-Cb); (d) Lithium Zinc chicken bone (Li/Zn-Cb$_2$).

### 6.3.4 FT-IR analysis

Fig. 6.3 illustrates the FT-IR spectra of raw chicken bone (Cb), lithium chicken bone (Li-Cb), and zinc chicken bone (Zn-Cb), and lithium zinc chicken bone (Li/Zn-Cb$_2$). It can be noticed from Fig. 6.3 that there are four distinguished groups: carbonate group at around 1411.9-1548.4 $cm^{-1}$, hydroxide group at around 3571-1-3641.1 $cm^{-1}$, and phosphate group at 950-1100 $cm^{-1}$ [220]. Samples of chicken bone loaded with metals showed a new characteristic peak of M-P group at around 1918-2340 $cm^{-1}$ (M: Zn, Li). New phases have been appeared after loading with zinc or lithium ion as confirmed by XRD analysis. The IR of split peak of C=O bond was noticed for samples including a Li$^+$ ion in its structure which show a good sensitivity towards the absorption of the ambient $CO_2$ at high temperature [46-32].
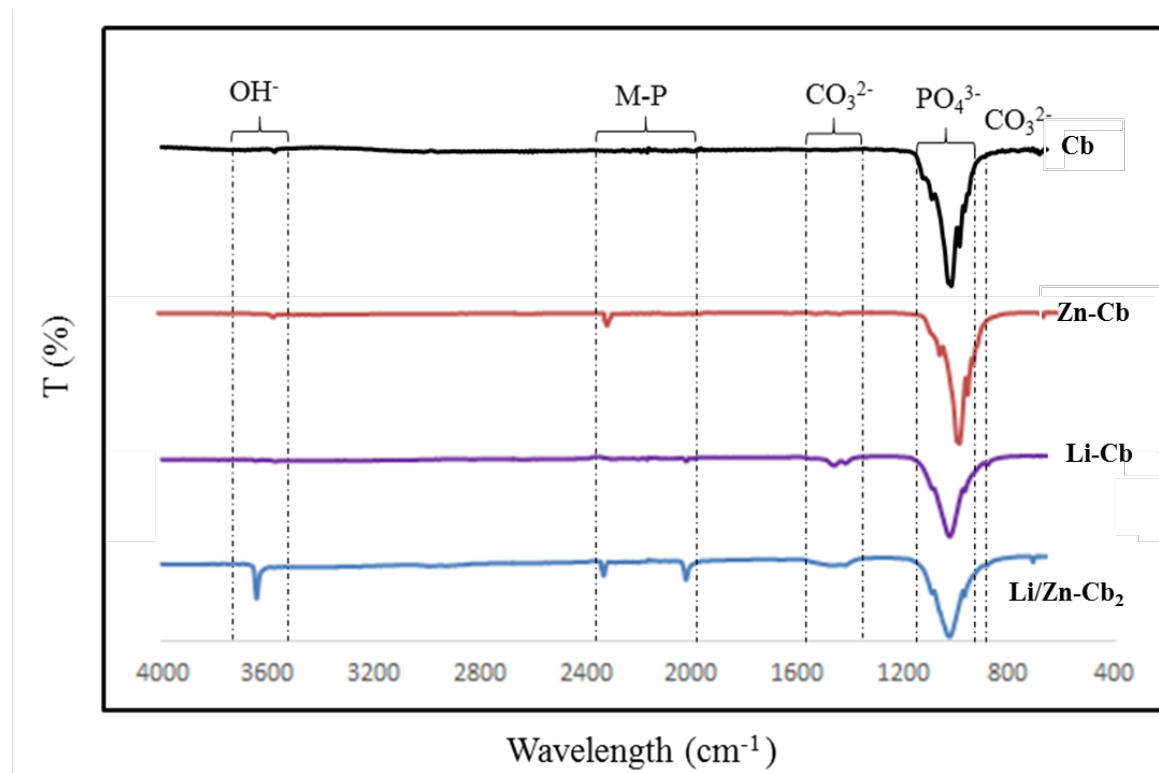


**Fig. 6.3.** FT-IR spectra of catalysts based chicken bone. M= Zn or Li.

**6.3.5 TGA/DSC analysis**

Fig. 6.4 shows the TGA/DSC profiles of as-prepared samples (Cb, Zn-Cb, Li-C, Li/Zn-Cb$_2$). For all samples, at temperature less than 200 ºC, the first weight loss in the TGA curve was observed which attributed to the release of the adsorbed water molecules from the sample (internal and external) [254]. While the second weight loss was occurred at temperature between (200-400 ºC) along with exothermic peaks in DSC profile which was associated with the decomposition of organic materials in the sample. At higher temperature (400 - 800 ºC), the third weight loss was noticed and corresponded to the formation of new materials/ phases as a results of interfering the support with the modification in composition such as lithiophosphate in the Li-Cb and Li/Zn-Cb samples and the formation of ZnO and calcium zinc oxide phosphate hydroxide in the Zn-Cb and Li/Zn-Cb$_2$ samples which were identified in the XRD analysis (Fig. 6.1). In addition, above 850 ºC, the TGA showed a constant line, indicating the completion of the decomposition process and therefore, the temperature of 850 ºC was chosen as the proper temperature for the calcination process.

**6.4 Influence of reaction parameters**

To evaluate the efficiency of the prepared catalyst (Li/Zn-Cb$_2$) for transesterification of waste canola oil (WCO) to FAMEs, the influence of various reaction parameters such as catalyst dosages, methanol to oil molar ratio, reaction time and reaction temperature were investigated and assessed. Fig. 6.5a shows the influence of different Li/Zn-Cb$_2$ dosages (1- 5 wt%) on the conversion to FAMEs. Each reaction was carried out at 60 ºC for 3 h using molar ratio of methanol to oil of 12:1. The results show that increasing the loading from 1% to 4% increases the conversion to FAMEs from 60% to 90%.

(a) Cb

(b) Zn-Cb

(c) Li-Cb
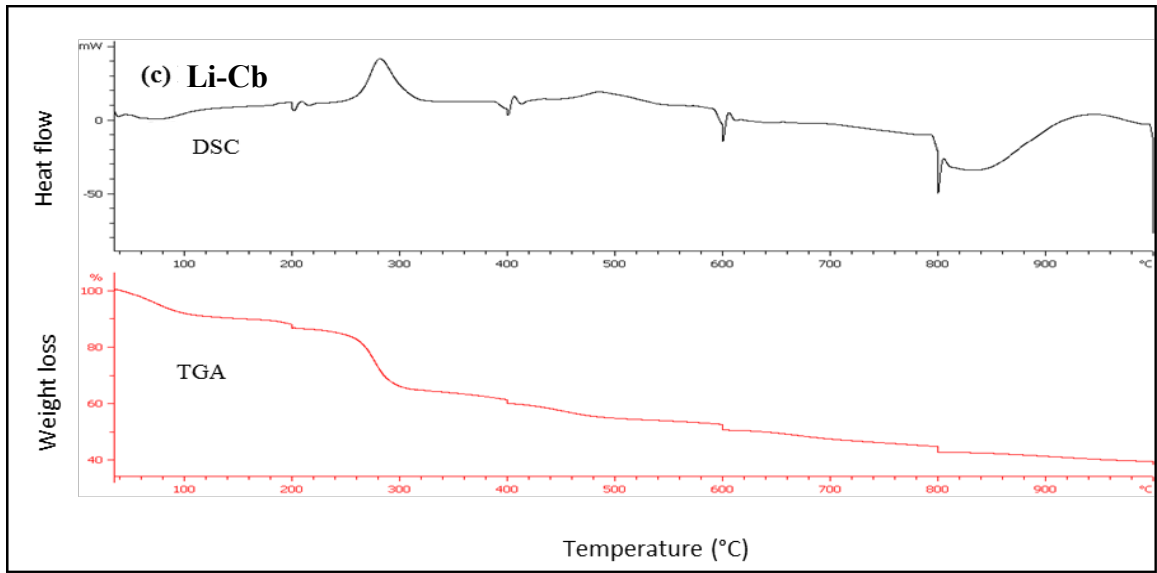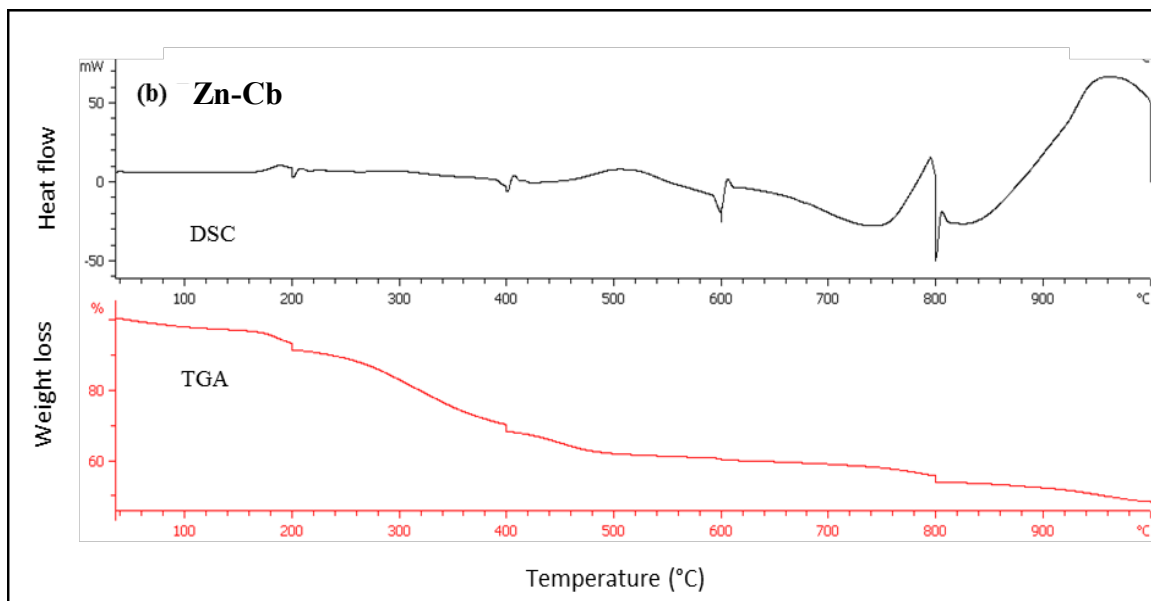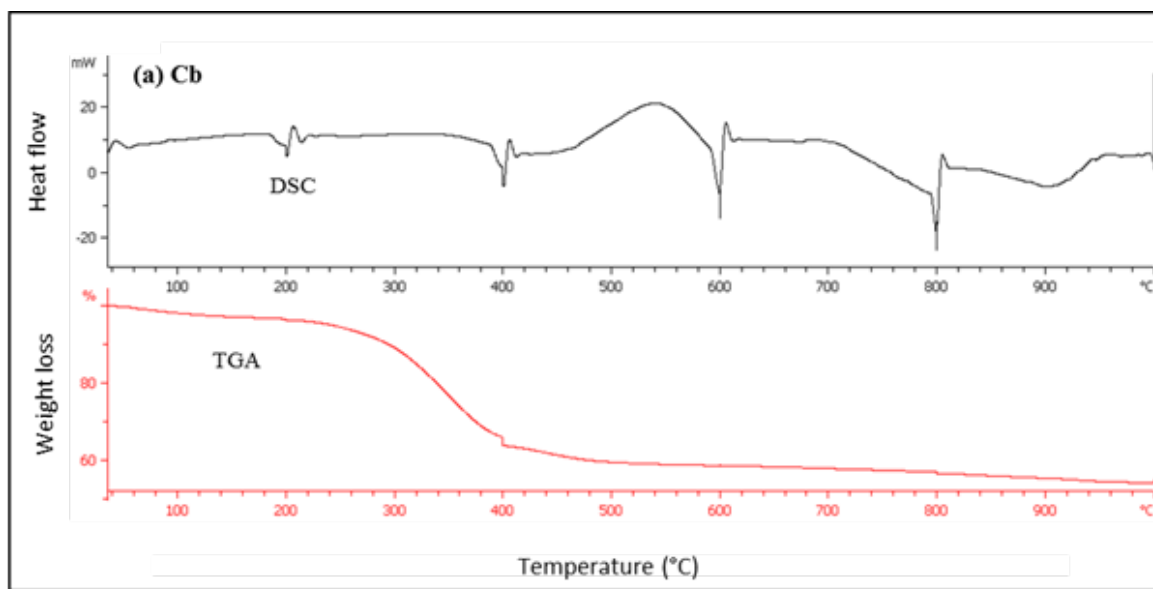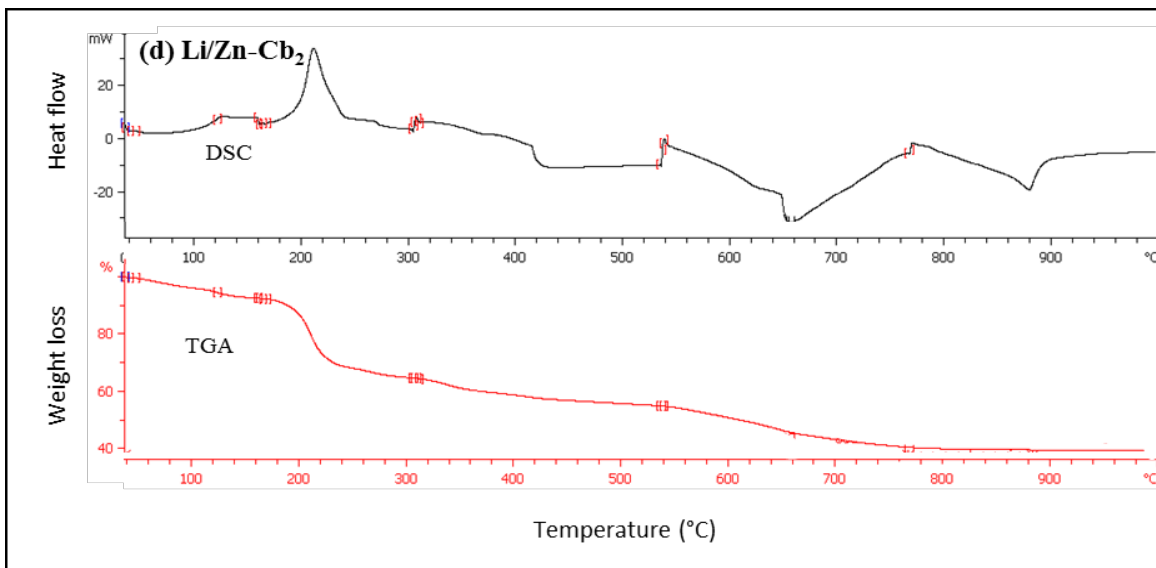
**Fig. 6.4**. TGA/DSC result of as-prepared samples: (a) raw chicken bone (Cb); (b) Zinc chicken bone (Zn-Cb); (c) Lithium chicken bone (Li-Cb); (d) Lithium Zinc chicken bone (Li/Zn-Cb$_2$). X axes is the heat flow in the DSC graph and weight loss in the TGA graph vs. y axes which is sample temperature.

The highest conversion of 90% was obtained at catalyst loading of 4%. Increasing the catalyst dosages will increase the active sites that favour the transesterification reaction and consequently increase the conversion to FAMEs [231]. However, the results also demonstrate that further increasing the catalyst dosage to 5%, will not enhance the conversion to FAMEs and slightly decreased to 89%. Probably, an excess amount of catalyst (catalyst loading above 4%) causes the formation of an emulsion which increases the viscosity of the reaction mixture and leads to the poor diffusion between the methanol–oil–catalyst systems [54, 255]. Therefore, the 4% Li/Zn-Cb$_2$ is the optimal catalyst loading in this reaction.

In order to drive the transesterification reaction towards biodiesel formation, excess amount of methanol is required due to the reversibility nature of the reaction [256]. Thus, the reaction was carried out by varying the MeOH:oil ratio from 6:1 to 20:1 to

assess the optimum value of methanol. Fig. 6.5b shows increasing the methanol to oil ratio from 6:1 to 18:1 increases the conversion to FAMEs from 65% to 96% respectively. However, the excess amount of methanol to 20:1 does not affect the conversion to FAMEs; the conversion was reached the equilibrium state with higher molar ratio (20:1, 96%). Excessive ethanol cannot increase the conversion to FAME due to the increased methanol–glycerol solubility which interferes with the glycerol separation [243]. Therefore, the optimum ratio of methanol to oil was 18:1.

The reaction temperature has a significant effect on carrying out the transesterification reaction. Fig. 6.5c, shows the influence of reaction temperature on the performance of the catalyst from 40 to 65 °C at 18:1 methanol:oil ratio with catalyst dosing of 4% and a reaction time of 3.5 h. The results clearly show that the FAME content was increased from 52% to 98% by increasing the temperature from 40 to 60°C. Referring to the kinetic performance, increasing reaction temperature enhances the reaction rate leading to raise the molecular collision and decline the activation energy limitation [240]. However, when the reaction was carried out at 65 °C, which is above the methanol boiling point, the conversion to FAMEs was slightly reduced to 97% due to the possibility of evaporating the methanol from the reaction media [54, 180]. Therefore, the optimal reaction temperature considered in this study was 60 °C.

The influence of the reaction time on the conversion to FAMEs was depicted in Fig. 6.5d. Generally, increasing the reaction time promotes the transesterification process towards completion. The results clearly show that the conversion to FAMEs increased with the reaction time up to 3.5 h, where a maximum FAME content of 98% was obtained and thereafter drop slightly to 97%, this is because a longer reaction time (above 3.5 h) enhanced the hydrolysis of ester (reverse transesterification) resulting in the loss of ester as well as causing more fatty acids to form soap [106,169].
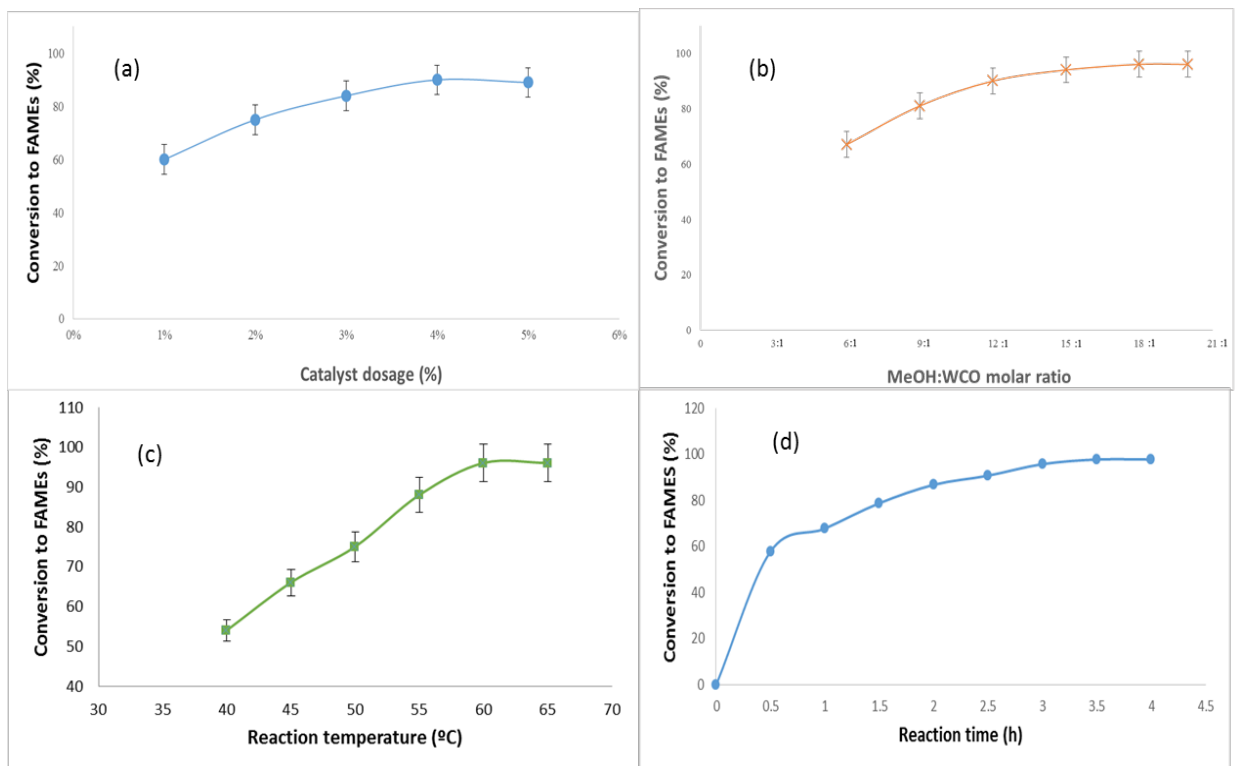
**Fig. 6.5.** Effect of: (a) the catalyst dosages (at MeOH:oil molar ratio= 12:1), (b) MeOH:WCO molar ratio ( at catalyst dosage 4%), (c) reaction temperature (at catalyst dosage 4%, MeOH:oil molar of 18:1, 3 h reaction time), and (d)  reaction time (at catalyst dosage 4%, MeOH:oil molar of 18:1, 60 °C reaction temperature) on the conversion to Fames ( 60 °C reaction temperature, 3 h reaction time).

## 6.5 The influence of ultrasonic at the optimum conditions of conventional transesterfication

### 6.5.1 Ultrasonication versus conventional transesterfication process

Conversion to FAMEs of 98% was achieved in the conventional transesterfication process (i.e. without ultrasound) and under the optimum conditions of 18:1, 60 °C, 3 h and 4 % of methanol: oil ratio, reaction temperature, reaction time and catalyst dosage. To verify the effect of sonication conditions on the conversion to FAMEs, an

experiment was carried out under the optimum conditions of the conventional transesterfication process and the results were compared. Fig. 6.6 illustrates the conversion in the ultrasound assisted process (ultrasonically agitated) and the mechanically agitated conventional process. It was found that conversion to FAMEs was less in the case of sonication (71%). Some authors have suggested in such kind of reaction, a longer reaction time causes a high content of monoglyceride (MG) as a result of low reaction rate to produce FAME and glycerol form monoglyceride (MG) [252]. Thus, more investigations were commenced to prove the effect of sonication on the ester conversion in the following sections. In this study, two parameters were investigated (reaction time and the catalyst dosage) as these parameters have the economic impact on the process while MeOH: oil molar ratio and reaction temperature were kept constant at 18:1 and 60 °C, respectively.

## 6.5.2 Effect of reaction time on conversion via ultrasonic technique

Fig. 6.7 shows the conversion to FAMEs under sonication conditions and without sonication at different reaction time (0.5 – 3.5 h). Each reaction was carried out at 60 °C using MeOH: oil molar ratio of 18:1 and catalyst dosage of 4%. In case of the conventional process without ultrasound, the conversion increases with increasing the reaction time and the maximum conversion was 98% at 3.5 h.
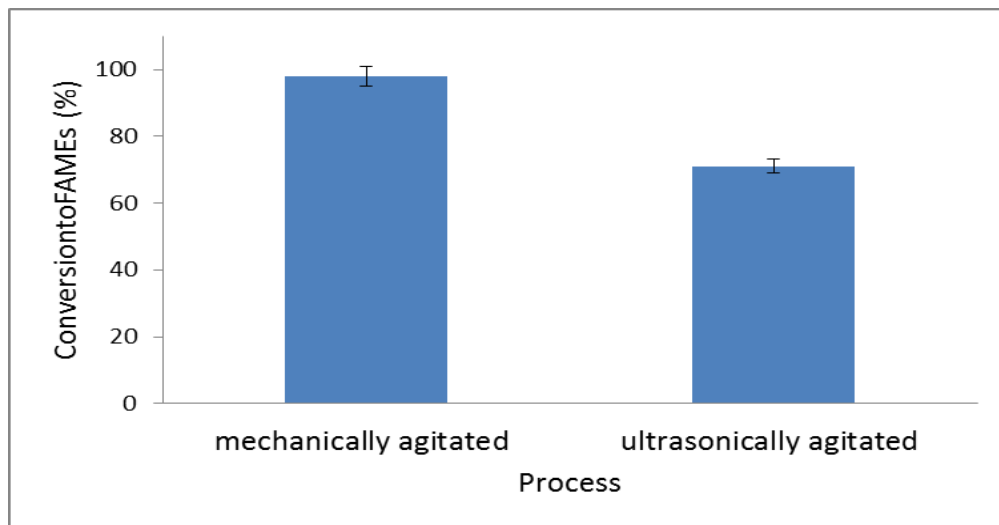
**Fig. 6.6**. The conversion to FAMEs in the ultrasound assisted process and the mechanically agitated process at the optimal conditions (temperature of 60 °C, MeOH: oil of 18:1, reaction time of 3 h and catalyst dosage of 4%).

The results of process under ultrasonic effect show that increasing the reaction time from 0.5 h to 1 h increases the conversion to FAMEs from 51% to 68% and the highest conversion of 71% was obtained at reaction time of 1.5 h. Enhancing the solubility of methanol in oil (reactants) by ultrasound irradiation resulted in eliminating the external mass transfer limitation between reactants and reflected in increasing the conversion to FAMEs [257]. However, increasing the reaction time beyond 1.5 h did not show further improving in the conversion because of reaching the equilibrium state. As can be observed from Fig. 6.7, conversion to FAMEs in the ultrasonic-assisted transesterfication process was lower than conversion in the conventional process about 27% at the candidate reaction conditions. This observed could be due to the inhomogeneity in the mixture resulting from the large quantity of catalyst and several positions of nucleus for bubbles are formed from the trapped gases [146] which could explain the lower conversion in ultrasonic-assisted

transesterfication process. Another explanation is incidence emulsion phase of oil and methanol that produced from irradiation of ultrasound as a result of cavitation was very fast in short mixing time and before being adsorbed on the catalyst surface [258]. Therefore, this phenomenon might inhibit the active sites of catalyst and result in reducing the conversion to FAMEs. In addition, The characteristics of agitation could influence the kinetic mechanism of catalyzed-transesterfication process specifically the adsorption step of the reactant on the catalyst surface. So, higher conversion in the mechanical-assisted process was resulted in [259]. Biodiesel production from waste cooking oil over alkaline modified zirconia catalyst. The same observation was noted by Choedkiatsakul et al. [145] in their demonstrating of transesterfication of refined palm oil by potassium phosphate ($K_3PO_4$) catalyst in ultrasound and mechanical-aided reactors. It was found that FAMEs yield of > 80 % in the mechanical stirring reactor is higher than the yield in the ultrasound reactor. Although the maximum conversion in ultrasonic- assisted process was less, it was achieved in a shorter reaction time. Hindryawati and Maniam [209] in their study used sodium loaded silica waste sponge (SWSS) to catalysed waste cooking oil transesterfication process assisted by ultrasound and achieved the maximum FAMEs content (98.2%) in 30 min while 80 min of reaction time was needed to reach the maximum FAMEs content (87.7%) in the mechanically agitated process. Thus, employing ultrasound technique for biodiesel production in short reaction time is of interest. So, more investigation is required and the catalyst dosage parameter was further investigated at 1.5 h of reaction time.
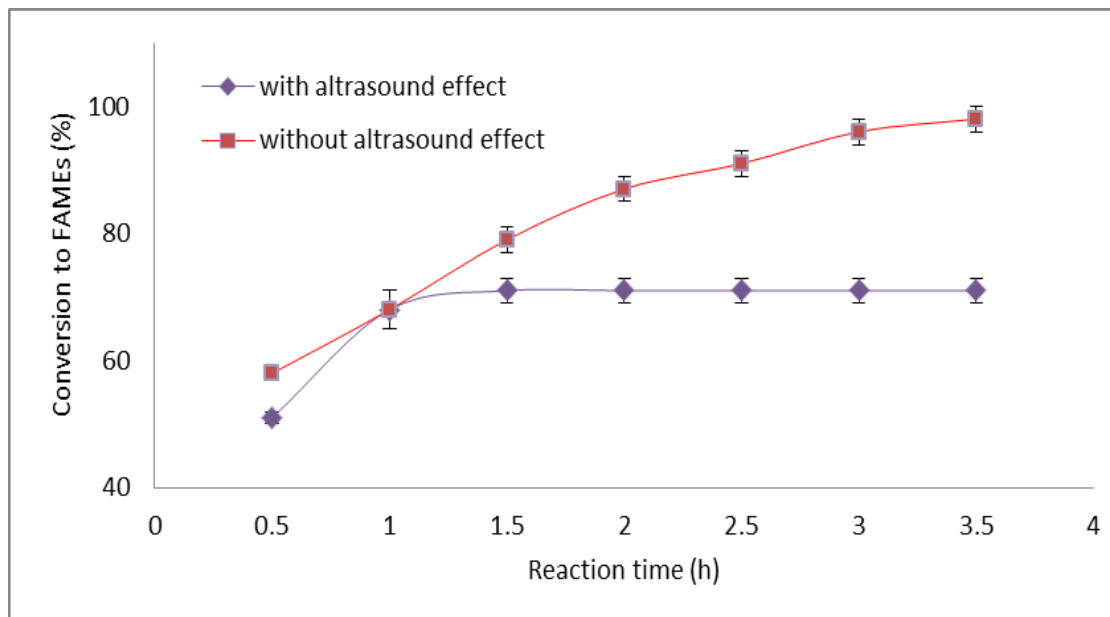
**Fig. 6.7.** The conversion to FAMEs under the ultrasound effect at (a) different reaction time (temperature of 60 °C, methanol:oil of 18:1 and catalyst dosage of 4%).

### 6.5.3 Effect of catalyst dosage on conversion via ultrasonic technique

The catalyst dosage effect was investigated under the sonication conditions as shown in Fig 6.8 and it was varied from 1 wt. % to 4 wt. %. The conversion to FAMEs was improved from 83% to 96% by increasing the catalyst dosage from 1 wt. % to 2 wt. %, respectively. However, the conversion was reduced beyond 2 wt. % from 96% to 71%. Similarly, Poosumas et al. [260] found that increasing the catalyst dosage to 2 wt. % enhanced the FAMEs yield to 80% and catalyst dosage greater than 3 wt. % did not show any improving in the FAMEs yield. The activity of ultrasonic cavitation has been enhanced by increasing the catalyst dosage. However, excess dosage of catalyst hinders the reactants bulk from access to the active sites of the catalyst and the energy of ultrasonic irradiation was scattered leaving the cavitation effect weaker [261]. Therefore, reactants were obstructed to reach the active sites on the catalyst

surface and resulting in lower conversion to FAMEs. The maximum conversion was found to be 96% at 2% of catalyst dosage, 60 °C of reaction temperature, 18:1 molar ratio of methanol to oil, and 1.5 h of reaction time. The highest conversion in the ultrasonic-assisted transesterfication process was achieved in the shorter time and less catalyst dosage in comparison with the conventional transesterfication process. The acoustic cavitation that was generated from ultrasound increased the inter facial area of the reaction and therefore resulted in a homogeneous suspension of the reactants (oil and methanol) which promotes the high conversion in a shorter reaction time and less catalyst dosage [209,262]. Thus, many advantages could be outlined from using ultrasound technique such as saving time, smaller dosage of catalyst and so on as reported by other authors [263].
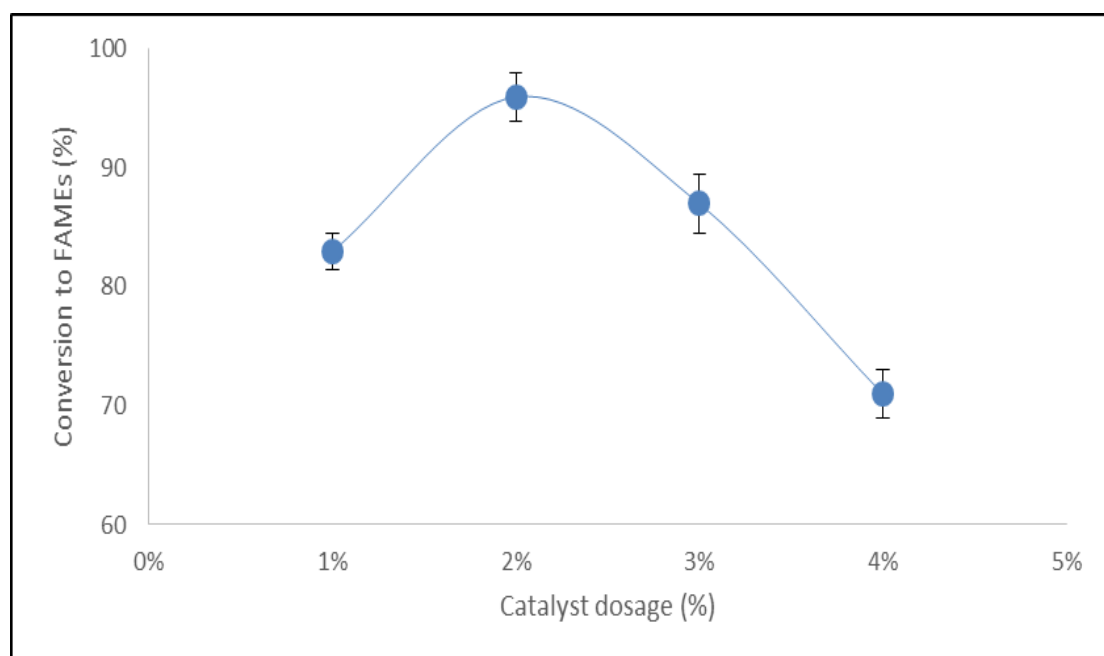


**Fig. 6.8.** The conversion to FAMEs under the ultrasound effect at different catalyst dosage (temperature of 60 °C, methanol:oil of 18:1 and reaction time of 1.5 h).

## 6.6 Reusability of catalyst

To assess the reusability of the prepared catalyst (Li/Zn-Cb$_2$), set of the transesterification reactions were conducted under the optimum conditions (18:1 MeOH:WCO, 4% of catalyst, 60 ºC reaction temperature and 3.5 h of reaction time). A fresh catalyst was used in the first experiment, while in the successive experiments the regenerated (used) catalyst was employed. After each experiment the catalyst was separated by filtration and washed three times with methanol and once with hexane then calcination at 850 ºC for 90 min, after that, it was directly subjected to the transesterification reaction under the optimum conditions. Fig. 6.9 shows the conversion to FAMEs was reduced by only 2% after 7 cycles, which could be attributed to the leaching of active sites.
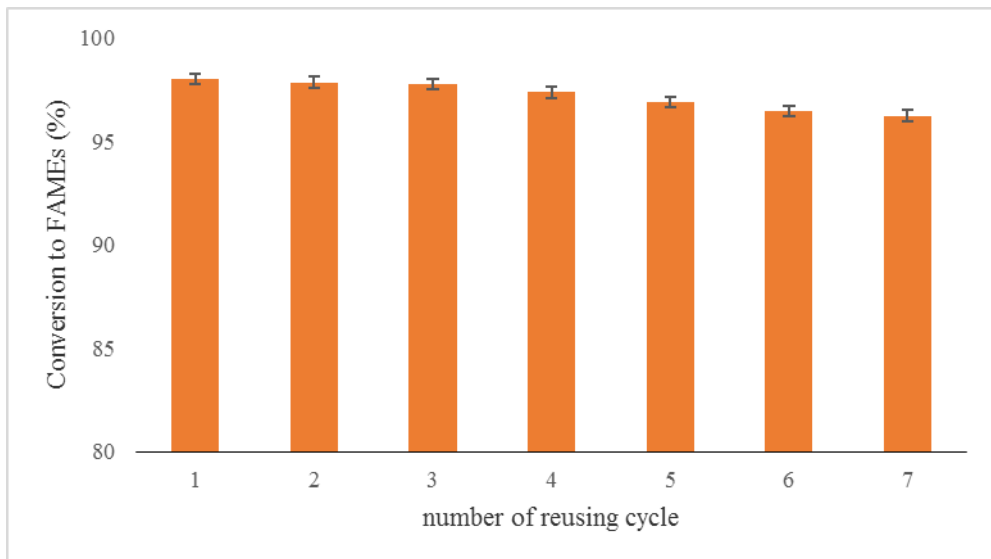


**Fig. 6.9.** Reusability of Li/Zn-Cb$_2$ catalyst. The optimum reaction condition: 60 ºC reaction temperature, 3.5 h of reaction time, catalyst dosage of 4% and 18:1 molar ratio of MeOH/WCO.

Therefore, to assess the catalyst stability, the catalyst was reacted with methanol under the optimum conditions (without oil) then the methanol was decanted and has

been reacted with oil in the absence of catalyst. The conversion from the latter was found to be 5% which means the reaction was totally carried out and controlled by the heterogeneous catalysed system with slight losing of the active sites which explained the slight decreasing in the conversion after seven consequence runs

## 6.7 Kinetic studies

The transesterification kinetics of WCO to FAME catalysed by Li/Zn-Cb$_2$ have been investigated at different reaction time and temperatures. Zero and pseudo first order kinetic models (Eqs. 4-1 and 4-7, respectively) were applied and fitted to the experimental results, under the following assumptions: (i) Using excess methanol in the reaction to accelerate the forward reaction to prefer the FAMEs formation and neglecting the reverse reaction (ii) Ignoring the intermediate reactions, the transesterification process could be considered as a single step.

$$\frac{dx}{dt} = K_{Me} \qquad (4\text{-}1)$$

$$-\ln(1 - X_{Me}) = kt \qquad (4-7)$$

Where $K_{Me}$ and $k$ are the reaction rate constants for the zero and pseudo first order, respectively, $X_{Me}$ is the conversion to FAMEs, and $t$ is the reaction time. The estimated parameters are summarized in Table 4 and suggest that the pseudo first order model is the best fit for canola oil transesterification at 60 ºC with a reaction rate constant of 0.6689 h$^{-1}$. Table (6-3) also reveals that the reaction rate constants increase with increasing the reaction temperatures.

To study the impact of the temperatures on the reaction rate, the activation energy ($Ea$) was determined by fitting the experimental results of different temperatures to Arrhenius equation, Eq. (4-9).

$$\ln k = \ln A - \frac{Ea}{RT} \qquad\qquad (4-9)$$

Where *Ea*, *R, k, A, T* are the activation energy (kJ mol$^{-1}$), universal gas constant (8.314 J mol$^{-1}$K$^{-1}$), reaction rate constant (h$^{-1}$), frequency factor (h$^{-1}$), and the reaction temperature (K), respectively. The estimated values for *A* and *Ea* were 2.6 × 10$^9$ h$^{-1}$ and 23.20 kJ mol$^{-1}$, respectively. The activation energy for the transesterification of waste canola oil applying the catalyst (Li/Zn-Cb) was lower than the activation energy obtained for base catalysed transesterification reaction, i.e. 33.6–84 kJ mol$^{-1}$ [241], indicates that the transesterification is much easier to carry out under the catalyst (Li/Zn-Cb$_2$) than the regular base catalyst.

**Table 6-3:** Estimated reaction rate constant at different reaction temperatures.

| Temp(ºC) | Rate constant (K) | | $R^2$ | |
|---|---|---|---|---|
| | zero order | Pseudo 1st order | zero order | Pseudo 1st order |
| 40ºC | 0.1091 | 0.1566 | 0.6869 | 0.719 |
| 45ºC | 0.1313 | 0.2057 | 0.7602 | 0.8455 |
| 50ºC | 0.1588 | 0.2727 | 0.821 | 0.9209 |
| 55ºC | 0.186 | 0.3946 | 0.7806 | 0.9154 |
| 60ºC | 0.2214 | 0.6689 | 0.8255 | 0.9828 |

## 6.8 Summary

Lithium/zinc chicken bone based catalyst (Li/Zn-Cb$_2$) was synthesised by the impregnation method for biodiesel production from waste canola oil. The performance of (Li/Zn-Cb$_2$) was investigated under different operation conditions. The highest FAME content obtained was 98% at 60 ºC, 3.5 h reaction time, and catalyst dosage of 4% and 18:1 molar ratio of MeOH/WCO. In the ultrasonic assisted process study, the maximum conversion was 96% which is close to the conversion by the conventional process (98%) but at the lower reaction time and catalyst dosage (1.5

h and 2% catalyst dosage, respectively). Thus, the ultrasonic technique offers energy savings by reducing the reaction time and economic process by reducing the used catalyst. The kinetics were best represented by the pseudo-first order model with 0.6689 $h^{-1}$ rate constant, and the associated frequency factor and activation energy were $2.6 \times 10^9$ $h^{-1}$ and 23.20 kJ $mol^{-1}$, respectively. Li/Zn-$Cb_2$ reused for 7 times with FAME content > 96%.

# CHAPTER 7

# Optimization of biodiesel production from waste canola oil

# by response surface methodology (RSM)

## 7.1 Introduction

The environmental issues such as the emission of greenhouse gases (NOx, SOx, CO, $CO_2$) and shortage in the fossil fuel reserve are results of increasing the consumption of fossil fuel [197]. These issues have encouraged the researchers to find a substitutional fuel which is a renewable and sustainable. Biodiesel, a mixture of mono-alkyl fatty acid esters, is a biodegradable, non-toxic and renewable fuel. These features make it as a promising alternative to the conventional fuel [61,215]. The process of biodiesel production includes the catalysed reaction between vegetable oils or animal fats with a short chain of alcohol (e.g. methanol and ethanol) by homogeneous or heterogeneous catalysts [232].

The conventional method to investigate the effect of reaction parameters on the progress of reaction is by varying a single parameter while keeping others constant, this method will result in a lack of knowledge of the interaction between the process parameters. Therefore, in order to obtain a comprehensive understanding of the impact of the selected parameter and its mutual interaction with other parameters on the process, an experimental design called response surface methodology (RSM) has been widely employed by researchers. RSM is defined as a mathematical and statistical method used to design experiments, analysis the results, modelling and evaluate the parameter influences and determines the optimal operating conditions to obtain the highest value of response.

The optimization of the biodiesel production by the response surface methodology (RSM) has been studied by several researchers [264,265]. Jahirul et al. [164] have investigated the effect of catalyst concentration, methanol to oil molar ratio and reaction temperature via response surface methodology (RSM) with BBD method for

biodiesel production via a two-step process of pre-esterification and transesterification of the beauty leaf plant. The responses of the statistical method were in line with the experimental results which indicate validity of this methodology in the industrial scale for optimization of beauty leaf oil-based biodiesel production. Mohamad et al. [266] have optimized catalyst dosage, ratio of vegetable palm oil (VPO) to methanol, and reaction time by RSM with central composite design (CCD) to demonstrate their influences on the biodiesel yield. It was concluded that the most effective factors on the transesterification of vegetable palm oil under UV light and catalysed by calcium oxide-based titanium dioxide (CaO-TiO$_2$) were reaction time and MeOH: oil molar ratio while the effect of catalyst dosage was the least significant. Therefore, the literatures reveal that the most significant parameters could be greatly predicted by response surface methodology (RSM) to investigate their impacts on the process.

Thus, in this chapter, it was selected Li/Zn-Cb catalyst for more detail's optimization as its most promised catalyst for WCO transesterification. Since our previous studies showed that the reaction temperature, MeOH: oil molar ration and catalyst dosage are the curtail factors in the reaction to maximize the conversion, they were chosen to optimize in the BBD method of RSM.

## 7.2 Materials and methods

The details of the experimental methods of this chapter have been described in chapter (3). However, in brief, the used chemicals and oil feedstock were given in Section 3.2.1, and the physico-chemical properties of waste canola oil (WCO) were tabulated in Table 3-1 in Section 3.2.1. The analytical methods were given in Sections 3.8.1-3.8.3. The applied catalyst (Li/Zn-Cb) was prepared as reported previously in

Section 3.3.3, and the catalyst characterisations were given in Sections 3.4.1-3.4.5. The experimental set-up and FAMEs analysis were given in Sections 3.5 and 3.8.3. The investigated parameters were given in Sections 3.6.1-3.6.4, for example in this chapter the catalyst dosage range was (1 – 5 wt.%), MeOH: oil molar ratio was (6:1 – 20:1), reaction time range (1 – 4 h), and reaction temperature range was (40 – 65 °C). The data were statistically analysed for significance by JMP statistical discovery TM software from SAS (version 13.1.0).

## 7.3 Experimental design and statistical analysis

The optimization of biodiesel production process via Li/Zn-Cb catalyst was performed by BBD method of RSM and the interaction between three independent factors were investigated. The biodiesel production process is significantly influenced by the reaction temperature ($x_1$), methanol to waste canola oil molar ratio ($x_2$) and catalyst dosage ($x_3$), thus, they were chosen for optimization. Based on our preliminary investigation, it was found that 3.5 h of reaction time is enough to complete the reaction, so, 3.5 h was chosen as the reaction time. The variance error could be increased when too many factors are applied. The reaction time and temperature are closely related; therefore, the reaction temperature was selected as the independent factor [165]. 15 experiments were conducted by varying the reaction temperature from 40 to 65 °C with a central point of 52.5, methanol to waste canola oil molar ratio from 6:1-20:1 with a central point of 13:1, and catalyst dosage 1 to 5 wt. % with a central point 3. The range of these factors were chosen based on our previous investigation that was carried out in the laboratory. The conversion to FAMEs (%) was selected as the response variable. Table 7-1 shows the levels of

coded and actual variables in the BBD design matrix for conversion to FAMEs (%).

The following equation (7-1) describes the relationship between the actual ($X_i$) and

coded ($x_i$) values of independent factors [267, 268].

$$x_i = \frac{X_i - X_0}{\Delta X_i} \qquad (7\text{-}1)$$

Where $x_i$ is the coded value of the actual value ($X_i$) while $X_i$ is the actual value of the

$i^{th}$ independent factor (i = 1, 2, 3…, k), $X_o$ is the actual value of the factor at the

centre, and $\Delta X_i$ is the step change value.

**Table 7-1:** The levels of coded and actual variables in the BBD design matrix for conversion to FAMEs (%).

| Run | Coded values | | | Actual values | | | Experimental conversion to FAMEs (%) | Predicted conversion to FAMEs (%) |
|-----|-----|-----|-----|-----|-----|-----|-----|-----|
| | $x_1$ | $x_2$ | $x_3$ | $X_1$ | $X_2$ | $X_3$ | | |
| 1 | − | − | 0 | 40 | 6 | 3 | 50.81 | 48.50 |
| 2 | − | + | 0 | 40 | 20 | 3 | 67 | 61.85 |
| 3 | + | − | 0 | 65 | 6 | 3 | 45 | 50.15 |
| 4 | + | + | 0 | 65 | 20 | 3 | 89 | 91.30 |
| 5 | 0 | − | − | 52.5 | 6 | 1 | 41.2 | 40.12 |
| 6 | 0 | − | + | 52.5 | 6 | 5 | 71 | 69.22 |
| 7 | 0 | + | − | 52.5 | 20 | 1 | 68 | 69.77 |
| 8 | 0 | + | + | 52.5 | 20 | 5 | 93 | 94.07 |
| 9 | − | 0 | − | 40 | 13 | 1 | 39 | 42.37 |
| 10 | + | 0 | − | 65 | 13 | 1 | 66 | 61.92 |
| 11 | − | 0 | + | 40 | 13 | 5 | 69 | 73.07 |
| 12 | + | 0 | + | 65 | 13 | 5 | 88 | 84.62 |
| 13 | 0 | 0 | 0 | 52.5 | 13 | 3 | 95 | 94.66 |
| 14 | 0 | 0 | 0 | 52.5 | 13 | 3 | 94 | 94.66 |
| 15 | 0 | 0 | 0 | 52.5 | 13 | 3 | 95 | 94.66 |

$X_1$, $X_2$ and $X_3$ are the actual values of reaction temperature, methanol to oil molar ration and catalyst dosage.

$x_1$, $x_2$, $x_3$ are the coded values of $X_1$, $X_2$ and $X_3$

A second-order polynomial equation was applied to calculate the predicted response (conversion to FAMEs) as shown below in Eq. (7-2) [269,270]:

$$Y = \beta_o + \sum_{j=1}^{k} \beta_j X_j + \sum_{j=1}^{k} \beta_{jj} X_j^2 + \sum_{i=1}^{k-1} \sum_{j=i+1}^{k} \beta_{ij} X_i X_j + \varepsilon \qquad (7\text{-}2)$$

Where Y is the predicted response factor (conversion to FAMEs), $\beta_o$ is the constant coefficient (i.e., intercept), i and j are the index number of patterns, k is the number of factors, and $\beta_j$, $\beta_{jj}$, $\beta_{ij}$ are the estimated coefficients from regression of linear, quadratic, and interaction effects, respectively. In this study, JMP statistical discovery TM software from SAS (version 13.1.0) was adopted for BBD experimental design, regression analysis and 3D response surface graphs plots. All runs were repeated in triplicate.

## 7.4 Results and discussion

### 7.4.1 Multiple regression analysis and analysis of variance (ANOVA)

The relationship between the response parameter (conversion to FAMEs) and the independent parameters (temperature, MeOH:oil molar ratio, and catalyst) were determined by the multiple regression analysis and developed a quadratic equation from the analysed results using Box Behnken Design in terms of coded variables and is shown in Eq. (7-3) whereas $x_1$, $x_2$ and $x_3$ represent the temperature, molar ratio and catalyst, respectively.

$$Conversion\,to\,FAMEs\,(\%) = 94.66 + 7.77375x_1 + 13.62x_2 + 13.35x_3 -$$
$$17.25708x_1^2 - 14.45708x_2^2 - 11.90958x_3^2 + 6.9525x_1x_2 - 2x_1x_3 - 1.2x_2x_3 \qquad (7-3)$$

Fig. 7.1 plotted the experimental and predicted response of esters conversion with a high value of the determination coefficient $R^2$ (0.98) which shows that the model is

adequacy to describe the relationship between the independent (input) variables ($X_1$, $X_2$, and $X_3$) and the response (output) variable (conversion to FAMEs) and is suited well with the obtained data. Analysis of variance (ANOVA), coefficient and significance of linear, interactive, and quadratic terms of model are shown in Table (7-2). P-value is the indication of the significance of each term in the model. It was reported that the term with p-value < 0.05 is statistically significant term. As can be seen from Table (7-2) that the conversion is influenced by the linear terms ($x_1$, $x_2$, and $x_3$). Similarly, the conversion was affected by the quadratic terms ($x_1^2$, $x_2^2$, $x_3^2$) and the interactive term ($x_1x_2$) whereas these terms comprise the p-value less than 0.05. While the p-value of the combined terms ($x_1x_3$ and $x_2x_3$) were greater than 0.05 (0.4666 and 0.6564, respectively) which mean they are less significant in comparison with the other independent parameters.
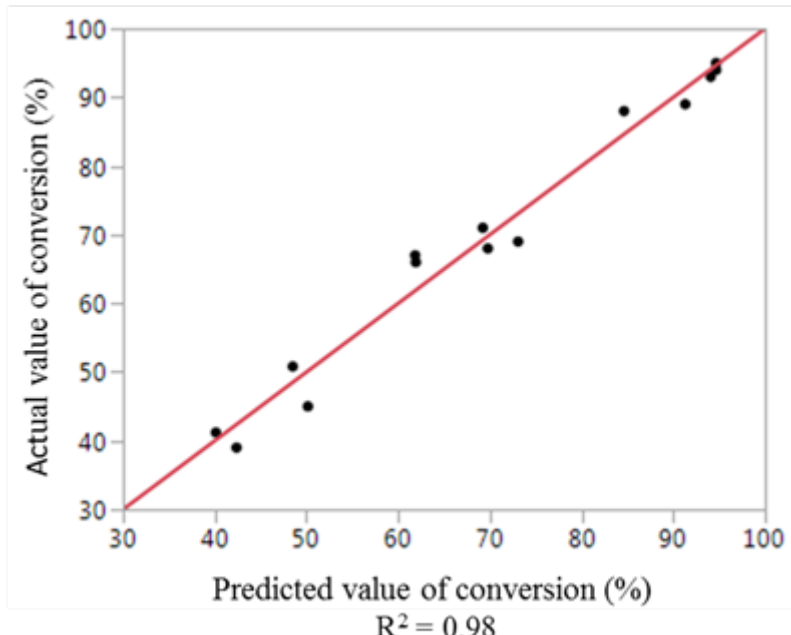


**Fig. 7.1**. Actual value of conversion to FAMEs versus predicted value.

## 7.4.2 BBD analysis and optimization the effects of reaction parameters on the producing of methyl esters

Table 7-1 shows the BBD matrix that was developed by RSM to study the effects of methanol to oil ratio, catalyst and temperature on the ester conversion which involved 15 experiments and the table displays the experimental and predicated results of conversion to FAMEs. Figs. 7.2- 7.4 illustrate the effects of reaction parameters (reaction temperature, methanol:oil molar ratio, and catalyst dosage) on the response factor (conversion to FAMEs) in three-dimensional surface (3-D) plots and 2D contour plots. In these figures, one independent parameter was kept constant at its centre value (coded zero), while the two remaining parameters were varied within the high and low limit of the experimental range.

**Table 7-2:** Analysis of variance (ANOVA)

| Term | Estimate | Std Error | t Ratio | Prob>\|t\| |
|---|---|---|---|---|
| Intercept | 94.66 | 2.93 | 32.29 | <.0001* |
| $x_1$ | 7.77 | 1.79 | 4.33 | 0.0075* |
| $x_2$ | 13.62 | 1.79 | 7.59 | 0.0006* |
| $x_3$ | 13.35 | 1.79 | 7.44 | 0.0007* |
| $x_1.x_2$ | 6.95 | 2.53 | 2.74 | 0.0409* |
| $x_1.x_3$ | -2.0 | 2.53 | -0.79 | 0.4666 |
| $x_2.x_3$ | -1.20 | 2.53 | -0.47 | 0.6564 |
| $x_1^2$ | -17.25 | 2.64 | -6.53 | 0.0013* |
| $x_2^2$ | -14.45 | 2.64 | -5.47 | 0.0028* |
| $x_3^2$ | -11.90 | 2.64 | -4.51 | 0.0064* |
| RSquare | 0.97 | | | |
| RSquare Adj | 0.93 | | | |

* indicates that the term with P-value <0.05 is statistically significant.

### 7.4.2.1 The effect of methanol:oil molar ratio and reaction temperature

Fig 7.2 illustrates the influence of interaction $x_1x_2$ on the conversion to FAMEs (Y) at constant catalyst dosage ($x_3$) of 3 wt. %. As can be observed from the surface plot, the combined influence of the increased methanol:oil molar ratio and reaction temperature leads to increase conversion to FAMEs up to the optimal values. The conversion to FAMEs increases with increasing MeOH:oil molar ratio at lower reaction temperature(40 °C). Excess MeOH:oil molar ratio is required to release the reaction products from the surface of catalyst and allow the active sites to increase in the reaction medium [271]. However, the conversion to FAMEs was less with higher methanol:oil molar ratio as a consequence of increasing the polarity which in turn increases glycerol solubility and make it difficult to separate from alkyl ester [271]. Moreover, higher value of reaction temperature leads to low conversion to FAMEs due to the lacking availability of methanol[162]. The highest conversion to FAMEs (95%) was obtained at 3wt.% of catalyst dosage, 13 of MeOH:oil and reaction temperature of 52.5 °C.
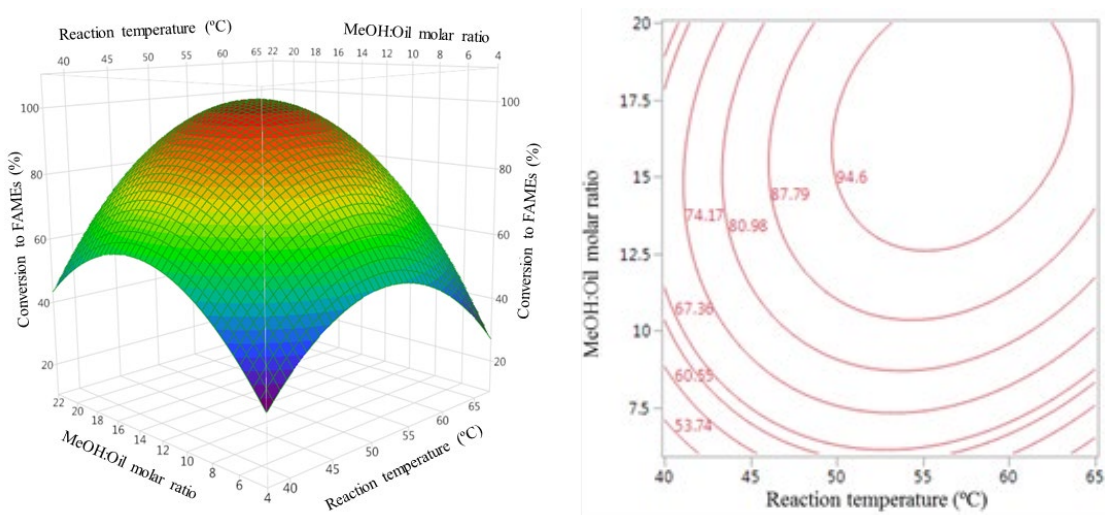


**Fig. 7.2.** Surface response plot and contour plot for conversion to FAMEs (%) of the effect of methanol:oil molar ratio and reaction temperature

## 7.4.2.2 The effect of catalyst dosage and reaction temperature

Fig. 7.3 demonstrates the trend of the conversion to FAMEs under the influence of reaction temperature and catalyst dosage ($x_1x_3$) while MeOH:oil molar ratio is constant at 13. The conversion to FAMEs is lower at low reaction temperature and catalyst dosage, as well as at a higher reaction temperature and catalyst dosage. Generally, increasing the catalyst dosage increases the conversion to FAMEs owing to increase the amount of active sites on the surface of the solid catalyst. While, higher dosage of the catalyst could slow down the reaction of oil-methanol-catalyst system and leads to the reduction in the conversion to FAMEs [271].
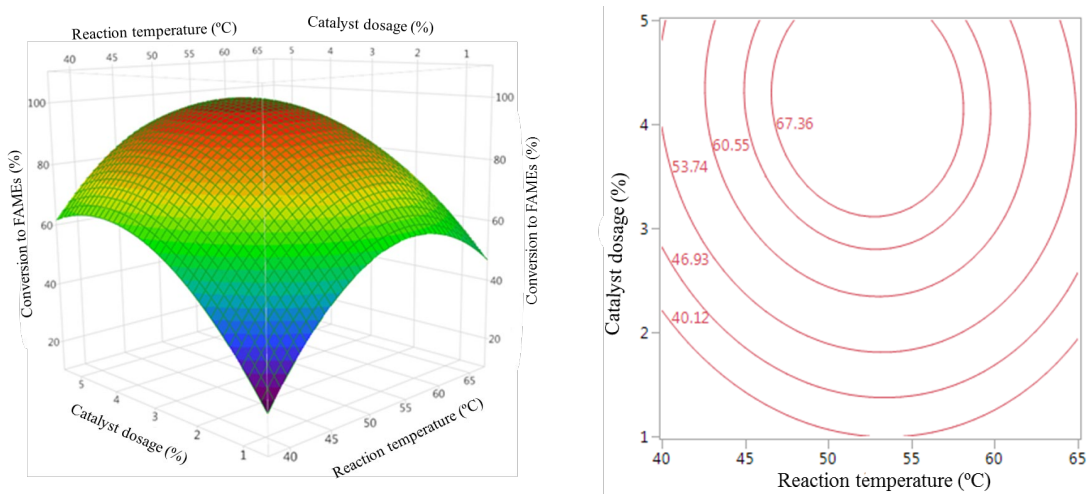


**Fig. 7.3.** Surface response plot and contour plot for conversion to FAMEs (%) of the effect of the catalyst dosage and reaction temperature

## 7.4.2.3 The effect of catalyst dosage and methanol: oil molar ratio

As can be seen from Fig. 7.3 that increasing the catalyst dosage and methanol: oil molar ratio ($x_2x_3$) initially resulted in increase the conversion to FAMEs and these finding where in line with our previous results (the conventional investigation factor by factor). However, a reverse effect on the conversion to FAMEs percentage can be

observed at the higher limit of the catalyst dosage and methanol: oil molar ratio. The findings were supported by finding of [126].
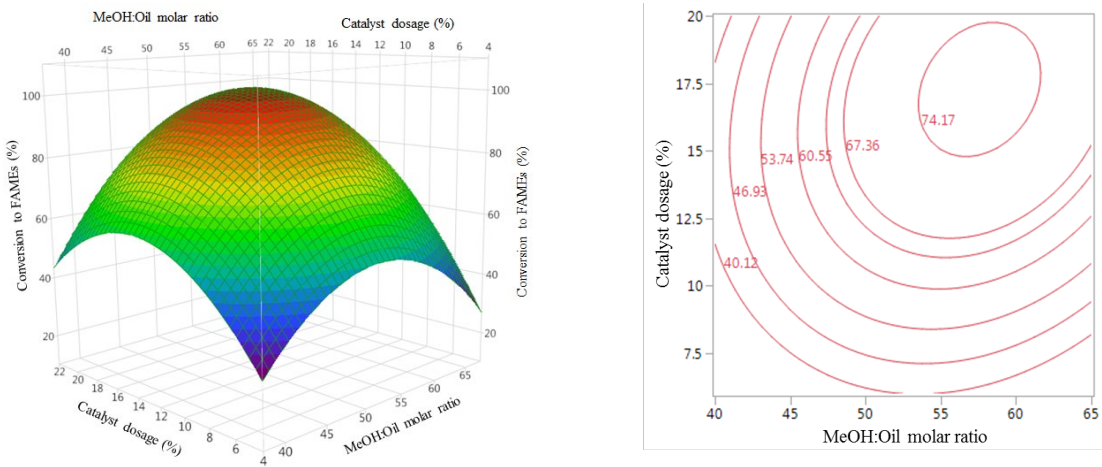


**Fig. 7.4.** Surface response plot and contour plot for conversion to FAMEs (%) of the effect of catalyst dosage and methanol: oil molar ratio.

### 7.4.3 Optimization of conversion to FAMEs

Consequently, the optimal conditions of independent variables for maximizing the biodiesel production process were estimated and the validity of model to predict the optimum value of response was evaluated. The optimal conditions were found to be 56.3 ºC reaction temperature, 17:1 molar ratio of methanol: oil and 4% of catalyst dosage in addition to the corresponding conversion under these conditions was predicted to be 100%. In order to verify the accuracy of the model analysis, three separated experiments were conducted under the optimum values of reaction temperature, methanol: oil molar ratio, and catalyst dosage. The average value of response was 97% which is close to the predicted value with the relative error of 3%. The results confirm that data were well-fitted with the second-order polynomial

model equation. Table 7-3 shows the optimum conditions and the experimental and predicted response.

**Table 7-3:** The optimum conditions of reaction temperature, methanol: oil molar ratio, and catalyst dosage along with the experimental and predicted response of ester conversion.

| Parameters | Value | Conversion to FAMEs (%) | | % error |
|---|---|---|---|---|
| | | Experimental value | Predicted value | |
| Reaction temperature, C | 56.3 | 97 | 100 | 3 |
| MeOH: oil molar ratio | 17:1 | | | |
| Catalyst dosage, wt. % | 4 | | | |

## 7.5 Summary

The conversion of waste canola oil to FAMEs in the transesterfication process by Li/Zn-Cb catalyst was demonstrated by the response surface methodology (RSM) based on the Box–Benkhen design (BBD) in order to sought the efficient and economic technique. The statistical analysis and variance analysis (ANOVA) showed that reaction temperature, methanol to oil molar ratio and catalyst dosage had the most significant influence on the conversion. In addition, the conversion was affected by the interaction between the reaction temperature and the molar ratio of methanol:oil. The quadratic model was well-fitted the experimental data as shown from the determination coefficient ($R^2$ =0.98) obtained from eq. (7-4). The highest conversion to FAMEs of 97% was achieved at 17:1 of methanol:oil molar ratio, 4% of catalyst dosage and 56.3 °C of reaction temperature.

**CHAPTER 8**

**Conclusions and Recommendations**

## 8.1  ntroduction

Biodiesel is currently being considered as a renewable source of energy and a promising alternative of fossil fuel. In this thesis, different lithium and chicken bone based solid catalysts (Li/TiO$_2$, Li-Cb and Li/Zn-Cb) were synthesized by wet impregnation method and characterized by  XRD, FT-IR, BET, TG-DSC and FESEM for biodiesel production. The performance of these catalysts were investigated under different conditions (reaction temperature, reaction time, catalyst dosage and methanol:oil molar ratio), using waste and fresh canola oil. Moreover, the transesterfication of waste canola oil was optimized using Response Surface Methodology (RSM) to understand the synergistic influence of the affecting parameter (reaction temperature, catalyst dosage and methanol:oil molar ratio) and the influence of ultrasonic at the optimum reaction conditions of the process was also evaluated. Therefore, the following conclusions have been drawn from the present study along with some proposed recommendations for future work.

### 8.1.1  Conclusions

- The activity of TiO$_2$ catalyst was enhanced by implanting lithium and the modified catalyst was evaluated for biodiesel production. The catalyst was prepared by impregnation method and the effect of preparation parameters such as concentration of lithium to TiO$_2$ and calcination temperature was investigated. The highest activity was shown by the catalyst that comprised of 30 wt. % of LiNO$_3$ concentration and 600 °C of calcination temperature (30LT600). The characterization showed that Li$_2$TiO$_4$ was the responsible compound for the high performance of 30LT600. The optimal reaction

141

conditions that identified for 30LT600 and conducted with transesterfication of fresh canola oil were 24:1 of methanol:oil ratio, 5% of catalyst dosage at 3 h of the reaction duration and 65 °C of reaction temperature and resulted in 98% of conversion to FAMEs. The kinetic studies have shown that the transesterfication reaction by 30LT600 could be carried out under mild reaction conditions of temperature and pressure. Transesterfication process was conducted with waste canola oil and the conversion was found to be 91.73%. In addition, the catalyst reusability was studied and it was found that upon four successive runs, the catalyst activity was declined due to two reasons: blocking the catalyst pores by triglyceride and glycerol as shown by TGA/DSC analysis and leaching of Li.

- The potential of Li impregnated chicken bone as a solid catalyst was evaluated for transesterfication of waste and fresh canola oil. The catalyst was developed by impregnating lithium onto chicken bone at various concentrations and it was thermally treated at different calcination temperatures in order to strengthen the basicity of chicken bone. The highest performance was found to the catalyst with 2 g of $LiNO_3$ implanted on chicken bone (Cb) and thermally treated at 850 °C (2Li-Cb850). The conversion was found to be 96.6% and 94.9% for transesterfication of fresh and waste canola oil, respectively, under the optimum reaction conditions (3 h of reaction time, 18:1 of methanol:oil molar ratio, 4wt % of catalyst loading, and reaction temperature of 60 °C). The catalyst was active for 5 successive runs with conversion > 82% at the optimum conditions with fresh canola oil. Moreover, pseudo first order was the fit model for the reaction at 60 °C with rate constant of 0.58 $h^{-1}$, 16.9

kJ/mol of activation energy and frequency factor of $2.49 \times 10^6$ h$^{-1}$ as revealed by the kinetic studies.

- Evaluating the optimum conditions for biodiesel production from waste canola oil via Lithium/zinc chicken bone based catalyst (Li/Zn-Cb2). The developed catalyst showed a high conversion (98%) after 3.5 h of reaction time, catalyst dosage of 4% and 18:1 molar ratio of MeOH/WCO at 60 ºC. Synthesizing catalyst from waste material and using waste oil as a source of feedstock contribute to making the biodiesel production process economical as well as get the wastes off the environment. The kinetic parameters were identified for the synthesized catalyst and it was found the reaction follows pseudo-first order model with a rate constant of 0.66 h$^{-1}$, frequency factor and activation energy were $2.6 \times 10^9$ h$^{-1}$ and 23.20 kJ mol$^{-1}$, respectively. The conversion was greater than 96% after 7 cycles of reuse.

- The effects of methanol to oil ratio, catalyst dosage and reaction temperature at constant reaction time (3.5 h) on the conversion to FAME were optimized statically by Response Surface Methodology (RSM), using a Box-Behnken method. Transesterfication process was conducted by Li/Zn-Cb catalyst and waste canola oil. The experimental design comprised 15 runs to verify the effects of the aforementioned reaction parameters (independent parameters) on the conversion to FAMEs (response factor). Analysis of variance (ANOVA), and significance of interaction of reaction parameters were discussed. Statistical optimization of the above parameters showed that 97% of conversion to FAMEs was obtained at 17:1 of methanol:oil molar ratio, 4% of catalyst dosage and 56.3 °C of reaction temperature.

- The influence of ultrasound conditions was demonstrated on the biodiesel production. The transesterfication process was carried out via Li/Zn-Cb catalyst with waste canola oil and assisted by ultrasound power. The investigation showed that 96% of conversion to FAMEs was achieved in a half dosage of catalyst (2%) that was used in process without ultrasound (4%) and in lower reaction time (1.5 h). Thus, the ultrasound assisted production process was economic by saving catalyst amount and reaction time.

## 8.1.2 Recommendations for further work

- In this work, we used methanol as a solvent in the transesterfication of oil, it is important to employ different types of solvents and compare the results of the conversion.

- The influence of water content and FFA on the performance of the prepared catalysts was not investigated. Therefore, these parameters should be considered in the future studies.

- The feasibility of applying the prepared catalysts (Li/TiO$_2$, Li-Cb and Li/Zn-Cb) for industrial scale of biodiesel production needs to be assessed and evaluated.

- Chicken bone as a waste biomass was used as a supporter for lithium and zinc ions, different kinds of biomass could be used and investigated for these ions (Li, Zn) for biodiesel production.

- This work focused on developing efficient catalysts for sustainable biodiesel production process. Thus, it would be interesting to conduct a life cycle analysis and economic assessment of the biodiesel production process.

- The major factor in losing the reproducibility of TiO$_2$ based catalysts was the leaching of lithium. Thus, enhancing the lithium saibility by employing different

kinds of supports or applying different preparation method such as co-precipitation method would be of interest.

## References

[1] Mardhiah, H. H., Ong, H. C., Masjuki, H., Lim, S., & Lee, H. (2017). A review on latest developments and future prospects of heterogeneous catalyst in biodiesel production from non-edible oils. Renewable and Sustainable Energy Reviews, 67, 1225-1236.

[2] Noraini, M., Ong, H. C., Badrul, M. J., & Chong, W. (2014). A review on potential enzymatic reaction for biofuel production from algae. Renewable and Sustainable Energy Reviews, 39, 24-34.

[3] Talebian-Kiakalaieh, A., Amin, N. A. S., & Mazaheri, H. (2013). A review on novel processes of biodiesel production from waste cooking oil. Applied Energy, 104, 683-710.

[4] Guldhe, A., Singh, B., Mutanda, T., Permaul, K., & Bux, F. (2015). Advances in synthesis of biodiesel via enzyme catalysis: Novel and sustainable approaches. Renewable and Sustainable Energy Reviews, 41, 1447-1464.

[5] Marinković, D. M., Stanković, M. V., Veličković, A. V., Avramović, J. M., Miladinović, M. R., Stamenković, O. O., Veljković, V. B., Jovanović, D. M. (2016). Calcium oxide as a promising heterogeneous catalyst for biodiesel production: Current state and perspectives. Renewable and Sustainable Energy Reviews, 56, 1387-1408.

[6] de Araújo, C. D. M., de Andrade, C. C., e Silva, E. D. S., & Dupas, F. A. (2013). Biodiesel production from used cooking oil: A review. Renewable and Sustainable Energy Reviews, 27, 445-452.

[7] Verma, P., & Sharma, M. (2015). Performance and emission characteristics of biodiesel fuelled diesel engines. International Journal of Renewable Energy Research, 5(1), 245-250.

[8] Saba, T., Estephane, J., El Khoury, B., El Khoury, M., Khazma, M., El Zakhem, H., & Aouad, S. (2016). Biodiesel production from refined sunflower vegetable oil over KOH/ZSM5 catalysts. Renewable Energy, 90, 301-306.

[9] Véras, I. C., Silva, F. A., Ferrão-Gonzales, A. D., & Moreau, V. H. (2011). One-step enzymatic production of fatty acid ethyl ester from high-acidity waste feedstocks in solvent-free media. Bioresource technology, 102(20), 9653-9658.

[10] Huang, J., Xia, J., Jiang, W., Li, Y., & Li, J. (2015). Biodiesel production from microalgae oil catalyzed by a recombinant lipase. Bioresource technology, 180, 47-53.

[11] Abdullah, A., Razali, N., Mootabadi, H., & Salamatinia, B. (2007). Critical technical areas for future improvement in biodiesel technologies. Environmental Research Letters, 2(3), 034001.

[12] Murillo, G., Ali, S. S., Sun, J., Yan, Y., Bartocci, P., El-Zawawy, N., ... & Fantozzi, F. (2019). Ultrasonic emulsification assisted immobilized Burkholderia cepacia lipase catalyzed transesterification of soybean oil for biodiesel production in a novel reactor design. Renewable Energy, 135, 1025-1034.

[13] Malhotra, R., & Ali, A. (2019). 5-Na/ZnO doped mesoporous silica as reusable solid catalyst for biodiesel production via transesterification of virgin cottonseed oil. Renewable Energy, 133, 606-619.

[14] Vyas, A. P., Verma, J. L., & Subrahmanyam, N. (2010). A review on FAME production processes. Fuel, 89(1), 1-9.

[15] Issariyakul, T., & Dalai, A. K. (2014). Biodiesel from vegetable oils. Renewable and Sustainable Energy Reviews, 31, 446-471.

[16] Lee, K. T., Lim, S., Pang, Y. L., Ong, H. C., & Chong, W. T. (2014). Integration of reactive extraction with supercritical fluids for process intensification of biodiesel production: Prospects and recent advances. Progress in Energy and Combustion Science, 45, 54-78.

[17] Banković-Ilić, I. B., Stojković, I. J., Stamenković, O. S., Veljkovic, V. B., & Hung, Y.-T. (2014). Waste animal fats as feedstocks for biodiesel production. Renewable and Sustainable Energy Reviews, 32, 238-254.

[18] Ramli, A., Farooq, M., Naeem, A., Khan, S., Hummayun, M., Iqbal, A., Ahmed, S., & Shah, L. A. (2017). Bifunctional Heterogeneous Catalysts for Biodiesel Production using Low Cost Feedstocks: A Future Perspective. In Frontiers in Bioenergy and Biofuels. InTech.

[19] Diesel, R. (1912). THE DIESEL OIL ENGINE. Naval Engineers Journal, 24(1), 653-692.

[20] Ibrehem, A. S., & Al-Salim, H. S. (2009). New Dynamic Analysis and System Identification of Biodiesel Production Process from Palm Oil. Bulletin of Chemical Reaction Engineering & Catalysis, 4(2), 61.

[21] Gorey, N., Ghosh, S., Srivastava, P., & Kumar, V. (2017, August). Characterization of Palm Oil as Biodiesel. In IOP Conference Series: Materials Science and Engineering (Vol. 225, No. 1, p. 012220). IOP Publishing.

[22] Sastry, S. V. A. R., & Murthy, C. V. R. (2012). Prospectus of biodiesel for future energy security. Elexir, Chemical Engg, 53, 12029-12034.

[23] Tekade, P. V., Mahodaya, O. A., Khandeshwar, G. R., & Joshi, B. D. (2012). Green synthesis of biodiesel from various vegetable oil and characterization by FT-IR spectroscopy. Sci. Rev. Chem. Commun, 2, 208-211.

[24] Pousa, G. P., Santos, A. L., & Suarez, P. A. (2007). History and policy of biodiesel in Brazil. Energy Policy, 35(11), 5393-5398.

[25] Yuan, W., & Yang, F. (2017). Chemical Conversion Process for Biodiesel Production. Biomass to Renewable Energy Processes, 299.

[26] Lin, L., Cunshan, Z., Vittayapadung, S., Xiangqian, S., & Mingdong, D. (2011). Opportunities and challenges for biodiesel fuel. Applied Energy, 88(4), 1020-1031.

[27] Adewale, P., Dumont, M.-J., & Ngadi, M. (2015). Recent trends of biodiesel production from animal fat wastes and associated production techniques. Renewable and Sustainable Energy Reviews, 45, 574-588.

[28] Narasimharao, K., Lee, A., & Wilson, K. (2007). Catalysts in production of biodiesel: a review. Journal of biobased materials and bioenergy, 1(1), 19-30.

[29] Pryde, E. H. (1983). Vegetable oils as diesel fuels: overview. Journal of the American Oil Chemists' Society, 60(8), 1557-1558.

[30] Ma, F., & Hanna, M. A. (1999). Biodiesel production: a review. Bioresource technology, 70(1), 1-15.

[31] Abbaszaadeh, A., Ghobadian, B., Omidkhah, M. R., & Najafi, G. (2012). Current biodiesel production technologies: a comparative review. *Energy Conversion and Management*, *63*, 138-148.

[32] Lam, S. S., Liew, R. K., Jusoh, A., Chong, C. T., Ani, F. N., & Chase, H. A. (2016). Progress in waste oil to sustainable energy, with emphasis on pyrolysis techniques. Renewable and Sustainable Energy Reviews, 53, 741-753.

[33] Singh, S. P., & Singh, D. (2010). Biodiesel production through the use of different sources and characterization of oils and their esters as the substitute of diesel: a review. Renewable and sustainable energy reviews, 14(1), 200-216.

[34] Ito, T., Sakurai, Y., Kakuta, Y., Sugano, M., & Hirano, K. (2012). Biodiesel production from waste animal fats using pyrolysis method. Fuel processing technology, 94(1), 47-52.

[35] Daud, N. M., Abdullah, S. R. S., Hasan, H. A., & Yaakob, Z. (2015). Production of biodiesel and its wastewater treatment technologies: a review. Process Safety and Environmental Protection, 94, 487-508.

[36] Siddiquee, M. N., & Rohani, S. (2011). Lipid extraction and biodiesel production from municipal sewage sludges: a review. Renewable and Sustainable Energy Reviews, 15(2), 1067-1072.

[37] Gnanaprakasam, A., Sivakumar, V. M., Surendhar, A., Thirumarimurugan, M., & Kannadasan, T. (2013). Recent strategy of biodiesel production from

waste cooking oil and process influencing parameters: a review. Journal of Energy, 2013.

[38] Atabani, A. E., Silitonga, A. S., Badruddin, I. A., Mahlia, T. M. I., Masjuki, H. H., & Mekhilef, S. (2012). A comprehensive review on biodiesel as an alternative energy resource and its characteristics. Renewable and sustainable energy reviews, 16(4), 2070-2093.

[39] Verma, P., & Sharma, M. (2016). Review of process parameters for biodiesel production from different feedstocks. Renewable and Sustainable Energy Reviews, 62, 1063-1071.

[40] Nurfitri, I., Maniam, G. P., Hindryawati, N., Yusoff, M. M., & Ganesan, S. (2013). Potential of feedstock and catalysts from waste in biodiesel preparation: a review. Energy Conversion and Management, 74, 395-402.

[41] Soltani, S., Rashid, U., Yunus, R., & Taufiq-Yap, Y. H. (2015). Synthesis of biodiesel through catalytic transesterification of various feedstocks using fast solvothermal technology: a critical review. Catalysis Reviews, 57(4), 407-435.

[42] Noiroj, K., Intarapong, P., Luengnaruemitchai, A., & Jai-In, S. (2009). A comparative study of KOH/Al 2 O 3 and KOH/NaY catalysts for biodiesel production via transesterification from palm oil. Renewable Energy, 34(4), 1145-1150.

[43] Nongbe, M. C., Ekou, T., Ekou, L., Yao, K. B., Le Grognec, E., & Felpin, F.-X. (2017). Biodiesel production from palm oil using sulfonated graphene catalyst. Renewable Energy, 106, 135-141.

[44] Nasreen, S., Liu, H., Skala, D., Waseem, A., & Wan, L. (2015). Preparation of biodiesel from soybean oil using La/Mn oxide catalyst. Fuel Processing Technology, 131, 290-296.

[45] Lu, Y., Zhang, Z., Xu, Y., Liu, Q., & Qian, G. (2015). CaFeAl mixed oxide derived heterogeneous catalysts for transesterification of soybean oil to biodiesel. Bioresource technology, 190, 438-441.

[46] González, E. A. Z., García-Guaderrama, M., Villalobos, M. R., Dellamary, F. L., Kandhual, S., Rout, N. P., Tiznado, H., & Arizaga, G. G. C. (2015). Potassium titanate as heterogeneous catalyst for methyl transesterification. Powder Technology, 280, 201-206.

[47] Salinas, D., Guerrero, S., Cross, A., Araya, P., & Wolf, E. (2016). Potassium titanate for the production of biodiesel. Fuel, 166, 237-244.

[48] Sánchez, B., Benitez, B., Querini, C., & Mendow, G. (2015). Transesterification of sunflower oil with ethanol using sodium ethoxide as catalyst. Effect of the reaction conditions. Fuel Processing Technology, 131, 29-35.

[49] Taufiq-Yap, Y., Lee, H., Yunus, R., & Juan, J. (2011). Transesterification of non-edible Jatropha curcas oil to biodiesel using binary Ca–Mg mixed oxide catalyst: effect of stoichiometric composition. Chemical Engineering Journal, 178, 342-347.

[50] Lee, H., Taufiq-Yap, Y., Hussein, M., & Yunus, R. (2013). Transesterification of jatropha oil with methanol over Mg–Zn mixed metal oxide catalysts. Energy, 49, 12-18.

[51] Taufiq-Yap, Y. H., Teo, S. H., Rashid, U., Islam, A., Hussien, M. Z., & Lee, K. T. (2014). Transesterification of Jatropha curcas crude oil to biodiesel on calcium lanthanum mixed oxide catalyst: effect of stoichiometric composition. Energy Conversion and Management, 88, 1290-1296.

[52] Ripa, M., Buonaurio, C., Mellino, S., Fiorentino, G., & Ulgiati, S. (2014). Recycling waste cooking oil into biodiesel: a life cycle assessment. International Journal of Performability Engineering, 10(4), 347-356.

[53] Refaat, A. (2010). Different techniques for the production of biodiesel from waste vegetable oil. International Journal of Environmental Science & Technology, 7(1), 183-213.

[54] Gurunathan, B., & Ravi, A. (2015). Biodiesel production from waste cooking oil using copper doped zinc oxide nanocomposite as heterogeneous catalyst. Bioresource technology, 188, 124-127.

[55] Amani, H., Ahmad, Z., & Hameed, B. (2014). Highly active alumina-supported Cs–Zr mixed oxide catalysts for low-temperature transesterification of waste cooking oil. Applied Catalysis A: General, 487, 16-25.

[56] Cai, Z.-Z., Wang, Y., Teng, Y.-L., Chong, K.-M., Wang, J.-W., Zhang, J.-W., & Yang, D.-P. (2015). A two-step biodiesel production process from waste cooking oil via recycling crude glycerol esterification catalyzed by alkali catalyst. Fuel Processing Technology, 137, 186-193.

[57] Ferrero, G. O., Almeida, M. F., Alvim-Ferraz, M. C., & Dias, J. M. (2015). Glycerol-enriched heterogeneous catalyst for biodiesel production from soybean oil and waste frying oil. Energy Conversion and Management, 89, 665-671.

[58] Srilatha, K., Devi, B. P., Lingaiah, N., Prasad, R., & Prasad, P. S. (2012). Biodiesel production from used cooking oil by two-step heterogeneous catalyzed process. Bioresource technology, 119, 306-311.

[59] Farooq, M., Ramli, A., & Subbarao, D. (2013). Biodiesel production from waste cooking oil using bifunctional heterogeneous solid catalysts. Journal of Cleaner Production, 59, 131-140.

[60] Gonçalves, A. L., Pires, J. C., & Simões, M. (2013). Green fuel production: processes applied to microalgae. Environmental chemistry letters, 11(4), 315-324.

[61] Krohn, B. J., McNeff, C. V., Yan, B., & Nowlan, D. (2011). Production of algae-based biodiesel using the continuous catalytic Mcgyan® process. Bioresource technology, 102(1), 94-100.

[62] Piloto-Rodríguez, R., Sánchez-Borroto, Y., Melo-Espinosa, E. A., & Verhelst, S. (2017). Assessment of diesel engine performance when fueled with biodiesel from algae and microalgae: An overview. Renewable and Sustainable Energy Reviews, 69, 833-842.

[63] Nautiyal, P., Subramanian, K., & Dastidar, M. (2014). Production and characterization of biodiesel from algae. Fuel Processing Technology, 120, 79-88.

[64] Vijayaraghavan, K., & Hemanathan, K. (2009). Biodiesel production from freshwater algae. Energy & Fuels, 23(11), 5448-5453.

[65] Hossain, A. S., Salleh, A., Boyce, A. N., Chowdhury, P., & Naqiuddin, M. (2008). Biodiesel fuel production from algae as renewable energy. American journal of biochemistry and biotechnology, 4(3), 250-254.

[66] Xu, R., & Mi, Y. (2011). Simplifying the process of microalgal biodiesel production through in situ transesterification technology. Journal of the American Oil Chemists' Society, 88(1), 91-99.

[67] Haas, M. J., & Wagner, K. (2011). Simplifying biodiesel production: the direct or in situ transesterification of algal biomass. European journal of lipid science and technology, 113(10), 1219-1229.

[68] Ehimen, E., Sun, Z., & Carrington, C. (2010). Variables affecting the in situ transesterification of microalgae lipids. Fuel, 89(3), 677-684.

[69] D'ippolito, S. A., Yori, J. C., Iturria, M. E., Pieck, C. L., & Vera, C. R. (2007). Analysis of a two-step, noncatalytic, supercritical biodiesel production process with heat recovery. Energy & Fuels, 21(1), 339-346.

[70] Juan, J. C., Kartika, D. A., Wu, T. Y., & Hin, T. Y. Y. (2011). Biodiesel production from jatropha oil by catalytic and non-catalytic approaches: an overview. Bioresource technology, 102(2), 452-460.

[71] Leung, D. Y., Wu, X., & Leung, M. K. H. (2010). A review on biodiesel production using catalyzed transesterification. Applied energy, 87(4), 1083-1095.

[72] Teo, S. H., Goto, M., & Taufiq-Yap, Y. H. (2015). Biodiesel production from Jatropha curcas L. oil with Ca and La mixed oxide catalyst in near supercritical methanol conditions. The Journal of Supercritical Fluids, 104, 243-250.

[73] Rathore, V., & Madras, G. (2007). Synthesis of biodiesel from edible and non-edible oils in supercritical alcohols and enzymatic synthesis in supercritical carbon dioxide. Fuel, 86(17-18), 2650-2659.

[74] Kiss, F. E., Micic, R. D., Tomić, M. D., Nikolić-Djorić, E. B., & Simikić, M. Đ. (2014). Supercritical transesterification: impact of different types of alcohol on biodiesel yield and LCA results. The Journal of Supercritical Fluids, 86, 23-32.

[75] Lam, M. K., Lee, K. T., & Mohamed, A. R. (2010). Homogeneous, heterogeneous and enzymatic catalysis for transesterification of high free fatty acid oil (waste cooking oil) to biodiesel: a review. Biotechnology advances, 28(4), 500-518.

[76] Vicente, G., Martınez, M., & Aracil, J. (2004). Integrated biodiesel production: a comparison of different homogeneous catalysts systems. Bioresource technology, 92(3), 297-305.

[77] Leung, D., & Guo, Y. (2006). Transesterification of neat and used frying oil: optimization for biodiesel production. Fuel Processing Technology, 87(10), 883-890.

[78] Atadashi, I., Aroua, M., Aziz, A. A., & Sulaiman, N. (2013). The effects of catalysts in biodiesel production: A review. Journal of Industrial and Engineering Chemistry, 19(1), 14-26.

[79] Cardoso, A. L., Neves, S. C., & da Silva, M. J. (2009). Kinetic study of alcoholysis of the fatty acids catalyzed by tin chloride (II): an alternative catalyst for biodiesel production. Energy & Fuels, 23(3), 1718-1722.

[80] Kulkarni, M. G., & Dalai, A. K. (2006). Waste cooking oil an economical source for biodiesel: a review. Industrial & engineering chemistry research, 45(9), 2901-2913.

[81] Jacobson, K., Gopinath, R., Meher, L. C., & Dalai, A. K. (2008). Solid acid catalyzed biodiesel production from waste cooking oil. Applied Catalysis B: Environmental, 85(1), 86-91.

[82] Lotero, E., Liu, Y., Lopez, D. E., Suwannakarn, K., Bruce, D. A., & Goodwin, J. G. (2005). Synthesis of biodiesel via acid catalysis. Industrial & engineering chemistry research, 44(14), 5353-5363.

[83] Balat, M., & Balat, H. (2010). Progress in biodiesel processing. Applied Energy, 87(6), 1815-1835.

[84] Lotero, E., Goodwin Jr, J. G., Bruce, D. A., Suwannakarn, K., Liu, Y., & Lopez, D. E. (2006). The catalysis of biodiesel synthesis. catalysis, 19(1), 41-83.

[85] Lin, L., Ying, D., Chaitep, S., & Vittayapadung, S. (2009). Biodiesel production from crude rice bran oil and properties as fuel. Applied Energy, 86(5), 681-688.

[86] Zheng, S., Kates, M., Dubé, M., & McLean, D. (2006). Acid-catalyzed production of biodiesel from waste frying oil. biomass and bioenergy, 30(3), 267-272.

[87] Aranda, D. A., Santos, R. T., Tapanes, N. C., Ramos, A. L. D., & Antunes, O. A. C. (2008). Acid-catalyzed homogeneous esterification reaction for biodiesel production from palm fatty acids. Catalysis letters, 122(1-2), 20-25.

[88] Melero, J. A., Bautista, L. F., Morales, G., Iglesias, J., & Sánchez-Vázquez, R. (2015). Acid-catalyzed production of biodiesel over arenesulfonic SBA-15: Insights into the role of water in the reaction network. Renewable Energy, 75, 425-432.

[89] Aransiola, E. F., Ojumu, T. V., Oyekola, O. O., Madzimbamuto, T. F., & Ikhu-Omoregbe, D. I. O. (2014). A review of current technology for biodiesel production: State of the art. Biomass and bioenergy, 61, 276-297.

[90] Borges, M. E., & Díaz, L. (2012). Recent developments on heterogeneous catalysts for biodiesel production by oil esterification and transesterification reactions: a review. Renewable and Sustainable Energy Reviews, 16(5), 2839-2849.

[91] Lu, H., Liu, Y., Zhou, H., Yang, Y., Chen, M., & Liang, B. (2009). Production of biodiesel from Jatropha curcas L. oil. Computers & Chemical Engineering, 33(5), 1091-1096.

[92] Wan, Z., Lim, J. K., & Hameed, B. H. (2015). Chromium–tungsten heterogeneous catalyst for esterification of palm fatty acid distillate to fatty acid methyl ester. Journal of the Taiwan Institute of Chemical Engineers, 54, 64-70.

[93] Dehghani, S., & Haghighi, M. (2017). Sono-sulfated zirconia nanocatalyst supported on MCM-41 for biodiesel production from sunflower oil: Influence of ultrasound irradiation power on catalytic properties and performance. Ultrasonics sonochemistry, 35, 142-151.

[94] Liu, R., Wang, X., Zhao, X., & Feng, P. (2008). Sulfonated ordered mesoporous carbon for catalytic preparation of biodiesel. Carbon, 46(13), 1664-1669.

[95] Liu, X., He, H., Wang, Y., Zhu, S., & Piao, X. (2008). Transesterification of soybean oil to biodiesel using CaO as a solid base catalyst. Fuel, 87(2), 216-221.

[96] Dossin, T. F., Reyniers, M.-F., & Marin, G. B. (2006). Kinetics of heterogeneously MgO-catalyzed transesterification. Applied Catalysis B: Environmental, 62(1), 35-45.

[97] Lee, H., Liao, J. D., Yang, J. W., Hsu, W. D., Liu, B. H., Chen, T. C., Sivashanmugan, K. & Gedanken, A. (2018). Continuous Waste Cooking Oil Transesterification with Microwave Heating and Strontium Oxide Catalyst. Chemical Engineering & Technology, 41(1), 192-198.

[98] Mutreja, V., Singh, S., & Ali, A. (2011). Biodiesel from mutton fat using KOH impregnated MgO as heterogeneous catalysts. Renewable Energy, 36(8), 2253-2258.

[99] Lertpanyapornchai, B., & Ngamcharussrivichai, C. (2015). Mesostructured Sr and Ti mixed oxides as heterogeneous base catalysts for transesterification of palm kernel oil with methanol. Chemical Engineering Journal, 264, 789-796.

[100] Thammachart, M., Meeyoo, V., Risksomboon, T., & Osuwan, S. (2001). Catalytic activity of CeO2–ZrO2 mixed oxide catalysts prepared via sol–gel technique: CO oxidation. Catalysis Today, 68(1-3), 53-61.

[101] Pasupulety, N., Rempel, G. L., & Ng, F. T. (2015). Studies on Mg-Zn mixed oxide catalyst for biodiesel production. Applied Catalysis A: General, 489, 77-85.

[102] Mutreja, V., Singh, S., & Ali, A. (2014). Potassium impregnated nanocrystalline mixed oxides of La and Mg as heterogeneous catalysts for transesterification. Renewable Energy, 62, 226-233.

[103] Mahesh, S. E., Ramanathan, A., Begum, K. M. S., & Narayanan, A. (2015). Biodiesel production from waste cooking oil using KBr impregnated CaO as catalyst. Energy Conversion and Management, 91, 442-4.

[104] Boro, J., Konwar, L. J., & Deka, D. (2014). Transesterification of non edible feedstock with lithium incorporated egg shell derived CaO for biodiesel production. Fuel Processing Technology, 122, 72-78.

[105] Kaur, M., & Ali, A. (2011). Lithium ion impregnated calcium oxide as nano catalyst for the biodiesel production from karanja and jatropha oils. Renewable Energy, 36(11), 2866-2871.

[106] Wan, L., Liu, H., & Skala, D. (2014). Biodiesel production from soybean oil in subcritical methanol using MnCO3/ZnO as catalyst. Applied Catalysis B: Environmental, 152, 352-359.

[107] Babu, N. S., Sree, R., Prasad, P. S., & Lingaiah, N. (2008). Room-temperature transesterification of edible and nonedible oils using a heterogeneous strong basic Mg/La catalyst. Energy & Fuels, 22(3), 1965-1971.

[108] Hájek, M., Kutálek, P., Smoláková, L., Troppová, I., Čapek, L., Kubička, D., Kocik, J., & Thanh, D. N. (2015). Transesterification of rapeseed oil by Mg–Al

mixed oxides with various Mg/Al molar ratio. Chemical Engineering Journal, 263, 160-167.

[109] Castro, C. S., Ferreti, C., Di Cosimo, J. I., & Assaf, J. M. (2013). Support influence on the basicity promotion of lithium-based mixed oxides for transesterification reaction. Fuel, 103, 632-638.

[110] Liu, Q., Wang, B., Wang, C., Tian, Z., Qu, W., Ma, H., & Xu, R. (2014). Basicities and transesterification activities of Zn–Al hydrotalcites-derived solid bases. Green Chemistry, 16(5), 2604-2613.

[111] Liu, L., Wen, Z., & Cui, G. (2015). Preparation of Ca/Zr mixed oxide catalysts through a birch-templating route for the synthesis of biodiesel via transesterification. Fuel, 158, 176-182.

[112] Singh, V., Bux, F., & Sharma, Y. C. (2016). A low cost one pot synthesis of biodiesel from waste frying oil (WFO) using a novel material, $\beta$-potassium dizirconate ($\beta$-$K_2Zr_2O_5$). Applied Energy, 172, 23-33.

[113] Xie, W., Han, Y., & Wang, H. (2018). Magnetic $Fe_3O_4$/MCM-41 composite-supported sodium silicate as heterogeneous catalysts for biodiesel production. Renewable Energy.

[114] Ognjanovic, N., Bezbradica, D., & Knezevic-Jugovic, Z. (2009). Enzymatic conversion of sunflower oil to biodiesel in a solvent-free system: process optimization and the immobilized system stability. Bioresource technology, 100(21), 5146-5154.

[115] Sim, J. H., Kamaruddin, A. H., & Bhatia, S. (2010). Biodiesel (FAME) productivity, catalytic efficiency and thermal stability of lipozyme TL IM for

crude palm oil transesterification with methanol. Journal of the American Oil Chemists' Society, 87(9), 1027-1034.

[116] Nasaruddin, R. R., Alam, M. Z., & Jami, M. S. (2014). Evaluation of solvent system for the enzymatic synthesis of ethanol-based biodiesel from sludge palm oil (SPO). Bioresource technology, 154, 155-161.

[117] Tran, D.-T., Chen, C.-L., & Chang, J.-S. (2013). Effect of solvents and oil content on direct transesterification of wet oil-bearing microalgal biomass of Chlorella vulgaris ESP-31 for biodiesel synthesis using immobilized lipase as the biocatalyst. Bioresource technology, 135, 213-221.

[118] Shah, S., & Gupta, M. N. (2007). Lipase catalyzed preparation of biodiesel from Jatropha oil in a solvent free system. Process Biochemistry, 42(3), 409-414.

[119] Chen, G., Ying, M., & Li, W. (2006). Enzymatic conversion of waste cooking oils into alternative fuel—biodiesel. Applied biochemistry and biotechnology, 132(1-3), 911-921.

[120] Tongboriboon, K., Cheirsilp, B., & Aran, H. (2010). Mixed lipases for efficient enzymatic synthesis of biodiesel from used palm oil and ethanol in a solvent-free system. Journal of Molecular Catalysis B: Enzymatic, 67(1), 52-59.

[121] Amini, Z., Ong, H. C., Harrison, M. D., Kusumo, F., Mazaheri, H., & Ilham, Z. (2017). Biodiesel production by lipase-catalyzed transesterification of Ocimum basilicum L.(sweet basil) seed oil. Energy Conversion and Management, 132, 82-90.

[122] Li, W., Li, R.-w., Li, Q., Du, W., & Liu, D. (2010). Acyl migration and kinetics study of 1 (3)-positional specific lipase of Rhizopus oryzae-catalyzed methanolysis of triglyceride for biodiesel production. Process Biochemistry, 45(12), 1888-1893.

[123] Royon, D., Daz, M., Ellenrieder, G., & Locatelli, S. (2007). Enzymatic production of biodiesel from cotton seed oil using t-butanol as a solvent. Bioresource technology, 98(3), 648-653.

[124] Nie, K., Xie, F., Wang, F., & Tan, T. (2006). Lipase catalyzed methanolysis to produce biodiesel: optimization of the biodiesel production. Journal of Molecular Catalysis B: Enzymatic, 43(1-4), 142-147.

[125] Viriya-Empikul, N., Krasae, P., Nualpaeng, W., Yoosuk, B., & Faungnawakij, K. (2012). Biodiesel production over Ca-based solid catalysts derived from industrial wastes. Fuel, 92(1), 239-244.

[126] Bet-Moushoul, E., Farhadi, K., Mansourpanah, Y., Nikbakht, A. M., Molaei, R., & Forough, M. (2016). Application of CaO-based/Au nanoparticles as heterogeneous nanocatalysts in biodiesel production. Fuel, 164, 119-127.

[127] Farooq, M., Ramli, A., & Naeem, A. (2015). Biodiesel production from low FFA waste cooking oil using heterogeneous catalyst derived from chicken bones. Renewable Energy, 76, 362-368.

[128] Suwannasom, P., Tansupo, P., & Ruangviriyachai, C. (2016). A bone-based catalyst for biodiesel production from waste cooking oil. Energy Sources, Part A: Recovery, Utilization, and Environmental Effects, 38(21), 3167-3173.

[129] Sharma, M., Khan, A. A., Puri, S., & Tuli, D. (2012). Wood ash as a potential heterogeneous catalyst for biodiesel synthesis. biomass and bioenergy, 41, 94-106.

[130] Win, T. T., & Khine, M. M. (2016). Chicken Eggshell Waste as a Suitable Catalyst for Transesterification of Palm Oil, Optimization for Biodiesel Production. In 5th International Conference on Food, Agricultural and Biological Sciences (ICFABS-2016) Dec (pp. 25-26).

[131] Cho, Y. B., & Seo, G. (2010). High activity of acid-treated quail eggshell catalysts in the transesterification of palm oil with methanol. Bioresource technology, 101(22), 8515-8519.

[132] Ilgen, O. (2011). Dolomite as a heterogeneous catalyst for transesterification of canola oil. Fuel Processing Technology, 92(3), 452-455.

[133] Ngamcharussrivichai, C., Nunthasanti, P., Tanachai, S., & Bunyakiat, K. (2010). Biodiesel production through transesterification over natural calciums. Fuel Processing Technology, 91(11), 1409-1415.

[134] Obadiah, A., Swaroopa, G. A., Kumar, S. V., Jeganathan, K. R., & Ramasubbu, A. (2012). Biodiesel production from palm oil using calcined waste animal bone as catalyst. Bioresource technology, 116, 512-516.

[135] Chakraborty, R., Bepari, S., & Banerjee, A. (2011). Application of calcined waste fish (Labeo rohita) scale as low-cost heterogeneous catalyst for biodiesel synthesis. Bioresource technology, 102(3), 3610-3618.

[136] Boey, P. L., Maniam, G. P., & Hamid, S. A. (2009). Biodiesel production via transesterification of palm olein using waste mud crab (Scylla serrata) shell as a heterogeneous catalyst. Bioresource Technology, 100(24), 6362-6368.

[137] Yang, L., Zhang, A., & Zheng, X. (2009). Shrimp shell catalyst for biodiesel production. Energy & Fuels, 23(8), 3859-3865.

[138] Ji, J., Wang, J., Li, Y., Yu, Y., & Xu, Z. (2006). Preparation of biodiesel with the help of ultrasonic and hydrodynamic cavitation. Ultrasonics, 44, e411-e414.

[139] Pal, A., Verma, A., Kachhwaha, S. S., & Maji, S. (2010). Biodiesel production through hydrodynamic cavitation and performance testing. Renewable Energy, 35(3), 619-624.

[140] Firoz, S. (2017). A review: advantages and disadvantages of biodiesel. Int Res J Eng Technol, 530-535.

[141] Marra, F., De Bonis, M. V., & Ruocco, G. (2010). Combined microwaves and convection heating: a conjugate approach. Journal of Food Engineering, 97(1), 31-39.

[142] Liu, C. Z., & Cheng, X. Y. (2009). Microwave-assisted acid pretreatment for enhancing biogas production from herbal-extraction process residue. Energy & Fuels, 23(12), 6152-6155.

[143] Azcan, N., & Danisman, A. (2007). Alkali catalyzed transesterification of cottonseed oil by microwave irradiation. Fuel, 86(17-18), 2639-2644.

[144] Singh, A. K., Fernando, S. D., & Hernandez, R. (2007). Base-catalyzed fast transesterification of soybean oil using ultrasonication. Energy & Fuels, 21(2), 1161-1164.

[145] Ho, W. W. S., Ng, H. K., & Gan, S. (2016). Advances in ultrasound-assisted transesterification for biodiesel production. Applied Thermal Engineering, 100, 553-563.

[146] Deshmane, V. G., & Adewuyi, Y. G. (2013). Synthesis and kinetics of biodiesel formation via calcium methoxide base catalyzed transesterification reaction in the absence and presence of ultrasound. Fuel, 107, 474-482.

[147] Pukale, D. D., Maddikeri, G. L., Gogate, P. R., Pandit, A. B., & Pratap, A. P. (2015). Ultrasound assisted transesterification of waste cooking oil using heterogeneous solid catalyst. Ultrasonics sonochemistry, 22, 278-286.

[148] Santos, F. F., Matos, L. J., Rodrigues, S., & Fernandes, F. A. (2009). Optimization of the production of methyl esters from soybean waste oil applying ultrasound technology. Energy & Fuels, 23(8), 4116-4120.

[149] Deshmane, V. G., Gogate, P. R., & Pandit, A. B. (2009). Ultrasound assisted synthesis of isopropyl esters from palm fatty acid distillate. *Ultrasonics sonochemistry*, *16*(3), 345-350.

[150] Georgogianni, K. G., Kontominas, M. G., Pomonis, P. J., Avlonitis, D., & Gergis, V. (2008). Alkaline conventional and in situ transesterification of cottonseed oil for the production of biodiesel. Energy & Fuels, 22(3), 2110-2115.

[151] Georgogianni, K. G., Kontominas, M. G., Pomonis, P. J., Avlonitis, D., & Gergis, V. (2008). Conventional and in situ transesterification of sunflower seed oil for the production of biodiesel. Fuel processing technology, 89(5), 503-509.

[152] Kelkar, M. A., Gogate, P. R., & Pandit, A. B. (2008). Intensification of esterification of acids for synthesis of biodiesel using acoustic and hydrodynamic cavitation. Ultrasonics Sonochemistry, 15(3), 188-194.

[153] Badday, A. S., Abdullah, A. Z., & Lee, K. T. (2014). Transesterification of crude Jatropha oil by activated carbon-supported heteropolyacid catalyst in an ultrasound-assisted reactor system. Renewable Energy, 62, 10-17.

[154] Choedkiatsakul, I., Ngaosuwan, K., & Assabumrungrat, S. (2013). Application of heterogeneous catalysts for transesterification of refined palm oil in ultrasound-assisted reactor. Fuel processing technology, 111, 22-28.

[155] Salamatinia, B., Mootabadi, H., Hashemizadeh, I., & Abdullah, A. Z. (2013). Intensification of biodiesel production from vegetable oils using ultrasonic-assisted process: optimization and kinetic. Chemical Engineering and Processing: Process Intensification, 73, 135-143.

[156] Feyzi, M., Hosseini, N., Yaghobi, N., & Ezzati, R. (2017). Preparation, characterization, kinetic and thermodynamic studies of MgO-La 2 O 3 nanocatalysts for biodiesel production from sunflower oil. Chemical Physics Letters, 677, 19-29.

[157] Özbay, N., Oktar, N., & Tapan, N. A. (2008). Esterification of free fatty acids in waste cooking oils (WCO): Role of ion-exchange resins. Fuel, 87(10), 1789-1798.

[158] Zabeti, M., Daud, W. M. A. W., & Aroua, M. K. (2009). Activity of solid catalysts for biodiesel production: a review. Fuel Processing Technology, 90(6), 770-777.

[159] Kumar, D., & Ali, A. (2012). Nanocrystalline K–CaO for the transesterification of a variety of feedstocks: Structure, kinetics and catalytic properties. *biomass and bioenergy*, *46*, 459-468.

[160] Olutoye, M. A., Wong, C. P., Chin, L. H., & Hameed, B. H. (2014). Synthesis of FAME from the methanolysis of palm fatty acid distillate using highly active solid oxide acid catalyst. Fuel Processing Technology, 124, 54-60.

[161] Hailegiorgis, S. M., Mahadzir, S., & Subbarao, D. (2013). Parametric study and optimization of in situ transesterification of Jatropha curcas L assisted by benzyltrimethylammonium hydroxide as a phase transfer catalyst via response surface methodology. Biomass and bioenergy, 49, 63-73.

[162] Girish, N., Niju, S. P., Begum, K. M. M. S., & Anantharaman, N. (2013). Utilization of a cost effective solid catalyst derived from natural white bivalve clam shell for transesterification of waste frying oil. Fuel, 111, 653-658.

[163] Dai, Y., Wu, J., Chen, C. & Chen, K. (2015). Evaluating the optimum operating parameters on transesterification reaction for biodiesel production over a LiAlO2 catalyst. Chemical    Engineering Journal, 280, 370-376.

[164] Jahirul, M. I., Koh, W., Brown, R. J., Senadeera, W., O'Hara, I., & Moghaddam, L. (2014). Biodiesel production from non-edible beauty leaf (Calophyllum inophyllum) oil: Process optimization using response surface methodology (RSM). Energies, 7(8), 5317-5331.

[165] Baroutian, S., Aroua, M. K., Raman, A. A. A., & Sulaiman, N. M. N. (2010). Potassium hydroxide catalyst supported on palm shell activated carbon for

transesterification of palm oil. Fuel Processing Technology, 91(11), 1378-1385.

[166] Boey, P. L., Ganesan, S., Lim, S. X., Lim, S. L., Maniam, G. P., & Khairuddean, M. (2011). Utilization of BA (boiler ash) as catalyst for transesterification of palm olein. Energy, 36(10), 5791-5796.

[167] Samart, C., Sreetongkittikul, P., & Sookman, C. (2009). Heterogeneous catalysis of transesterification of soybean oil using KI/mesoporous silica. Fuel Processing Technology, 90(7-8), 922-925.

[168] Leclercq, E., Finiels, A., & Moreau, C. (2001). Transesterification of rapeseed oil in the presence of basic zeolites and related solid catalysts. Journal of the American Oil Chemists' Society, 78(11), 1161-1165.

[169] Ho, W. W. S., Ng, H. K., Gan, S., & Tan, S. H. (2014). Evaluation of palm oil mill fly ash supported calcium oxide as a heterogeneous base catalyst in biodiesel synthesis from crude palm oil. Energy Conversion and Management, 88, 1167-1178.

[170] Malhotra, R., & Ali, A. (2018). Lithium-doped ceria supported SBA− 15 as mesoporous solid reusable and heterogeneous catalyst for biodiesel production via simultaneous esterification and transesterification of waste cottonseed oil. Renewable Energy, 119, 32-44.

[171] Helwani, Z., Aziz, N., Kim, J., & Othman, M. R. (2016). Improving the yield of Jatropha curcas's FAME through sol–gel derived meso-porous hydrotalcites. Renewable energy, 86, 68-74.

[172] Wen, L., Wang, Y., Lu, D., Hu, S., & Han, H. (2010). Preparation of KF/CaO nanocatalyst and its application in biodiesel production from Chinese tallow seed oil. Fuel, 89(9), 2267-2271.

[173] Hindryawati, N., Maniam, G. P., Karim, M. R., & Chong, K. F. (2014). Transesterification of used cooking oil over alkali metal (Li, Na, K) supported rice husk silica as potential solid base catalyst. Engineering Science and Technology, an International Journal, 17(2), 95-103.

[174] Yan, S., Salley, S. O., & Ng, K. S. (2009). Simultaneous transesterification and esterification of unrefined or waste oils over ZnO-La2O3 catalysts. Applied Catalysis A: General, 353(2), 203-212.

[175] Singh, A. K., & Fernando, S. D. (2007). Reaction kinetics of soybean oil transesterification using heterogeneous metal oxide catalysts. Chemical Engineering & Technology, 30(12), 1716-1720.

[176] Hagen, J. (2015). Industrial catalysis: a practical approach: John Wiley & Sons.

[177] Xiao, Y., Gao, L., Xiao, G., & Lv, J. (2010). Kinetics of the transesterification reaction catalyzed by solid base in a fixed-bed reactor. Energy & Fuels, 24(11), 5829-5833.

[178] Hattori, H., Shima, M., & Kabashima, H. (2000). Alcoholysis of ester and epoxide catalyzed by solid bases. Studies in surface science and catalysis, 130, 3507-3512.

[179] Rattanaphra, D., Harvey, A. P., Thanapimmetha, A., & Srinophakun, P. (2012). Simultaneous transesterification and esterification for biodiesel production with and without a sulphated zirconia catalyst. Fuel, 97, 467-475.

[180] Birla, A., Singh, B., Upadhyay, S. N., & Sharma, Y. C. (2012). Kinetics studies of synthesis of biodiesel from waste frying oil using a heterogeneous catalyst derived from snail shell. Bioresource Technology, 106, 95-100.

[181] Vujicic, D., Comic, D., Zarubica, A., Micic, R., & Boskovic, G. (2010). Kinetics of biodiesel synthesis from sunflower oil over CaO heterogeneous catalyst. Fuel, 89(8), 2054-2061.

[182] Maneerung, T., Kawi, S., Dai, Y., & Wang, C. H. (2016). Sustainable biodiesel production via transesterification of waste cooking oil by using CaO catalysts prepared from chicken manure. Energy Conversion and Management, 123, 487-497.

[183] Kaur, N., & Ali, A. (2014). Kinetics and reusability of Zr/CaO as heterogeneous catalyst for the ethanolysis and methanolysis of Jatropha crucas oil. Fuel Processing Technology, 119, 173-184.

[184] Wu, W., Zhu, M., & Zhang, D. (2017). An experimental and kinetic study of canola oil transesterification catalyzed by mesoporous alumina supported potassium. Applied Catalysis A: General, 530, 166-173.

[185] Emeji, I. C., Afolabi, A. S., Abdulkareem, A. S., & Kalala, J. (2015, October). Characterization and kinetics of biofuel produced from waste cooking oil. In *Proceedings of the World Congress on Engineering and Computer Science* (Vol. 2, pp. 21-23).

[186] Dang, T. H., Chen, B. H., & Lee, D. J. (2013). Application of kaolin-based catalysts in biodiesel production via transesterification of vegetable oils in excess methanol. Bioresource technology, 145, 175-181.

[187] Jeong, G. T., Yang, H. S., & Park, D. H. (2009). Optimization of transesterification of animal fat ester using response surface methodology. Bioresource technology, 100(1), 25-30.

[188] Dias, J. M., Alvim-Ferraz, M. C., Almeida, M. F., Díaz, J. D. M., Polo, M. S., & Utrilla, J. R. (2012). Selection of heterogeneous catalysts for biodiesel production from animal fat. Fuel, 94, 418-425.

[189] Baskar, G., Selvakumari, I. A. E., & Aiswarya, R. (2018). Biodiesel production from castor oil using heterogeneous Ni doped ZnO nanocatalyst. Bioresource technology, 250, 793-798.

[190] Chakraborty, R., & Das, S. K. (2012). Optimization of biodiesel synthesis from waste frying soybean oil using fish scale-supported Ni catalyst. Industrial & Engineering Chemistry Research, 51(25), 8404-8414.

[191] Hameed, B. H., Lai, L. F., & Chin, L. H. (2009). Production of biodiesel from palm oil (Elaeis guineensis) using heterogeneous catalyst: an optimized process. Fuel Processing Technology, 90(4), 606-610.

[192] Costarrosa, L., Leiva-Candia, D. E., Cubero-Atienza, A. J., Ruiz, J. J., & Dorado, M. P. (2018). Optimization of the Transesterification of Waste Cooking Oil with Mg-Al Hydrotalcite Using Response Surface Methodology. Energies, 11(2), 302.

[193] Mahdavi, V., & Monajemi, A. (2014). Optimization of operational conditions for biodiesel production from cottonseed oil on CaO–MgO/Al2O3 solid base catalysts. Journal of the Taiwan Institute of Chemical Engineers, 45(5), 2286-2292.

[194] Liao, C. C., & Chung, T. W. (2013). Optimization of process conditions using response surface methodology for the microwave-assisted transesterification of Jatropha oil with KOH impregnated CaO as catalyst. Chemical Engineering Research and Design, 91(12), 2457-2464.

[195] Znad, H., & Frangeskides, Z. (2014). Chicken drumstick bones as an efficient biosorbent for copper (II) removal from aqueous solution. Desalination and Water Treatment, 52(7-9), 1560-1570.

[196] Predojević, Z. J. (2008). The production of biodiesel from waste frying oils: A comparison of different purification steps. Fuel, 87(17-18), 3522-3528.

[197] Kumar, D. & Ali, A. (2010). Nanocrystalline lithium ion impregnated calcium oxide as heterogeneous catalyst for transesterification of high moisture containing cotton seed oil. Energy Fuels, 24, 2091–2097.

[198] Gonçalves, A. M., Lima-Corrêa, R. A., Assaf, J. M., & Nogueira, A. R. (2017). Lithium and calcium based perovskite type oxides for ethylic transesterification. *Catalysis Today*, *279*, 177-186.

[199] Kaur, N. & Ali, A. (2013). Lithium ions-supported magnesium oxide as nano-sized solid catalyst for biodiesel preparation from muton fat. Energy Sources, Part A: Recovery, Utilization, and Environmental Effects, 35:2, 184-192.

[200] Wen, Z., Yu, X., Tu, S., Yan, J., Dahlquist, E. (2010). Biodiesel from waste cooking oil catalyzed by TiO-MgO mixed oxides. Bioresource Technology, 101, 9570-9576.

[201] Xie, W., Yang, Z., Chun, H. (2007). Catalytic properties of Lithium-Doped ZnO catalysts used for biodiesel preparations. Ind. Eng. Chem. Res., 46, 7942-7949.

[202] Amani, H., Asif, M., & Hameed, B. H. (2016). Transesterification of waste cooking palm oil and palm oil to fatty acid methyl ester using cesium-modified silica catalyst. Journal of the Taiwan Institute of Chemical Engineers, 58, 226-234.

[203] Salinas, D., Araya, P., Guerrero, S. (2012). Study of potassium-supported TiO2 catalysts for the production of biodiesel. Applied Catalysis B: Environmental, 117– 118, 260– 267.

[204] Yu, X., Wena, Z., Li, H., Tu, S.,Yan, J. (2011). Transesterification of Pistacia chinensis oil for biodiesel catalyzed by CaO–CeO2 mixed oxides. Fuel, 90, 1868–1874.

[205] Li, F., Li, H., Wang, L. & Cao, Y. (2015). Waste carbide slag as a solid base catalyst for effective synthesis of biodiesel via transesterification of soybean oil with methanol. Fuel Processing Technology 131, 421–429.

[206] Olutoye, M.A., Wong, S.W., Chin, L.H., Amani, H., Asif, M., Hameed, B.H. (2016). Synthesis of fatty acid methyl esters via the transesterification of waste cooking oil by methanol with a barium-modified montmorillonite K10 catalyst. Renewable Energy, 86, 392-398.

[207] Syamsuddin, Y., Murat, M.N., Hameed B.H. (2016). Synthesis of fatty acid methyl ester from the transesterification of high- and low-acid-content crude palm oil (Elaeis guineensis) and karanj oil (Pongamia pinnata) over a calcium–lanthanum–aluminium mixed-oxides catalyst. Bioresource Technology, 214, 248–252.

[208] Moradi, G.R., Mohadesi, M., Ghanbari, M., Moradi, M.J., Hosseini, Sh., Davoodbeygi, Y. (2015). Kinetic comparison of two basic heterogeneous catalysts obtained from sustainable resources for transesterification of waste cooking oil. Biofuel Research Journal 6, 236-241.

[209] Hindryawati, N, Maniam, G.P. (2015). Novel utilization of waste marine sponge (Demospongiae) as a catalyst in ultrasound-assisted transesterification of waste cooking oil. Ultrasonics Sonochemistry, 22, 454–462.

[210] Georgogianni, K.G., Kontominas, M.G., Tegou, E., Avlonitis, D., Vergis, V., (2007) Biodiesel production: reaction and process parameters of alkali-catalysed transesterification of waste frying-oils, Energy Fuels, 21, 3023–3027.

[211] Utlu, Z., (2007) Evaluation of biodiesel obtained from waste cooking oil, Energy Sources, Part A, 29, 1295–1304.

[212] Refaat, A.A., Attia, N.K., Sibak, H.A., El Sheltawy, S.T., El Diwani, G.I., (2008) Production optimisation and quality assessment of biodiesel from waste vegetable oil, Int J Environ Sci Technol, 5, 75–82.

[213] Phan, A. N., Phan T. M., (2008) Biodiesel production from waste cooking oils, Fuel, 87, 3490–3496.

[214] Lee, J. Y., Yoo, C., Jun, S. Y., Ahn, C. Y., & Oh, H. M. (2010). Comparison of several methods for effective lipid extraction from microalgae. *Bioresource technology*, *101*(1), S75-S77.

[215] Huang, D., Han, S., Han, Z., & Lin, Y. (2012). Biodiesel production catalyzed by Rhizomucor miehei lipase-displaying Pichia pastoris whole cells in an isooctane system. Biochemical engineering journal, 63, 10-14.

[216] Helwani, Z., Othman, M. R., Aziz, N., Fernando, W. J. N., & Kim, J. (2009). Technologies for production of biodiesel focusing on green catalytic techniques: a review. Fuel Processing Technology, 90(12), 1502-1514.

[217] Tan, Y. H., Abdullah, M. O., Nolasco-Hipolito, C., & Taufiq-Yap, Y. H. (2015). Waste ostrich-and chicken-eggshells as heterogeneous base catalyst for biodiesel production from used cooking oil: Catalyst characterization and biodiesel yield performance. Applied Energy, 160, 58-70.

[218] Punsuvon, V., Nokkaew, R., Somkliang, P., Tapanwong, M., & Karnasuta, S. (2015). The optimization of esterification reaction for biodiesel production from animal fat. Energy Sources, Part A: Recovery, Utilization, and Environmental Effects, 37(8), 846-853.

[219] Lim, B. P., Maniam, G. P., & Hamid, S. A. (2009). Biodiesel from adsorbed waste oil on spent bleaching clay using CaO as a heterogeneous catalyst. European Journal of Scientific Research, 33(2), 347-357.

[220] Manalu, J. L., Soegijono, B., & Indrani, D. J. (2015). Characterization of Hydroxyapatite Derived from Bovine Bone. Asian Journal of Applied Sciences (ISSN: 2321–0893), 3(04).

[221] Yan, B., Zhang, Y., Chen, G., Shan, R., Ma, W., & Liu, C. (2016). The utilization of hydroxyapatite-supported CaO-CeO$_2$ catalyst for biodiesel production. Energy Conversion and Management, 130, 156-164.

[222] Viriya-Empikul, N., Krasae, P., Puttasawat, B., Yoosuk, B., Chollacoop, N., & Faungnawakij, K. (2010). Waste shells of mollusk and egg as biodiesel production catalysts. Bioresource technology, 101(10), 3765-3767.

[223] Maleki, H., Kazemeini, M., Larimi, A. S., & Khorasheh, F. (2017). Transesterification of canola oil and methanol by lithium impregnated CaO–La$_2$O$_3$ mixed oxide for biodiesel synthesis. Journal of Industrial and Engineering Chemistry, 47, 399-404.

[224] Yang, Z., & Xie, W. (2007). Soybean oil transesterification over zinc oxide modified with alkali earth metals. Fuel processing technology, 88(6), 631-638.

[225] Islam, A., Taufiq-Yap, Y. H., Ravindra, P., Teo, S. H., Sivasangar, S., & Chan, E. S. (2015). Biodiesel synthesis over millimetric γ-Al2O3/KI catalyst. Energy, 89, 965-973.

[226] Kong, B., Yu, J., Savino, K., Zhu, Y., & Guan, B. (2012). Synthesis of α-calcium sulfate hemihydrate submicron-rods in water/n-hexanol/CTAB reverse microemulsion. *Colloids and Surfaces A: Physicochemical and Engineering Aspects*, *409*, 88-93.

[227] Wang, Y.-T., Fang, Z., Zhang, F., & Xue, B.-J. (2015). One-step production of biodiesel from oils with high acid value by activated Mg–Al hydrotalcite nanoparticles. Bioresource technology, 193, 84-89.

[228] Khemthong, P., Luadthong, C., Nualpaeng, W., Changsuwan, P., Tongprem, P., Viriya-Empikul, N., & Faungnawakij, K. (2012). Industrial eggshell wastes

as the heterogeneous catalysts for microwave-assisted biodiesel production. *Catalysis Today*, *190*(1), 112-116.

[229] Wan, L., Liu, H., & Skala, D. (2014). Biodiesel production from soybean oil in subcritical methanol using MnCO3/ZnO as catalyst. *Applied Catalysis B: Environmental*, *152*, 352-359.

[230] Amani, H., Ahmad, Z., Hameed, B.H. (2014). Synthesis of fatty acid methyl esters via the methanolysis of palm oil over Ca3.5xZr0.5yAlxO3 mixed oxide catalyst. Renewable Energy, 66, 680-685.

[231] Deng, X., Fang, Z., Liu, Y.-h., & Yu, C.-L. (2011). Production of biodiesel from Jatropha oil catalyzed by nanosized solid basic catalyst. Energy, 36(2), 777-784.

[232] Yan, S., Kim, M., Salley, S. O., & Ng, K. S. (2009). Oil transesterification over calcium oxides modified with lanthanum. *Applied Catalysis A: General*, *360*(2), 163-170.

[233] Kumar, D., & Ali, A. (2013). Transesterification of low-quality triglycerides over a Zn/CaO heterogeneous catalyst: kinetics and reusability studies. *Energy & Fuels*, *27*(7), 3758-3768.

[234] Stamenković, O. S., Veličković, A. V., & Veljković, V. B. (2011). The production of biodiesel from vegetable oils by ethanolysis: current state and perspectives. Fuel, 90(11), 3141-3155.

[235] Singh, A. K., & Fernando, S. D. (2009). Preparation and reaction kinetics studies of Na-based mixed metal oxide for transesterification. *Energy & Fuels*, *23*(10), 5160-5164.

[236] Kawashima, A., Matsubara, K., & Honda, K. (2008). Development of heterogeneous base catalysts for biodiesel production. *Bioresource technology*, *99*(9), 3439-3443.

[237] Tittabut, T., & Trakarnpruk, W. (2008). Metal-loaded MgAl oxides for transesterification of glyceryl tributyrate and palm oil. *Industrial & Engineering Chemistry Research*, *47*(7), 2176-2181.

[238] Xie, W., Peng, H., & Chen, L. (2006). Calcined Mg–Al hydrotalcites as solid base catalysts for methanolysis of soybean oil. *Journal of Molecular Catalysis A: Chemical*, *246*(1-2), 24-32.

[239] Yoosuk, B., Krasae, P., Puttasawat, B., Udomsap, P., Viriya-empikul, N., & Faungnawakij, K. (2010). Magnesia modified with strontium as a solid base catalyst for transesterification of palm olein. *Chemical Engineering Journal*, *162*(1), 58-66.

[240] Chen, G., Shan, R., Shi, J., Liu, C., & Yan, B. (2015). Biodiesel production from palm oil using active and stable K doped hydroxyapatite catalysts. *Energy conversion and management*, *98*, 463-469.

[241] Wei, Z., Xu, C., & Li, B. (2009). Application of waste eggshell as low-cost solid catalyst for biodiesel production. *Bioresource technology*, *100*(11), 2883-2885.

[242] Nakatani, N., Takamori, H., Takeda, K., & Sakugawa, H. (2009). Transesterification of soybean oil using combusted oyster shell waste as a catalyst. *Bioresource Technology*, *100*(3), 1510-1513.

[243] Kotwal, M. S., Niphadkar, P. S., Deshpande, S. S., Bokade, V. V., & Joshi, P. N. (2009). Transesterification of sunflower oil catalyzed by flyash-based solid catalysts. *Fuel*, *88*(9), 1773-1778.

[244] Aderemi, B. O., & Hameed, B. H. (2009). Alum as a heterogeneous catalyst for the transesterification of palm oil. *Applied Catalysis A: General*, *370*(1-2), 54-58.

[245] Jazie, A. A., Pramanik, H., Sinha, A. S. K., & Jazie, A. A. (2013). Egg shell as eco-friendly catalyst for transesterification of rapeseed oil: optimization for biodiesel production. *International Journal of Sustainable Development and Green Economics*, *2*(1), 27-32.

[246] Azócar, L., Heipieper, H. J., & Navia, R. (2010). Biotechnological processes for biodiesel production using alternative oils. *Applied microbiology and biotechnology*, *88*(3), 621-636.

[247] Al-Jammal, N., Al-Hamamre, Z., & Alnaief, M. (2016). Manufacturing of zeolite based catalyst from zeolite tuft for biodiesel production from waste sunflower oil. Renewable Energy, 93, 449-459.

[248] Agrawal, S., Singh, B., & Sharma, Y. C. (2012). Exoskeleton of a mollusk (Pila globosa) as a heterogeneous catalyst for synthesis of biodiesel using used frying oil. *Industrial & Engineering Chemistry Research*, *51*(37), 11875-11880.

[249] Cercado, A. P., Ballesteros Jr, F., & Capareda, S. (2018). Ultrasound assisted transesterification of microalgae using synthesized novel catalyst. Sustainable Environment Research, 28(5), 234-239.

[250] Maceiras, R., Alfonsín, V., Cancela, Á., & Sánchez, Á. (2017). Biodiesel Production from Waste Frying Oil by Ultrasound-Assisted Transesterification. Chemical Engineering & Technology, 40(9), 1713-1719.

[251] Maghami, M., Sadrameli, S. M., & Ghobadian, B. (2015). Production of biodiesel from fishmeal plant waste oil using ultrasonic and conventional methods. Applied Thermal Engineering, 75, 575-579.

[252] Bai, R., Wang, S., Mei, F., Li, T., & Li, G. (2011). Synthesis of glycerol carbonate from glycerol and dimethyl carbonate catalyzed by KF modified hydroxyapatite. Journal of Industrial and Engineering Chemistry, 17(4), 777-781.

[253] Taufiq-Yap, Y. H., Lee, H. V., Hussein, M. Z., & Yunus, R. (2011). Calcium-based mixed oxide catalysts for methanolysis of Jatropha curcas oil to biodiesel. Biomass and bioenergy, 35(2), 827-834.

[254] Tantirungrotechai, J., Chotmongkolsap, P., & Pohmakotr, M. (2010). Synthesis, characterization, and activity in transesterification of mesoporous Mg–Al mixed-metal oxides. *Microporous and Mesoporous Materials*, *128*(1-3), 41-47.

[255] Tang, Y., Xu, J., Zhang, J., & Lu, Y. (2013). Biodiesel production from vegetable oil by using modified CaO as solid basic catalysts. *Journal of Cleaner Production*, *42*, 198-203.

[256] Alsharifi, M., Znad, H., Hena, S., & Ang, M. (2017). Biodiesel production from canola oil using novel Li/TiO2 as a heterogeneous catalyst prepared via impregnation method. *Renewable Energy*, *114*, 1077-1089.

[257] Gole, V. L., & Gogate, P. R. (2012). A review on intensification of synthesis of biodiesel from sustainable feed stock using sonochemical reactors. Chemical Engineering and Processing: Process Intensification, 53, 1-9.

[258] Vichare, N. P., Gogate, P. R., Dindore, V. Y., & Pandit, A. B. (2001). Mixing time analysis of a sonochemical reactor. Ultrasonics Sonochemistry, 8(1), 23-33.

[259] Omar, W. N. N. W., & Amin, N. A. S. (2011). Biodiesel production from waste cooking oil over alkaline modified zirconia catalyst. Fuel Processing Technology, 92(12), 2397-2405.

[260] Poosumas, J., Ngaosuwan, K., Quitain, A. T., & Assabumrungrat, S. (2016). Role of ultrasonic irradiation on transesterification of palm oil using calcium oxide as a solid base catalyst. Energy conversion and management, 120, 62-70.

[261] Zhao, H., Zhang, G., Chong, S., Zhang, N., & Liu, Y. (2015). MnO2/CeO2 for catalytic ultrasonic decolorization of methyl orange: Process parameters and mechanisms. Ultrasonics sonochemistry, 27, 474-479.

[262] Malani, R. S., Shinde, V., Ayachit, S., Goyal, A., & Moholkar, V. S. (2019). Ultrasound–assisted biodiesel production using heterogeneous base catalyst and mixed non–edible oils. Ultrasonics sonochemistry, 52, 232-243.

[263] Darwin, S., Egi, A., & Achmad, P. (2010). Transesterification of biodiesel from waste cooking oil using ultrasonic technique. In International conference on environment Malaysia.

[264] Uddin, M. R., Ferdous, K., Uddin, M. R., Khan, M. R., & Islam, M. A. (2013). Synthesis of biodiesel from waste cooking oil. Chemical engineering and science, 1(2), 22-26.

[265] Betiku, E., Etim, A. O., Pereao, O., & Ojumu, T. V. (2017). Two-Step Conversion of Neem (Azadirachta indica) Seed Oil into Fatty Methyl Esters Using a Heterogeneous Biomass-Based Catalyst: An Example of Cocoa Pod Husk. Energy & Fuels, 31(6), 6182-6193.

[266] Mohamad, M., Ngadi, N., Wong, S. L., Jusoh, M., & Yahya, N. Y. (2017). Prediction of biodiesel yield during transesterification process using response surface methodology. Fuel, 190, 104-112.

[267] Al-Mohammedawi, H. H., Znad, H., & Eroglu, E. (2018). Synergistic effects and optimization of photo-fermentative hydrogen production of Rhodobacter sphaeroides DSM 158. International Journal of Hydrogen Energy, 43(33), 15823-15834.

[268] Alvarez-Guzmán, C. L., Balderas-Hernández, V. E., González-García, R., Ornelas-Salas, J. T., Vidal-Limón, A. M., Cisneros-de la Cueva, S., & De Leon-Rodriguez, A. (2017). Optimization of hydrogen production by the psychrophilic strain G088. International Journal of Hydrogen Energy, 42(6), 3630-3640.

[269] Alawi, N. M., Barifcani, A., & Abid, H. R. (2018). Optimisation of CH4 and CO2 conversion and selectivity of H2 and CO for the dry reforming of methane by a microwave plasma technique using a Box–Behnken design. Asia-Pacific Journal of Chemical Engineering, 13(6), e2254.

[270] Alketife, A. M., Judd, S., & Znad, H. (2017). Synergistic effects and optimization of nitrogen and phosphorus concentrations on the growth and nutrient uptake of a freshwater Chlorella vulgaris. Environmental technology, 38(1), 94-102.

[271] Hasni, K., Ilham, Z., Dharma, S., & Varman, M. (2017). Optimization of biodiesel production from Brucea javanica seeds oil as novel non-edible feedstock using response surface methodology. Energy Conversion and Management, 149, 392-400.

Every reasonable effort has been made to acknowledge the owners of copyright

material. I would be pleased to hear from any copyright owner who has been

omitted or incorrectly acknowledged.

## Appendix A: Articles copyright and Co-author attribution statement

## Co-Author Attribution Statement

Paper 1: Alsharifi, M., Znad, H., Hena, S., & Ang, M. (2017). Biodiesel production from canola oil using novel Li/TiO2 as a heterogeneous catalyst prepared via impregnation method. Renewable Energy, 114, 1077-1089.

| | Conception & design | Acquisition Of data & method | Data Conditioning & manipulation | Analysis & Statistical method | Interpretation & discussion | Final approval |
|---|---|---|---|---|---|---|
| Dr. Hussein Znad | X | | X | X | | X |
| I acknowledge that these represent my contribution to the above research output. Signed. | | | | | | |
| Dr. Sufia Hena | X | | | X | X | X |
| I acknowledge that these represent my contribution to the above research output. Signed. | | | | | | |

Paper 2: Alsharifi, M., & Znad, H. (2019). Development of a lithium based chicken bone (Li-Cb) composite as an efficient catalyst for biodiesel production. Renewable Energy, 136, 856-864.

| | Conception And design | Acquisition Of data & method | Data Conditioning & manipulation | Analysis & Statistical method | Interpretation & discussion | Final approval |
|---|---|---|---|---|---|---|
| Dr. Hussein Znad | X | | X | X | | X |
| I acknowledge that these represent my contribution to the above research output. Signed. | | | | | | |

Paper 3: Alsharifi, M., & Znad, H. (2020). Transesterification of waste canola oil by lithium/zinc composite supported on waste chicken bone as an effective catalyst. Renewable Energy, 151, 740-749.

| | Conception And design | Acquisition Of data & method | Data Conditioning & manipulation | Analysis & Statistical method | Interpretation & discussion | Final approval |
|---|---|---|---|---|---|---|
| Dr. Hussein Znad | X | | X | X | | X |
| I acknowledge that these represent my contribution to the above research output. Signed. | | | | | | |